

Spatial and Temporal Patterns of Erosion in Western China and Tibet

Amanda C. Henck

A dissertation  
submitted in partial fulfillment of the  
requirements for the degree of

Doctor of Philosophy

University of Washington  
2010

Program Authorized to Offer Degree:  
Geological Sciences

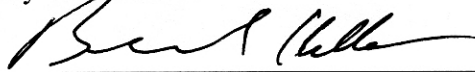
University of Washington  
Graduate School

This is to certify that I have examined this copy of a doctoral dissertation by

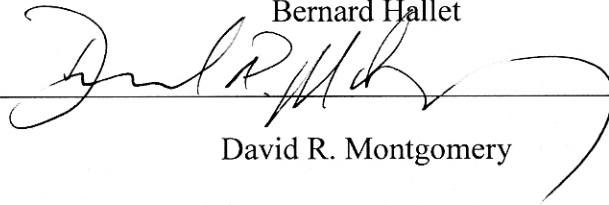
Amanda C. Henck

and have found that it is complete and satisfactory in all respects,  
and that any and all revisions required by the final  
examining committee have been made.

Chairs of the Supervisory Committee:

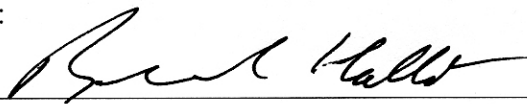


Bernard Hallet

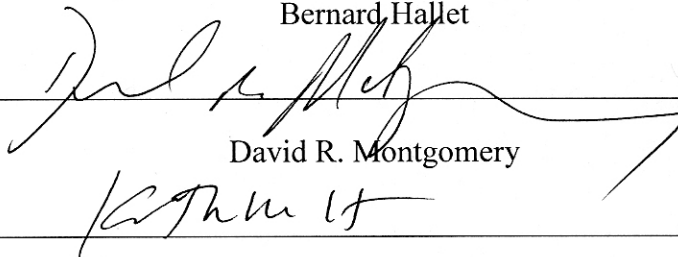


David R. Montgomery

Reading Committee:



Bernard Hallet



David R. Montgomery



Katharine W. Huntington

Date: 2/10/10

In presenting this dissertation in partial fulfillment of the requirements for the doctoral degree at the University of Washington, I agree that the Library shall make its copies freely available for inspection. I further agree that extensive copying of this dissertation is allowable only for scholarly purposes, consistent with "fair use" as prescribed in the U. S. Copyright Law. Requests for copying or reproduction of this dissertation may be referred to ProQuest Information and Learning, 300 North Zeeb Road, Ann Arbor, MI 48106-1346, 1-800-521-0600, to whom the author has granted "the right to reproduce and sell (a) copies of the manuscript in microform and/or (b) printed copies of the manuscript made from microform."

Signature \_\_\_\_\_

Date \_\_\_\_\_

University of Washington

**Abstract**

Spatial and Temporal Patterns of Erosion in Western China and Tibet

Amanda C. Henck

Chairs of the Supervisory Committee:

David R. Montgomery, Professor  
Department of Earth and Space Sciences

Bernard Hallet, Professor  
Department of Earth and Space Sciences

Two parallel debates are ongoing about how tectonics and climate interact to set erosion rates and how humans alter these erosion rates; these issues form the basis for my dissertation. Using the eastern margin of the Tibetan Plateau as a natural laboratory to inform these two debates, I conduct detailed studies of millennial and decadal erosion rates in southwest China and southeast Tibet, focusing specifically on the Three Rivers Region (TRR) as well as other rivers in Tibet and Yunnan. The TRR is where the Salween, Mekong, and Yangtze Rivers flow parallel to one another incised in 3000-m deep gorges. To further understand controls on annual sediment yield, I calculate effective discharges for the same region. I find two patterns in the millennial erosion rates. First is an along river trend of increasing erosion rates as the rivers leave the dry, flat Tibetan Plateau and enter the wet, steep gorges of the TRR. In the Salween and Mekong Rivers, erosion rates are well correlated with relief and stream power, while in the Yangtze River they are correlated with rainfall. Second is a pattern across the rivers. In the lower basins of the TRR the erosion rates in the Salween are 200 times higher than the erosion rates in the Yangtze River across a region with little variation in stream power and no variation in relief or rainfall, suggesting a strong tectonic control on erosion rates.

Using daily sediment concentration and discharge records, I calculate mean annual sediment yield for 44 stations in Tibet and Yunnan. I find that sediment yield is weakly correlated with mean annual rainfall and fraction of land under cultivation and that there are no systematic trends in the sediment yield data over time. To further investigate the controls on these sediment yields, I calculate effective discharge for all of these stations. The effective discharge calculations shed light on a long-standing debate about whether small and frequent or large and infrequent events transport more sediment. In this monsoon region, I find that effective discharge recurs throughout the monsoon and is controlled by monsoon base flow rather than individual storm events.

## TABLE OF CONTENTS

LIST OF FIGURES .....	iii
LIST OF TABLES .....	iv
Chapter 1: Introduction .....	1
Tectonic and geomorphic context .....	2
Chapters 2-4 .....	4
Conclusions .....	6
Notes for chapter 1 .....	7
Chapter 2: Spatial controls on erosion in the Three Rivers Region .....	10
Introduction .....	10
Samples and methods .....	15
Results .....	22
Discussion .....	28
Conclusion .....	37
Acknowledgements .....	39
Figures for chapter 2 .....	40
Tables for chapter 2 .....	47
Notes for chapter 2 .....	65
Chapter 3: The myth of Communist land degradation: new evidence from local erosion and basin-wide sediment yield in SW China and SE Tibet .....	76
Introduction .....	76
Methods .....	82
Results .....	85
Discussion .....	89
Conclusions .....	94
Acknowledgements .....	96

Figures for chapter 3 .....	97
Tables for chapter 3.....	106
Notes for chapter 3 .....	114
Chapter 4: Monsoon control of effective discharge, Yunnan and Tibet .....	121
Introduction .....	121
Methods.....	124
Results and discussion .....	126
Conclusions .....	127
Acknowledgments.....	129
Figures for chapter 4 .....	130
Tables for chapter 4.....	132
Notes for chapter 4 .....	134
Bibliography.....	138

## LIST OF FIGURES

Figure 2.1: Context map of the study region .....	40
Figure 2.2: Location of samples and topography for the TRR. ....	41
Figure 2.3: Erosion rates measured for the TRR .....	42
Figure 2.4: Geomorphic parameters for the region.....	43
Figure 2.5: Relationship between erosion and geomorphic parameters .....	44
Figure 2.6: Basin area vs. cumulative sediment yield for each river. ....	45
Figure 2.7: Longitudinal profiles for main stem of each river.....	46
Figure 3.1: Location of the study region.....	97
Figure 3.2: Details on location and quality of sediment yield data.....	98
Figure 3.3: Geomorphic and anthropogenic data about the region.....	99
Figure 3.4: Scatter plots showing the relation between various geomorphic and anthropogenic metrics and sediment yield.....	100
Figure 3.5: Sediment yield and sediment rating curve parameters as a function of time.....	102
Figure 3.6: Erosion rate calculated from sediment yield as a function of erosion rate measured over millennial timescales from <sup>10</sup> Be data.....	104
Figure 3.7: Cumulative sediment yield as a function of upstream area. ....	105
Figure 4.1: Map showing location of stations analyzed.....	130
Figure 4.2: Histograms of distribution of RI.....	130
Figure 4.3: RI as a function of ratio of effective discharge to mean daily discharge, basin area, and years of data available. ....	131
Figure 4.4: Hydrographs (thin black line) and Q <sub>eff</sub> (wider grey line) .....	131



## LIST OF TABLES

Table 2.1: Details on location and sequence of samples used in analysis. ....	47
Table 2.2: Concentrations of $^{10}\text{Be}$ and derived erosion rates for entire upstream basins (a) and intermediate reaches between samples (b).....	50
Table 2.3: Details on data collection and preparation.....	52
Table 2.4: CRONUS calculator input. ....	56
Table 2.5: Information for calculating intermediate erosion rates.....	61
Table 3.1: Summary details on all the stations .....	106
Table 4.1: Details on stations and effective discharge calculations.....	132

## **ACKNOWLEDGEMENTS**

Thank you to the numerous people who helped me along this journey, including (but not at all limited to): my husband, Josh, for being here through the tumultuous final year; my parents, for encouraging my love of science; Steve and Tom for the fantastic research, teaching, and mentoring I got from UWWW and the IGERT program; Dave for guiding me along the way in large and small ways and editing just about every draft of every paper; Kate for jumping in at the last minute and providing me with much needed female mentoring; Bernard for inspiring me to think broadly; John for guidance and mentoring in and out of his lab; Greg for advice and guidance from day 1; Patsy and John for field work assistance; Liang Chuan for unbelievable access to data; Harvey for every GIS question I ever had; and too many others to mention here who have supported me along the way. Thank you.

## **DEDICATION**

To Granddaddy, who would have been 87 on my defense date, 19 January 2010.

## Chapter 1: Introduction

Recent attention in geomorphology has focused on how climate, tectonics, and erosion interact to form landscapes (e.g., Burbank et al., 2003; Dadson et al., 2003; Reiners et al., 2003). In addition to these natural interactions, human disturbances to the environment have prompted research on how humans act as geomorphic agents (Hooke, 1999; 2000) and, in some places, contribute disproportionately to erosion rates while in others have no discernable effect (von Blanckenburg, 2005). The margins of the Tibetan Plateau have emerged as a natural laboratory for climate-tectonics-erosion research because of steep hillslopes and high rates of tectonic activity (Burbank et al., 1996; Zeitler et al., 2001; Burbank et al., 2003). However, these regions are less ideal for studying human altered landscapes as reflected in sediment yield because many regions are ungauged or gauge records are extremely short. I take advantage of a relatively long period of record for a set of sediment gauges in Tibet and Yunnan to combine these two lines of research on the eastern margin of the Tibetan Plateau.

This dissertation addresses broad questions related to controls on erosion over multiple spatial and temporal scales in southwest China and southeast Tibet. I capitalize on the coincidence of a geomorphically interesting area with long records of modern sediment yield to conduct a detailed study of how geomorphic and anthropogenic parameters interact to set rates of landscape denudation in this part of the world. To do this I calculate basin-averaged erosion rates using both  $^{10}\text{Be}$  in

detrital quartz and records up to 27 years in duration of sediment yield from Chinese hydrology stations. I compare these erosion rates to relevant geomorphic parameters: stream power, rainfall, and mean local relief. For the modern data I examine the role humans play in accelerating and controlling erosion. I analyze annual sediment rating curves and time series of annual sediment yield as well as the relationship between mean annual sediment yield and indices of development such as population density and the fraction of land under cultivation. As a further investigation of controls on erosion and annual sediment yield, I calculate effective discharge for all the Chinese hydrology stations to determine if small and frequent events or large and infrequent events have a greater control on sediment yield.

### **Tectonic and geomorphic context**

Roughly 36-40 mm/yr of convergence between India and Eurasia since early Cenozoic time (DeCelles et al., 2002) has resulted in the high rates of uplift, deep exhumation, and substantial thickening of the crust that characterize the Himalayan-Tibetan system. The central Tibetan plateau has subdued topography with a mean elevation of over 5 km and is internally drained (Fielding et al., 1994). The northern margin of the plateau is sharply defined by the narrow eastern and western Kunlun Shan. The steep southern topographic front of the plateau is defined by the 2500-km long Himalayan ranges, which stretch between two structural syntaxes centered on major metamorphic massifs, Nanga Parbat (8125 m) in the west and Namche Barwa (7782 m) to the east (Zeitler et al., 2001).

Deformation in the central Himalaya is characterized by north-dipping, primarily convergent structures and more limited east-west extension since Miocene time (Hodges, 2000). The syntaxes are characterized by intense deformation propagating outward from the indenter corners, shortening, and rotation of crustal material along major strike-slip faults (Wang and Burchfiel, 2000; Zeitler et al., 2001; Koons et al., 2005).

In contrast to the clear topographic boundaries to the north and south of the Tibetan plateau, the eastern and western margins of the plateau are less-well defined, transitioning gradually from the low-relief plateau interior to the deeply incised margin. To the west, the gentle topography of the plateau transitions gradually into the high relief Karakoram and Pamir Mountains (Searle and Turrill, 1991; Burtman and Molnar, 1993). Although the steepest far-eastern margin of the plateau is clearly defined at the edge of the Sichuan basin by the Longmen Shan, the southeastern and northeastern margins of the plateau are more diffuse. At the southeastern margin, the low-relief surface of the plateau is incised by deep gorges carved by the Tsangpo, Salween, Mekong, and Yangtze Rivers (Burg et al., 1997; Liu and Zhong, 1997; Hallet and Molnar, 2001; Zeitler et al., 2001). My dissertation is focused on these incised rivers and the Red River in the far southeastern margin of the Plateau.

## Chapters 2-4

Chapters 2-4 were prepared for publication individually, resulting in some unavoidable overlap between chapters. Although formatted specifically for this dissertation, the content of each chapter is identical to what was submitted for publication.

Chapter 2 characterizes the spatial patterns in erosion rates in the Three Rivers Region (TRR) in southwest China and southeast Tibet using  $^{10}\text{Be}$  in detrital quartz and investigates correlations between erosion rates and various geomorphic characteristics. The TRR is where the Salween, Mekong, and Yangtze Rivers are incised in 3000-m deep gorges parallel to and within 100 km of one another. For fifty main-stem and tributary basins in the region I measured  $^{10}\text{Be}$  concentrations in detrital sediment and calculated basin-wide erosion rates. The region has two distinct spatial patterns evident in the erosion rates. The first is a downstream increase in erosion rates as the rivers leave the high, dry Tibetan Plateau and enter the wet, steep gorges of the TRR. In the Salween River erosion rates correlate well with mean local relief, in the Mekong River with mean normalized stream power and relief, and in the Yangtze River with rainfall. The second pattern is across the trend of the rivers in the narrow gorges of the lower basins. Erosion rates along the Salween River are 200 times higher than those along the Yangtze River, which is only 100 km away. For this pattern of erosion rates to be sustained over time, there must be a gradient in rock uplift. I propose that this region is an example of a

transition from tectonically controlled erosion rates in the Salween River to climatically controlled erosion rates in the Yangtze River.

Chapter 3 is a study of the controls on modern erosion rates over decadal timescales and investigates the scientific basis for claims that modern policies have increased sediment loading to rivers. Recent environmental policies in China ban logging and farming in much of western China because of perceptions that sediment loading to rivers is causing increased flooding to downstream areas. Using up to 27 years of daily discharge and total suspended sediment data and extensive GIS data, I analyze time series of sediment yield, time series of sediment rating curve parameters (as a method of measuring river response to sediment loading which is insensitive to temporal variation in discharge), and correlations between mean annual sediment yield and metrics of development such as land use and population density. I find that sediment yield is weakly correlated to the fraction of land under cultivation and to rainfall, but that there are no systematic trends in the annual sediment yields or sediment rating curve parameters. This suggests that if human activities have increased erosion locally, the sediment is being stored in the system and not exported in the major rivers. This conclusion calls into question the longstanding argument that Communist policies greatly increased erosion rates throughout China, causing systematic increases in flooding in downstream areas.



In chapter 4 I look more closely at the long-standing question of whether large and infrequent storms or small and frequent events control sediment yield on an decadal basis. I find that effective discharge in this part of the world happens during the summer monsoon with an average recurrence interval of 11 days, at flows which are approximately the base flow of the monsoon. Instead of being a storm-by-storm based system in which large storms move the most sediment, sediment is mobilized for up to two or three months every summer during the monsoon.

## **Conclusions**

As one moves from large spatial and temporal scales of characterizing erosion rates to smaller and shorter scales, the controls on erosion rates in the TRR changes. On the longer, millennial timescale that  $^{10}\text{Be}$  measures, the erosion rate along the Salween and Mekong Rivers depends on stream power and relief and transition to rainfall controlling the erosion rate along the Yangtze River. However, across the TRR, erosion rate decreases eastward by nearly three orders of magnitude in only 100 km, suggesting a strong tectonic control. Over shorter, decadal timescales erosion rate is primarily a function of the fraction of land under cultivation and mean annual rainfall in a watershed. A detailed investigation of the discharges that are dominant in transporting sediment reveals that the base flow of the monsoon (directly tied to monsoon rainfall) dominates sediment transport in this region.

## Notes for chapter 1

- Burbank, D. W., Blythe, A. E., Putkonen, J., Pratt-Sitaula, B., Gabet, E., Oskin, M., Barros, A., and Ojha, T. P. (2003). Decoupling of erosion and precipitation in the Himalayas. *Nature* 426, 652-655.
- Burbank, D. W., Leland, J., Fielding, E., Anderson, R. S., Brozovic, N., Reid, M. R., and Duncan, C. (1996). Bedrock incision, rock uplift and threshold hillslopes in the northwestern Himalayas. *Nature* 379, 505-510.
- Burg, J. P., Davy, P., Nievergelt, P., Oberli, F., Seward, D., Diao, Z. Z., and Meier, M. (1997). Exhumation during crustal folding in the Namche-Barwa syntaxis. *Terra Nova* 9, 53-56.
- Burtman, V. S., and Molnar, P. (1993). Geological and geophysical evidence for deep subduction of continental crust beneath the Pamir. *Geological Society of America Special Paper* 281, 1-76.
- Dadson, S. J., Hovius, N., Chen, H. G., Dade, W. B., Hsieh, M. L., Willett, S. D., Hu, J. C., Horng, M. J., Chen, M. C., Stark, C. P., Lague, D., and Lin, J. C. (2003). Links between erosion, runoff variability and seismicity in the Taiwan orogen. *Nature* 426, 648-651.
- DeCelles, P. G., Robinson, D. M., and Zandt, G. (2002). Implications of shortening in the Himalayan fold-thrust belt for uplift of the Tibetan Plateau. *Tectonics* 21, 10.1029/2001TC001322.
- Fielding, E., Isacks, B., Barazangi, M., and Duncan, C. (1994). How flat is Tibet. *Geology* 22, 163-167.
- Hallet, B., and Molnar, P. (2001). Distorted drainage basins as markers of crustal strain east of the Himalaya. *Journal of Geophysical Research-Solid Earth* 106, 13697-13709.

- Hodges, K. V. (2000). Tectonics of the Himalaya and southern Tibet from two perspectives. *Geological Society of America Bulletin* 112, 324-350.
- Hooke, R. L. (1999). Spatial distribution of human geomorphic activity in the United States: Comparison with rivers. *Earth Surface Processes and Landforms* 24, 687-692.
- Hooke, R. L. (2000). On the history of humans as geomorphic agents. *Geology* 28, 843-846.
- Koons, P. O., Hallet, B., Henck, A., Liu, Y., and Zeitler, P. K. (2005). Topographic expression of crustal velocity curls: an example from Eastern Himalaya to Burma. *Eos Transactions AGU; Fall Meeting Supplement* 87.
- Liu, Y., and Zhong, D. (1997). Petrology of high-pressure granulites from the eastern Himalayan syntaxis. *Journal of Metamorphic Geology* 15, 451-466.
- Reiners, P. W., Ehlers, T. A., Mitchell, S. G., and Montgomery, D. R. (2003). Coupled spatial variations in precipitation and long-term erosion rates across the Washington Cascades. *Nature* 426, 645-647.
- Searle, M. P., and Tirrul, R. (1991). Structural and Thermal Evolution of the Karakoram Crust. *Journal of the Geological Society* 148, 65-82.
- von Blanckenburg, F. (2005). The control mechanisms of erosion and weathering at basin scale from cosmogenic nuclides in river sediment. *Earth and Planetary Science Letters* 237, 462-479.
- Wang, E., and Burchfiel, B. (2000). Late Cenozoic to Holocene deformation in southwestern Sichuan and adjacent Yunnan, China, and its role in formation of the southeastern part of the Tibetan Plateau. *Geological Society of America Bulletin* 112, 413-423.

Zeitler, P. K., Meltzer, A. S., Koons, P. O., Craw, D., Hallet, B., Chamberlain, C. P., Kidd, W. S. F., Park, S. K., Seeber, L., Bishop, M., and Shroder, J. (2001). Erosion, Himalayan geodynamics, and the geomorphology of metamorphism. *GSA Today* January 2001, 4-9.

## **Chapter 2: Spatial controls on erosion in the Three Rivers Region**

### **Introduction**

According to conventional geomorphological views, erosion rates generally increase with the steepness of hillslopes, as measured by mean local relief (Ahnert, 1970) up to a limiting or threshold slope (Roering et al., 1999; Montgomery and Brandon, 2002), or with the capacity of rivers to transport sediment and incise bedrock, as measured by stream power (Whipple and Tucker, 1999; Finlayson et al., 2002; Finnegan et al., 2005). Some workers have proposed that in regions with large gradients in rainfall, climatic variations may lead to larger variations in erosion rates than either changes in hillslope steepness or stream power (Montgomery et al., 2001; Reiners et al., 2003; Anders et al., 2006; 2008), whereas others have stressed that in tectonically active areas, the coupling of tectonic activity with erosion is strong enough to dominate the spatial pattern of erosion rates (Zeitler et al., 2001; Burbank et al., 2003; Finnegan et al., 2008).

Here we explore the spatial pattern of basin-wide erosion rates averaged over millennial timescales in the Three Rivers Region (TRR) (Fig. 1) of western China. We evaluate the relative importance of hillslope steepness, river power, and modern precipitation in accounting for variation in these rates, as well as consider the tectonic context of the study region. Large variations in hillslope and river steepness and climate exist across the Salween, Mekong, and Yangtze River

drainages in the TRR, an area adjacent to the zone of active deformation resulting from ongoing India-Asia collision.

### **Tectonic and geomorphic setting**

Located at the eastern limit of the India-Eurasia collision and southeastern margin of the Tibetan plateau, the TRR is defined by the elongate, roughly parallel drainages of the Salween (Nu Jiang), Mekong (Lancang Jiang), and Yangtze (Jinsha Jiang) Rivers. Elevation decreases gradually across the Tibetan plateau margin, and is characterized by what has been inferred to be a low-relief surface that has been dissected by the three rivers and their tributaries (Royden et al., 1997; Clark and Royden, 2000; Clark et al., 2004; Schoenbohm et al., 2004; Clark et al., 2005a; 2005b; 2006; Schoenbohm et al., 2006a; 2006b). The Salween, Mekong, and Yangtze drainages are shallowly incised into the ~5 km-high surface of the plateau in their upper reaches, becoming more deeply incised downstream as they converge in the narrowest part of the TRR adjacent to the eastern Himalayan syntaxis (Burg et al., 1997; Liu and Zhong, 1997; Hallet and Molnar, 2001; Zeitler et al., 2001). This great orogenic bend at the northeast corner of the indenting Indian plate marks the abrupt transition between the east-west trending thrusts of the Himalaya and right-lateral strike-slip structures accommodating the northward motion of India relative to China (Burg et al., 1997). Crustal strain and thickening associated with ongoing India-Eurasia collision since the early Cenozoic has resulted in bending of structural fabrics, topography, and plate velocity vectors

around the syntaxis (Royden et al., 1997; Hallet and Molnar, 2001; Tapponnier et al., 2001; Zhang et al., 2004; Sol et al., 2007). It has been suggested that the extremely close spacing of the Three Rivers and pronounced distortion of their drainage basins around the northeast corner of the Indian plate reflect the large crustal strains near the syntaxis (Brookfield, 1998; Hallet and Molnar, 2001), others have argued that the modern configuration of drainages in the TRR reflects river incision and river capture events rather than large-magnitude tectonic shear (Clark et al., 2004).

Little is known about rates of erosion or exhumation in the TRR, but they must vary substantially in both space and time to be consistent with the immediately adjacent regions where exhumation rates to the west greatly exceed those to the east of the TRR. Modern erosion and longer term exhumation west of the TRR in the structural core of the syntaxis are extremely rapid, estimated at 7-21 mm/yr on the basis of mixing models of detrital zircon U-Pb ages, zircon fission track ages, and suspended sediment estimates for the Siang River, the main tributary of the Brahmaputra (Stewart et al., 2008). Erosion rates from  $^{10}\text{Be}$  in detrital quartz vary between 1 and 6 mm/yr over timescales of  $10^2$ - $10^3$  years in this area (Finnegan et al., 2008, data repository). Rapid cooling over the last 3 to 10 Ma is indicated by a suite of thermobarometric and geochronologic data (Booth et al., 2009),  $^{40}\text{Ar}/^{39}\text{Ar}$  in hornblende (ca. 8 Ma, Ding et al., 2001) and biotite (0.9-2.5 Ma, Malloy, 2004), fission tracks in zircon and apatite (0.2-0.5 Ma, Burg et al., 1997;

Seward and Burg, 2008), and (U-Th)/He in zircon (0.3-1.0 Ma, Malloy, 2004) point to rapid long-term denudation at up to 10 mm/yr sustained for at least the last 3 to 10 Ma. In contrast, one transect of bedrock zircon and apatite fission track data from the Yangtze (Jinsha) River suggest long-term exhumation rates in the region of 0.38 mm/yr for at least 10 Ma (Ouimet, 2007). East of the TRR, low erosion rates from  $^{10}\text{Be}$  in detrital sediments also were reported in the Yalong and Dadu Rivers (0.14 to 3.5 mm/yr) and lower-relief areas of eastern Tibet (0.01 to 0.02 mm/yr), although rates are in excess of 2 mm/yr near Gongga Shan (Ouimet et al., 2009). In the same area of eastern Tibet, Kirby et al. (2002) and Clark et al. (2005b) inferred long-term exhumation rates of up to 0.25-0.5 mm/yr from  $^{40}\text{Ar}/^{39}\text{Ar}$  data, suggesting that an increase in rock cooling rates after ca. 9 to 13 Ma marked the initiation of regional uplift and river incision (Clark et al., 2005b; Ouimet, 2007). Similarly, work by Enkelmann et al. (2006) near the northeastern margin of the plateau indicates an increase in denudation rates from 0.02 mm/yr to 0.2 mm/yr in the middle Miocene. Although these study areas are separated by many hundreds of kilometers, the general spatial pattern suggests that long-term erosion rates along the plateau margin decrease with distance from the actively deforming syntaxis.

Erosion rates on either side of the TRR have been examined in light of local relief, precipitation, and stream power patterns correlating with erosion rates. Researchers working primarily in eastern and northeastern Tibet have argued that



erosion is tied to mean local relief (Clark et al., 2004; 2005a), proposing that rapid erosion and incision of the plateau margin initiated as crustal thickening related to plateau growth and uplift advanced eastward. West of the TRR in the core of the syntaxis, Finnegan et al. (2008) reported a spatially coincident area of rapid erosion and extremely high stream power and local relief where the Tsangpo river carves one of the deepest gorges on Earth into an actively deforming metamorphic massif, centered on two major mountains, Namche Barwa (7782 m) and Gyala Peri (7294 m). These spatial patterns suggest that active erosion may be closely related to relief, stream power, or local deformation (Finnegan et al., 2008) but not to precipitation, which is more intense at the Himalayan range front (Anders et al., 2006) far south of the zone of most rapid denudation.

Across the eastern margin of the Tibetan Plateau the tectonic setting changes dramatically from the zone of active convergence and rotation at the eastern Himalayan syntaxis (Sol et al., 2007) to eastern Tibet where surface uplift appears to have been achieved without significant shortening along surface structures (e.g., Royden et al., 1997). Here we examine erosion rates in the TRR in order to better understand how topography reflects the interaction of surface and tectonic processes in a region with a steep gradient in exhumation rates in eastern Tibet.

## Samples and methods

### Erosion rates from cosmogenic $^{10}\text{Be}$

In order to quantify the spatial distribution of millennial erosion rates in the TRR, we calculated basin-wide erosion rates from measured cosmogenic  $^{10}\text{Be}$  in modern stream sediments. Beryllium-10 is produced *in situ* when cosmic rays interact with the uppermost layer of Earth's surface, and is carried by detrital sediment after detachment and erosion. The concentration of  $^{10}\text{Be}$  can be used to quantify basin-wide average erosion rates, as originally discussed by Brown et al. (1995), Bierman and Steig (1996), and Granger et al. (1996).

We analyzed *in-situ*-produced  $^{10}\text{Be}$  in 45 samples of detrital quartz from sand collected in catchments of varying size ( $\sim 2 \text{ km}^2$  to  $>300,000 \text{ km}^2$ ) throughout the TRR (Fig. 2, Table 1). Instead of working with samples only from small tributary basins as is commonly done (see reviews by Bierman, 2004; von Blanckenburg, 2005), we collected samples from a wide range of main stem and tributary locations in each of the TRR basins. Twenty-seven samples were taken from main stem reaches of the Salween, Mekong and Yangtze, or from the lower reaches of major tributaries close to their junctions with these rivers. The remaining nineteen samples are from headwater tributaries. All samples were collected from active parts of the flood plain, or from sandbars immediately adjacent to rivers.

Samples were sieved and prepared using standard laboratory methods (Kohl and Nishiizumi, 1992; Bierman, 2004; Stone, 2004). To obtain the most representative sampling of the large catchments investigated, we extracted quartz from the 180-425  $\mu\text{m}$  size fraction of most samples. The lower limit of 180  $\mu\text{m}$  was selected because insufficient amounts of the finer grain size fractions survived the HF etching procedure used to concentrate and purify quartz. The upper limit of 425  $\mu\text{m}$  was selected because many samples had only fine sand. Two headwater catchment samples contained insufficient 180-425  $\mu\text{m}$  quartz for analysis, and thus we analyzed the 425-850  $\mu\text{m}$  fraction. In three additional samples, one from the main stems of each of the Three Rivers, we measured *in-situ*-produced  $^{10}\text{Be}$  in both the 180-425  $\mu\text{m}$  and 425-850  $\mu\text{m}$  fractions to evaluate potential effects of grain size on erosion rate estimates.

Beryllium isotopic measurements were made at PRIME laboratory, Purdue University, and erosion rates averaged over the contributing area upstream of each sample were calculated from the data using the CRONUS online calculator (Balco et al., 2008). Isotopic values reported in Table 2 are referenced to revised values of the KNSTD Be isotope standards (Nishiizumi et al., 2007) and erosion rates are calculated using the corresponding value of  $^{10}\text{Be}$  half-life. The upstream basin information for each sample was calculated for basins defined by the WWF Hydrosheds data (USGS, 2008). The average  $^{10}\text{Be}$  production rate for each basin was calculated using the standard procedure to account for latitude, longitude, and

effective elevation (the elevation which will result in the correct basin-averaged production rate) for each basin (Balco, 2006).

First we calculated erosion rates for the entire upstream area of all samples using the CRONUS Online Calculator. Erosion rates for intermediate reaches were then determined from the differences in erosion rate and contributing area of successive samples (following Vance et al., 2003). Errors reported for the intermediate reaches are the sum of fully propagated independent, internal (and independent) errors and the average external (and dependent) errors of contributing samples.

### **Potential drivers of erosion**

Previous workers have suggested that erosion rates correlate with stream power, mean local relief, or mean annual rainfall. As described in the following sections, we examine spatial patterns of all three across the TRR and compare them to the observed pattern of millennial basin-averaged erosion rates.

### ***Rivers – predicting erosion rate patterns using stream power***

Fluvial erosion rates are widely thought to increase with stream power (e.g., Whipple and Tucker, 1999; Montgomery et al., 2001; Finnegan et al., 2005; Whittaker et al., 2007; Finnegan et al., 2008), especially in regions with threshold or near-threshold hillslopes. Following the methods of Finlayson et al. (2002) and Finnegan et al. (2005), we computed values of stream power along the main stem

and major tributaries of each of the Three Rivers. Stream power per unit area of channel bed (unit stream power,  $\Omega$ ) is defined as:

$$\Omega = \rho g Q S / W, \quad (1)$$

where  $\rho$  is density of water,  $g$  is the acceleration due to gravity,  $Q$  is discharge,  $S$  is channel slope, and  $W$  is channel width. However, since direct width measurements are generally difficult to obtain, it is often assumed that width scales as  $Q^{0.5}$  (e.g., Finlayson et al., 2002), yielding

$$\Omega = k Q^{0.5} S, \quad (2)$$

where  $k$  is an empirically defined constant that scales the relationship between discharge and channel width and includes the density and gravity terms from (1). However, Finnegan et al. (2005) refined the discharge-to-width relationship to take into account the fact that, for any fixed discharge, increased slope decreases channel width in bedrock rivers, proposing:

$$\Omega = k Q^{5/8} S^{19/16} \quad (3)$$

as a more realistic representation for bedrock rivers. Although the  $k$  terms in equations (2) and (3) are similarly defined and include density and gravity terms, they are not identical because the hydraulic geometry relationship between discharge, slope, and channel width is not the same for both equations.

Our calculations employ both equations (2) and (3) and use the Hydrosheds digital elevation model (DEM) (USGS, 2008) derived from the Shuttle Radar Topography Mission (SRTM) data for topography. We used Tropical Rainfall

Measuring Mission (TRMM) satellite data to calculate discharge by routing the mean annual rainfall down river channels defined by SRTM data and ignoring evaporative and other water losses. All values were averaged over a 1-km stretch of river, thus removing some of the DEM artifacts. Following Finlayson et al. (2002), we normalize the stream power values to the maximum value calculated for the TRR (20079700 and 1463720000 using equations (2) and (3), respectively, and where  $Q$  is in  $\text{m}^3/\text{s}$  and slope in  $\text{m}/\text{m}$ ). This assumes that  $k$  is constant across the entire region and additionally removes the need to estimate the fraction of rainfall that becomes discharge, as well as scaling factors associated with hydraulic geometries when using discharge and slope to estimate width. Thus, normalized unit stream powers reported in this paper are expressed as the fraction of maximum stream power in the TRR. Errors in this calculation come from errors in estimating channel slope using SRTM data, from assuming that  $k$  is spatially constant, and from errors in TRMM data and estimating discharge using these data. SRTM elevations used are reported to have an accuracy of  $\pm 16$  m over an approximately 90 m grid (USGS, 2008) suggesting errors in slope across a single pixel of 15%. Our slopes are averaged over 1 km, making these errors even smaller. We have no way to evaluate the errors in assuming  $k$  is constant across the region. Errors in using TRMM data to estimate rainfall are reported to be 15 – 50% (Anders et al., 2006). Errors inherent in assuming that rainfall routed down rivers is discharge will

increase that error estimate, making it likely that the discharge estimate is the largest error in the calculations.

***Hillslopes – predicting erosion rates with mean local relief***

Ahnert (1970) proposed a simple linear function between erosion rates and local relief in mountainous areas:

$$E = 0.2R, \quad (4)$$

where E is erosion in mm/yr and R is local relief in km, averaged over the area for which E was measured. Montgomery and Brandon (2002) observed that in tectonically active areas, the erosion rate increases rapidly for small increases in relief. They proposed that in such areas (i.e., in active orogenic settings characterized by high rates of rock uplift) where hillslopes are steep, erosion rates increase primarily through increased frequency of landslides (Montgomery and Brandon, 2002). Their compilation of relief and erosion-rate data from tectonically active and other regions is well described by a power law:

$$E = 1.4 \times 10^{-6} R^{1.8}, \quad (5)$$

where R is in meters (Montgomery and Brandon, 2002). They further showed that mean local relief is a measure of hillslope steepness, which is less dependent on quality and scale of DEMs but well correlated with measured erosion rates worldwide.

For our analysis, we calculated local relief for a 5 km radius window over SRTM-derived DEMs (USGS, 2008a). The resulting local relief values were then

used to calculate mean local relief for each of the basins for which we measured erosion rates.

### ***Climate – predicting erosion rates from mean annual rainfall***

Recent research into spatial controls on erosion has increasingly focused on the suggestion that if gradients in rainfall are sufficient, they will dominantly influence erosion rate patterns (e.g., Montgomery et al., 2001; Reiners et al., 2003; Anders et al., 2006; 2008). Along these lines, theoretical modeling over the last 10 years generally has assumed that the potential of rivers to erode increases with discharge, and, therefore, that climate and erosion rates are strongly linked over many time scales (e.g., Willett et al., 1993; Tucker and Slingerland, 1994; Whipple et al., 1999; Willett, 1999; Willett et al., 2001). Drawing on this modeling, Anders et al. (2006) suggested evidence for co-evolution of precipitation patterns and topography in the Himalaya. Empirical studies have demonstrated a strong correlation between modern precipitation values and long-term erosion rates in a variety of orogenic settings including the Washington Cascades (Reiners et al., 2003), the Eastern Cordillera of Columbia (Mora et al., 2008), and the Bolivian Andes (Barnes and Pelletier, 2006). However, considerable debate has focused on the extent to which precipitation patterns and erosion may be linked in the Himalaya. Burbank et al. (2003) argued that erosion, exhumation, and rainfall are spatially decoupled based on the lack of variation in bedrock apatite fission track ages across a transect of the Nepal Himalaya with large variations in rainfall. In



contrast, other studies in the same region have concluded that decadal erosion rates and Quaternary deformation measured from offset on faults scale well with modern patterns of rainfall (e.g., Gabet et al., 2004; Hodges et al., 2004; Thiede et al., 2004).

We test the hypothesis that modern rainfall rates correlate well with erosion rates in the TRR. To enable direct comparison of results with previous studies and due to limitations of calculating rainfall values using TRMM data, we used mean annual rainfall for our analysis. We calculated mean annual rainfall patterns throughout the TRR using average annual precipitation for 1 km x 1 km pixels over 2000 – 2006 using the TRMM satellite data and the methods described by Anders et al. (2006). TRMM data are acquired on a schedule such that data are collected over all periods of a day but not all the time, capturing daily variability in rainfall but not the total amount of rainfall. As a result, the mean annual values we report likely underestimate actual rainfall but portray an accurate spatial distribution of rainfall and are likely to have errors of 15 – 50% (Anders et al., 2006).

## **Results**

### **<sup>10</sup>Be erosion rates**

Two trends emerge from the <sup>10</sup>Be erosion rate measurements for the TRR. The first is the expected result that in each of the Three Rivers drainages, erosion rates increase with distance downstream, corresponding to the transition from

gentle river gradients on the relatively dry, low relief Tibetan Plateau to steeper gradients and higher relief and rainfall in the narrow gorges. The second trend – unexpected on the basis of geomorphic features of the landscape – is the two order of magnitude westward decrease in erosion rates from the Salween River gorge ( $8\pm 2$  mm/yr) to the Yangtze River gorge ( $0.0126\pm 0.0014$  mm/yr) over a span of only 100 km in the narrowest part of the TRR (Table 2; Fig. 3).

Basin-averaged erosion rates in the Salween River drainage generally decrease northward from a peak rate of  $8\pm 3$  mm/yr to  $0.024\pm 0.005$  mm/yr, with a mean erosion rate of 0.68 mm/yr. Erosion rates were calculated for eight intermediate reaches in the Salween basin. Errors in erosion rate estimates are relatively high for these intermediate reaches; they average 31%, compared to the 13% average for the basin-wide erosion rates. The highest erosion rate estimate in this drainage is for the narrowest portion of the TRR between  $\sim 25$  and  $27^\circ\text{N}$  (i.e., between 05-3R-13b-SAL and 05-3R-12-SAL).

The Mekong River basin exhibits a smaller range of erosion rates than the Salween; rates range from  $0.017\pm 0.002$  to  $0.5\pm 0.7$  mm/yr with a mean value of 0.21 mm/yr. Erosion rates were calculated for four intermediate reaches in the Mekong River basin. As with the Salween, errors for these intermediate reaches of the Mekong are significantly higher (mean error of 94%) than the errors in basin-wide erosion rate measurements (mean error of 14%) and erosion rates are highest

in the most southern portions of the basin and decrease to the north. The highest erosion rates in the Mekong River basin are in small tributary channels.

Unlike the Salween and Mekong river drainages, the Yangtze drainage generally exhibits uniformly low erosion rates ( $<0.15$  mm/yr) with the exception of one tributary channel north of the narrowest portion of the TRR ( $0.8 \pm 0.19$  mm/yr). In the Yangtze River basin, erosion rates were calculated for 7 intermediate reaches. As with the Salween and Mekong basins, errors for the erosion rate estimates for these reaches are relatively high, averaging 37% compared to 13% for the basin-wide erosion rates.

In order to confirm that limiting the range of grain sizes analyzed does not significantly impact our results; we measured  $^{10}\text{Be}$  in two different grain size fractions (180-850  $\mu\text{m}$  and 180-425  $\mu\text{m}$ ) for three samples. In all three cases the difference in rate estimated for the two size fractions is less than the spread of rate estimates based on duplicate 180-425  $\mu\text{m}$  preparations of sample 06-3R-27-MEK ( $3.8 \pm 0.13 \times 10^5$  vs.  $4.3 \pm 0.13 \times 10^5$  atoms  $^{10}\text{Be}/\text{g}$ ), and corresponds to negligible ( $\pm 0.01$  mm/yr for 05-3R-11b-SAL and 06-3R-26-MEK and  $\pm 0.001$  mm/yr for 05-3R-17-YANG) differences in apparent erosion rate. For consistency with the rest of the data set we refer to the results from the 180-425  $\mu\text{m}$  fractions of these samples in the following discussion and calculations. In the case of the duplicate analyses the same grain size of sample 06-3R-27-MEK, which yielded erosion rates

identical within analytical error, we favor the lower  $^{10}\text{Be}$  concentration because it implies an erosion rate that is compatible with samples upstream.

To confirm that successive samples on the main stem of rivers are representative of the upstream area, we analyzed the trends in cumulative sediment yield measured along each river. The cumulative sediment yield (erosion rate times upstream area) increases within measurement errors downstream along the main stem of each of the three rivers (Fig. 6), suggesting that the samples are indeed representative of the average erosion rate for the region (see Validity of Erosion Rates in the Discussion for a more detailed discussion).

### **Patterns of stream power, local relief, and mean annual precipitation**

Whereas millennial erosion rates are highest near the Eastern Himalayan syntaxis, the highest values of normalized unit stream power, local relief, and mean annual rainfall generally are restricted to the narrowest parts of the TRR drainage (Fig. 4). To highlight overall regional trends in stream power, local relief, and precipitation across the TRR, we present values of these variables over the entire region. Basin averaged values are used for correlation analysis with erosion rates.

Normalized unit stream power (hereafter “stream power”) indices calculated using equations (2) and (3) are highest on the main stems of the Salween, Mekong, and Yangtze Rivers where they flow through the narrowest parts of the TRR (~25-28°N) (Fig. 4a-b). The increase in calculated stream power where the basins narrow and main stem channels steepen is more pronounced using equation (2) than

equation (3), although the general pattern is similar. The main difference is that when normalized unit stream power is calculated using equation (3), which more heavily weights channel slope, the region of high normalized unit stream power is significantly smaller along the Yangtze River than it is when calculated using equation (2). The mean normalized unit stream power along the main stem of the lower reaches of the Salween, Mekong, and Yangtze Rivers shows a decrease of a factor of two to three from the Salween to the Yangtze River (from 0.011 to 0.007 and from 0.009 to 0.003 using equations (2) and (3), respectively), mirroring the decrease in erosion rates across this region.

The overall range of local relief in the TRR is 50 m to 3000 m, with the areas of highest local relief being found along the main stems of the Salween, Mekong, and Yangtze Rivers (Figure 4c), especially along the narrowest sections of the TRR, between 24 and 30°N in the Salween basin, and north of 26°N in the Mekong basin. Local relief in the Yangtze River basin remains high from the southern limit of the Yangtze drainage in the study area from 27°N to 34°N.

The mean annual rainfall in the TRR varies by a factor of five, from less than 250 mm/yr to over 1250 mm/yr (Fig. 4d). Generally, annual precipitation decreases to the north and east of the peak rainfall areas. The southern reaches of the Salween and Mekong Rivers (south of 27°N and 26°N, respectively) receive the highest annual precipitation of any of the main stem channels of the TRR. The northernmost regions of the Yangtze (north of ~33°N) are the driest. Along the

main stem of the Salween, the rainfall increases downstream two-fold from under 500 mm/yr to over 1000 mm/yr in a distance of 500 km. Mean annual rainfall along the Mekong River is more variable and increases from 500 mm/yr in the northern reaches to 1250 mm/yr in the southern reaches.

### **Predictive power of geomorphic parameters**

Here we examine the aspects of the spatial variability in erosion rates that can and cannot be explained with the geomorphologic and climatic parameters used herein. First we analyze patterns for the region as a whole, then for each individual watershed, and finally for the west to east gradient in erosion rates in the lower basins in more detail.

Taking the TRR as a whole, mean annual rainfall, mean local relief, and mean normalized stream power each is weakly correlated with erosion rate ( $r = 0.64, 0.69,$  and  $0.53,$  respectively). A multiple regression of erosion rate as a function of mean local relief and mean annual rainfall has better explanatory power ( $r = 0.75$ ); stream power does not improve the correlation. This analysis suggests that these typical geomorphic parameters across a broad region only weakly explain variability in erosion rates across the TRR.

We analyzed independently the erosion rates for each river. All three rivers have increasing erosion rates with increasing distance downstream. However, there are subtle differences in which parameters best explain the spatial variability in erosion rates for each river. Erosion rates in the Salween River basin are well

correlated with mean local relief ( $r = 0.86$ ). Multiple regressions which include stream power and/or rainfall only marginally improve the correlation ( $r = 0.89$ ), suggesting that mean local relief is the best indicator of erosion rates in the Salween River (Fig. 5a-c). Erosion rates in the Mekong River basin are well correlated with a multiple regression of stream power and relief ( $r = 0.78$ ); adding rainfall to the regression does not improve the correlation (Fig. 5d-f). Finally, in the Yangtze River basin, erosion rates are best correlated with mean annual rainfall ( $r = 0.71$ ). Counterintuitively, Yangtze River basin erosion rates are inversely correlated to stream power ( $r = -0.27$ ) and are only weakly correlated with relief ( $r = 0.42$ ) (Fig. 5g-i), suggesting that there rainfall dominates the spatial pattern of erosion rates. Multiple regressions of erosion rates as a function of these parameters do not improve the correlation.

## **Discussion**

Taken as a whole, erosion rates in the TRR are weakly correlated with mean annual rainfall and mean local relief. Across the region erosion rates increase as the rivers leave the dry, flat Tibetan Plateau and enter the steep, wetter gorges in the lower basins. However, the correlation between erosion rates and geomorphic and climatic parameters varies from basin to basin. Erosion rates correlate best with relief in the Salween River, stream power in the Mekong River, and rainfall in the Yangtze River. Yet, despite these correlations, the strongest gradient in the region

is a two order of magnitude decrease in erosion rates west to east across the lower basins, an area with a two-fold decrease in stream power along the main stem of each river but little variability in rainfall or local relief. Below we explore assumptions that go into erosion rate estimates, possible geomorphic mechanisms that may be responsible for this gradient in erosion rates, implications for regional uplift patterns, and implications for geomorphic controls on erosion rates.

### **Validity of erosion rates**

In order to attribute patterns of erosion rates to geomorphologic, climatic, or tectonic drivers with confidence, we must evaluate the validity of assumptions required to calculate basin averaged erosion rates from  $^{10}\text{Be}$  in detrital sediments. Calculating basin-averaged erosion rates from *in-situ*-produced  $^{10}\text{Be}$  concentrations depends on a suite of assumptions (Brown et al., 1995; Bierman and Steig, 1996; Granger et al., 1996): erosion has been steady over time, sediment storage in the basin is minimal, quartz is contributed in proportion to erosion rate, and samples are well mixed. Below we evaluate these assumptions for our data and infer that the erosion rates reported above are valid for the TRR.

The assumption that erosion has been steady over the time in which the last few meters were eroded from basin surfaces ensures that the removal rate of  $^{10}\text{Be}$  by erosion balances the production rate of  $^{10}\text{Be}$  in the underlying surface. This is likely to be true for the more rapidly eroding basins (i.e., with rates  $\geq 0.1$  mm/yr), where erosion rates are averaged over a  $10^3$ - $10^4$ -year timescale for  $^{10}\text{Be}$  build-up. In



the smallest basins (i.e.,  $\leq 25 \text{ km}^2$ ), sediment production by intermittent landsliding may be a source of imbalance between  $^{10}\text{Be}$  removal and production, and is likely to bias erosion estimates from small catchments towards high values (Niemi et al., 2005). However, it is unlikely to be a significant factor in our high erosion rate estimates ( $>0.1 \text{ mm/yr}$ ) for the main stems of the Salween and Mekong, for which most sampled drainage areas were large ( $10^4 - 10^5 \text{ km}^2$ ).

It is necessary for sediment transit from source to sampling point to be rapid and storage minimal to ensure that  $^{10}\text{Be}$  measured in sediments represent the erosion rate from the hillslope rather than storage in the basin. This assumption is likely to be met in the mountainous terrain of the TRR, especially in the main stem gorges of the Three Rivers where stream power is high, slopes are steep, and sediment storage is minimal.

For samples to represent the average erosion rate of the entire upstream area, all surfaces in the basins must shed quartz in proportion to their erosion rates. This assumption, which amounts to the requirement that quartz be uniformly distributed in all bedrock throughout the region, is unlikely to be met, but is difficult to evaluate. Generalized, large-scale geologic maps exist for the region (the best digital map is the Global GIS Database (USGS, 2001)), but are not diagnostic of quartz content. Quartz yields from the sediment samples ranged from 5 – 54% (more typically  $\sim 10\text{-}35\%$ ; see data repository table 1 for complete results), likely reflecting variable source rock types. Because  $^{10}\text{Be}$  concentrations are only

measured in quartz, our results disproportionately reflect erosion rates of quartz-rich rock types.

Our final assumption is that the samples are well-mixed averages of the quartz supplied to the rivers throughout the basins upstream. To maximize the chance of obtaining well-mixed samples from the large basins studied, we used the finest-grained sediment fraction practicable (180-425  $\mu\text{m}$ ). For samples collected in a sequence progressing downstream in a drainage network, this assumption was tested directly and shown to be reasonable by confirming that the cumulative sediment yield inferred from the calculated erosion-rate (the product of erosion rate obtained from the  $^{10}\text{Be}$  content of each sample and drainage area) increases downstream (Fig. 6).

Although we cannot evaluate the validity of the assumption quartz is distributed similarly throughout the basins, we see no reason why an uneven distribution of quartz in the watersheds could account for the observed systematic spatial variation in erosion rates by two orders of magnitude across this region. Therefore, we conclude that our reported erosion rates are valid for the TRR.

### **Spatial patterns of erosion**

The two order of magnitude decrease in erosion rates across a region with only a two to three-fold decrease in stream power and little change in relief or rainfall suggests that standard geomorphic and climatic parameters alone cannot explain the observed erosion rates in the lower TRR. This sharp decrease in erosion

rates is in a region of increasing distance from the India-Asia collision, and we hypothesize that the decrease in erosion rates is related to a decrease in tectonic activity across this region. Below we analyze mean elevation, mean local relief, and longitudinal profiles in the context of measured erosion rates to ascertain gradients in rock uplift across the region.

As expected for reaches with higher stream power, the Mekong and Salween Rivers have steeper gradients in the lower basins than the Yangtze River (Fig. 7). This steeper gradient and commensurately higher stream power suggest that the Salween and Mekong Rivers have more potential to incise their beds, and thus erode faster, than the Yangtze River. The same pattern is seen in the erosion rate data – the Salween River is eroding much faster than the Yangtze River. If these erosion rates were to persist for millions of years in the absence of a gradient in rock uplift, the Salween would relatively quickly be eroded to being less steep than the Yangtze and would have a correspondingly lower stream power.

Similarly, below the knick points, the basins have approximately the same mean elevation. If the Salween River maintains an erosion rate 200 times higher than the Yangtze River, then in the absence of a gradient in rock uplift, the mean elevation of the Salween would be lowering with respect to the Yangtze basin. Finally, each of the rivers has approximately the same mean local relief. In the absence of a gradient in rock uplift, the local relief in the Salween basin would be decreasing with respect to that in the Yangtze. Thus, in order to maintain the

present topography and measured erosion rates, there is likely a gradient in rock uplift across the TRR.

Over shorter timescales (i.e., the timescale of  $^{10}\text{Be}$  erosion rates), two possible geomorphic mechanisms have been proposed through which gradients in tectonic activity (such as rock uplift) may affect erosion rates by changing the efficiency of the river to incise. The first possibility is that proximity to the deformation front of the India-Asia collision resulted in increased erodibility of rocks in the Salween and Mekong Rivers relative to the Yangtze River. Molnar et al. (2007) suggest that tectonic activity could affect erosion rates through increased bedrock fracturing, thereby decreasing the resistance of the bedrock to erosion. As the relationship between fracturing rate and the size of fractures is potentially highly non-linear, a large increase in erosion rate may result from a modest change in the fracture size or density of the bedrock even if the unit stream power was spatially uniform.

A second possibility is that in response to proximity to the India-Asia collision, the quantity of sediment stored on and protecting the bedrock bed of the rivers changes from the Salween to the Yangtze River. Fluvial incision depends on the amount of sediment available to work as tools (and increase erosion) or armor the bed (and decrease erosion), and a river may respond to changing tectonic conditions through adjustments in the quantity of sediment on the river bed (Sklar and Dietrich, 2001). In the case of the TRR, the Salween River's higher erosion

rate means that there is a higher flux of sediment through the Salween River than the Yangtze River. The Salween River also has a higher stream power. The combination provides the Salween with more tools and more power with which to move them, thus enabling it to sustain a higher erosion rate than the Yangtze River.

We find a strong spatial gradient in erosion rates and controls on erosion rates across an inferred gradient in rock uplift. Although all three rivers have the same pattern of increasing erosion rates as they flow off the Tibetan Plateau, the geomorphic and climatic parameters which correlate best with erosion rate transition from relief in the Salween River to rainfall in the Yangtze River. Simultaneously, the two order of magnitude decrease in erosion rates from west to east in the lower basins across a region with no gradient in rainfall or relief and only a two to three-fold decrease in stream power demonstrates the influence of a tectonic gradient.

### **Implications for general erosion controls**

The spatial transition in the role of geomorphic parameters in setting patterns of erosion rates in the TRR suggests that in regions with strong gradients in tectonic activity, topographic and climatic information can prove insufficient for predicting spatial patterns of erosion rates. In this region, simply using relief or rainfall to predict intra-regional patterns in erosion would correctly predict that erosion rates increase as the rivers leave the Tibetan Plateau and enter the lower basins. However, this analysis would break down for the lower basins. In the lower

basins, all three rivers have mean local relief between 1200 and 1700 m, mean annual rainfall between 500 and 800 mm/yr, and mean normalized stream power between 0.002 and 0.005. This range of geomorphic and climatic parameters does not forecast the nearly three order of magnitude decrease in erosion rates across this region. Instead, a gradient in rock uplift is needed to explain the striking decrease in erosion rates from the Salween to Yangtze Rivers.

This changing control on erosion rates across a gradient in tectonic activity offers potential insights to reconcile diverse studies of basin-wide erosion rates. Many of the numerous recent studies of controls on basin-wide erosion rates either invoke rainfall or some combination of river and hillslope steepness, relief, and tectonics to explain patterns of erosion rates. Many of the studies which suggest that rainfall is the best predictor for basin-averaged erosion rates are in regions with relatively low rates of rock uplift, such as Australia (Bierman and Caffee, 2002; Tomkins et al., 2007), the Cascades (Reiners et al., 2003), the Alps (Wittmann et al., 2007; Champagnac et al., 2009; Demoulin et al., 2009), the Eastern Cordillera of Columbia (Mora et al., 2008), and the Sierra Nevada (Dixon et al., 2009). In contrast, studies which suggest that relief or hillslope steepness is the major predictor for erosion rate patterns are primarily based in tectonically active areas such as the San Bernardino Mountains (Binnie et al., 2007), the Himalaya (Vance et al., 2003), northeastern Tibet (Harkins et al., 2007), and the Andes (Safran et al., 2005; Aalto et al., 2006; Barnes and Pelletier, 2006). Following Montgomery and

Brandon (2002), other studies in tectonically active areas such as the Flinders Range (Quigley et al., 2007), the Apennines (Cyr and Granger, 2008), the Himalaya (Burbank et al., 2003; Finnegan et al., 2008), the Kun Lun Shan (Lal et al., 2004), Sichuan (Ouimet et al., 2009), and northwestern Tibet (Kong et al., 2007) note a limit to hillslope steepness and mean local relief and therefore independence between relief and erosion rates above a critical value. This independence is inferred to be a signature of strong tectonic control on erosion rates.

Based on our data from the TRR, we propose that these diverse studies may be explained by varying control of geomorphic and climatic parameters in different tectonic settings. Our Salween River data suggest that when rock uplift is high, erosion rates correlate best with mean local relief until they reach threshold steepness and erosion rates are decoupled from hillslope steepness and local relief. However, in regions with little to no active rock uplift, erosion rates will broadly correlate with rainfall, as we see in the Yangtze River basin. This model, in which the primary driver of erosion shifts from tectonics and mean local relief to rainfall as the landscape transitions from being tectonically active to relatively inactive, may help reconcile a number of results from these studies.

However, some areas do not follow this conceptual model. For example, in arid, tectonically active regions with extreme gradients in rainfall, some researchers have found a correlation between rainfall and erosion rate (i.e., Jayko, 2005; Kober et al.,

2007), likely due to the large gradient in rainfall overwhelming modest gradients in rock uplift. Additionally, in tectonically inactive areas such as passive margins and escarpments, other researchers have found no correlation between erosion rate and rainfall (i.e., Bierman and Caffee, 2001; Riebe et al., 2001; Matmon et al., 2003a; 2003b; von Blanckenburg et al., 2004; Vanacker et al., 2007). However, these studies come from regions where erosion rates are controlled by a propagating base level fall, such as is typical along old escarpments. Hence, the regional tectonic-climatic context is the most important factor in determining which geomorphic parameters will correlate best with erosion rates.

## **Conclusion**

Two strong spatial gradients are evident in the  $^{10}\text{Be}$ -derived erosion rates in the TRR. First, as the rivers leave the Tibetan Plateau and enter the steep, wet gorges in the lower basins, erosion rates predictably increase. Second, a steep transverse gradient in erosion rates exists across the TRR in the lower basins of each of the rivers where erosion rates are high. Here erosion rates decrease eastward by two orders of magnitude from the Salween to the Yangtze Rivers. We hypothesize that a west-to-east decrease in tectonic activity is responsible for the large decrease in erosion rates over a region with little variability in standard climatic or geomorphic parameters. Over longer timescales, we infer a gradient in rock uplift which approximately balances the gradient in erosion rates across the



region. On the shorter timescales represented by the  $^{10}\text{Be}$  erosion rates, we propose that either changing tools available for incision and/or density of rock fracturing may provide a geomorphic mechanism by which the river can respond to the gradient in tectonic activity. The shift in parameters which best correlate with erosion rates in each of the rivers suggests that tectonic setting is at least as important as climatic and geomorphic parameters in predicting spatial patterns of erosion rates.

**Acknowledgements**

This chapter was submitted for publication with Katharine W. Huntington, John O. Stone, David R. Montgomery, and Bernard Hallet as coauthors. We thank Greg Balco for help with analysis, many useful discussions during this project, and a helpful review of the paper, Joy Laydbak for help in lab, Patsy Garcia and John Weller for field work assistance, and Harvey Greenberg for GIS help. This material is based upon work supported by the National Science Foundation under Grant No. EAR003561, the University of Washington Quaternary Research Center and Department of Earth and Space Sciences, the Geological Society of America Fahnestock Award, the Geological Society of America Mackin Award, and the UW Graduate School Top Scholar Award. Henck was supported by NSF-IGERT Grant No. 0333408 and an NSF Graduate Research Fellowship.

## Figures for chapter 2

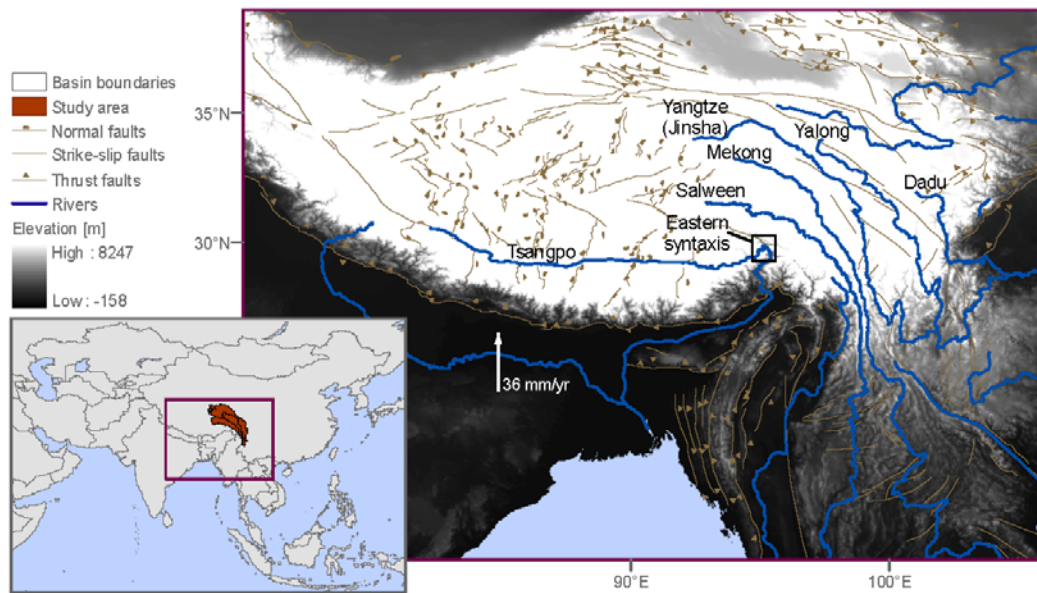


**Figure 2.1: Context map of the study region showing major structures, topography, and major rivers. Fault data are from Taylor and Yin (2009).**

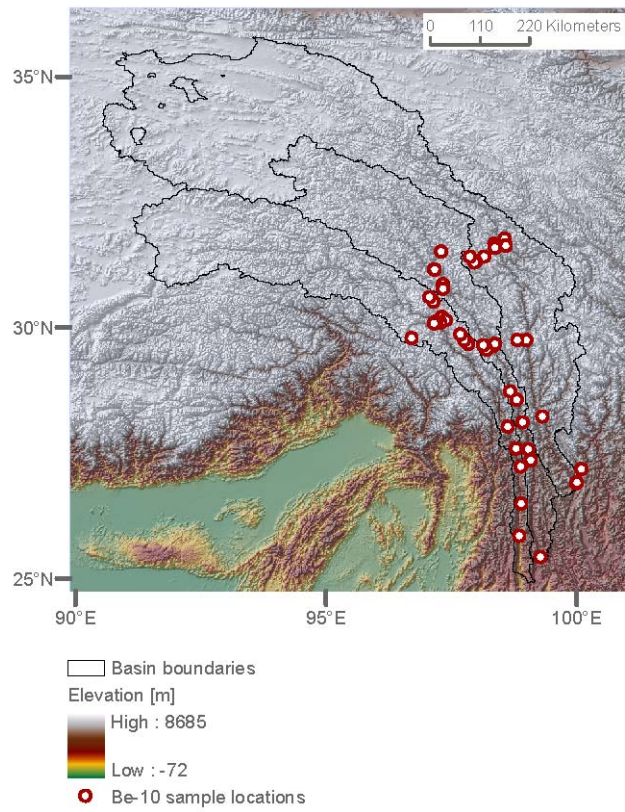


**Figure 2.2: Location of samples and topography for the TRR.**

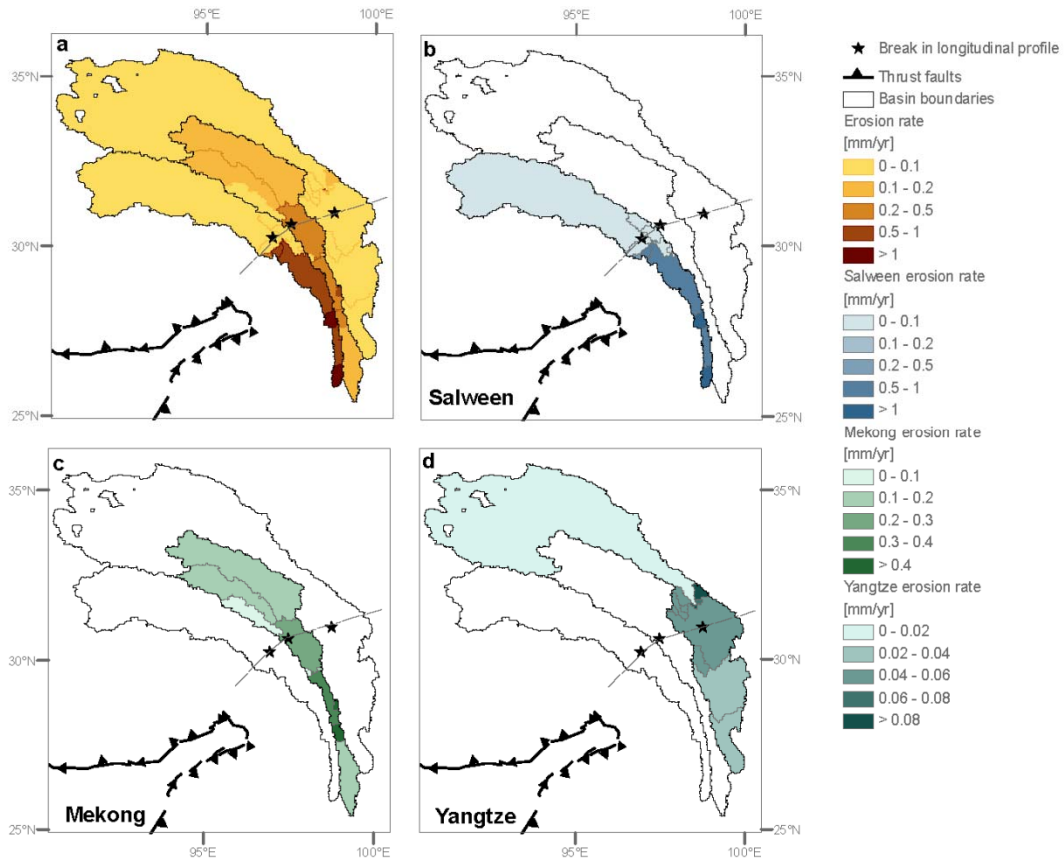


**Figure 2.3: Erosion rates measured for the TRR are shown for the region as a whole and for each individual basin. Break in longitudinal profile where the slope of each river increases, corresponding with the river leaving the Tibetan Plateau, is marked with a line which divides each basin into the upper and lower basins. For each watershed there is a trend in increasing erosion rate as the rivers move from the relatively flat Tibetan Plateau into the deeply dissected gorges of the TRR. There is also an across-basin trend in the lower basins where erosion rate decreases sharply from the Salween to Yangtze Rivers.**

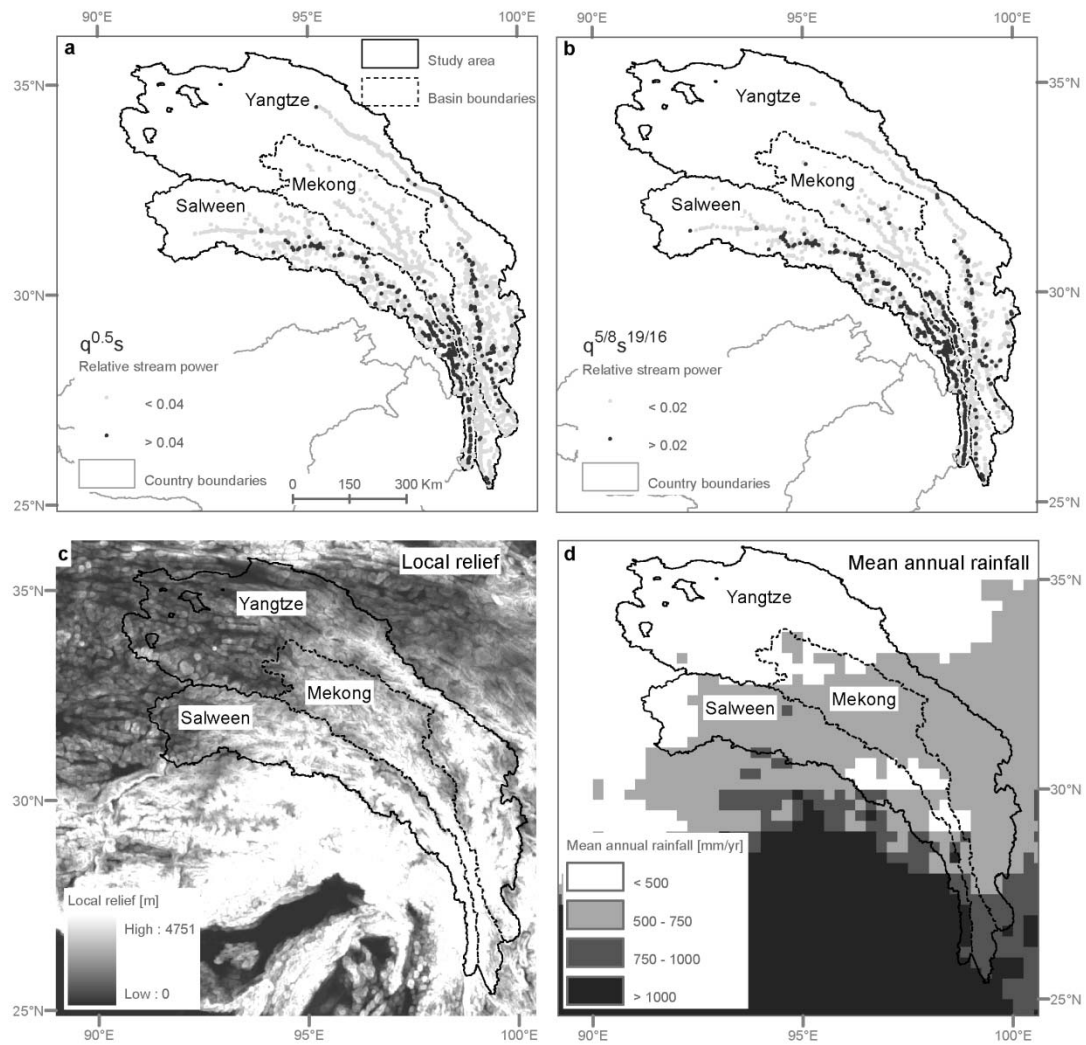


**Figure 2.4: Geomorphic parameters for the region. (a-b) Stream power calculated using equations (2) and (3), respectively. Black dots show the points in the 75<sup>th</sup> percentile of relative stream power values. Note the higher stream power values in the lower basins. (c) Mean local relief throughout the region. (d) Mean annual rainfall for the region.**

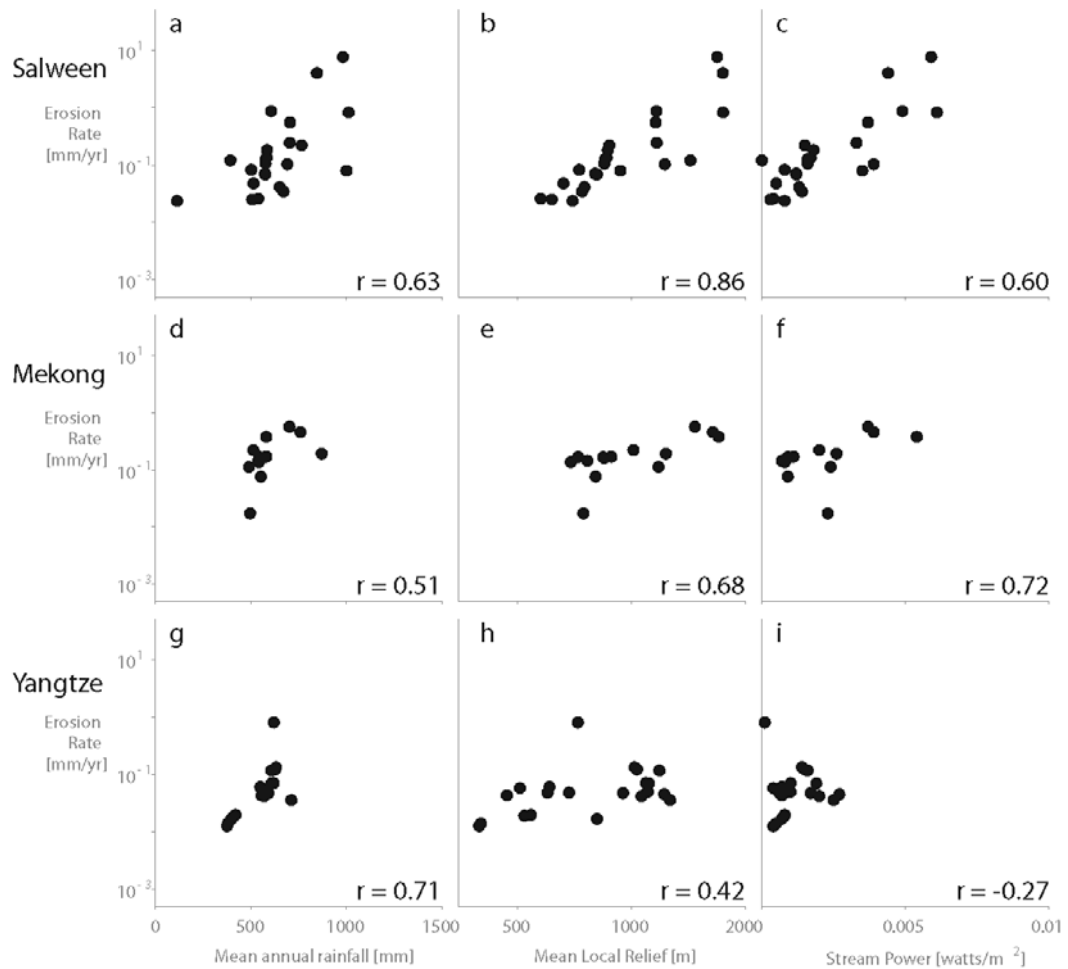


**Figure 2.5: Relationship between erosion and geomorphic parameters for each basin taken separately. Salween River is shown across top row (a-c), Mekong River in the middle (d-f), and Yangtze River on the bottom (g-i). The left column shows erosion rate as a function of rainfall (a, d, g), the middle column shows erosion rate as a function of relief (b, e, h), and the right column shows erosion rate as a function of stream power (calculated using equation (3)) (c, f, i). When the region is examined as a whole (i.e., all the basins are considered together) correlations are weaker ( $r = 0.69$ ,  $0.64$ , and  $0.53$  for rainfall, relief, and stream power, respectively). Using equation (2) instead of equation (3) does not change correlations.**

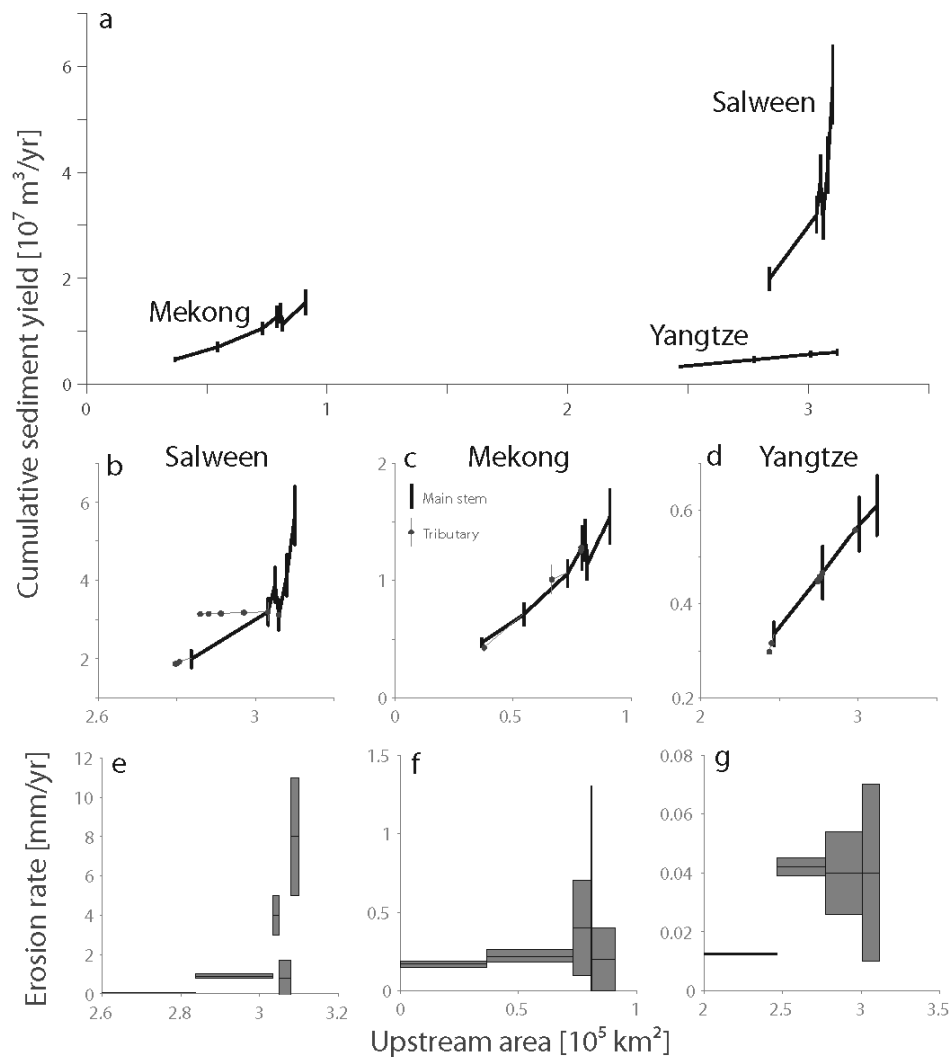


**Figure 2.6: Basin area vs. cumulative sediment yield for each river. This analysis shows that the sample results agree with one another within measurement errors and shows the relative differences between each of the rivers. The slope of the line connecting basin area vs. cumulative sediment yield data is the erosion rate. As the trends for each of the three rivers must intersect the origin (i.e., 0 sediment yield for 0 contributing area), the plots clearly show the increase in erosion rate as the rivers leave the Tibetan Plateau and flow into the incised gorges. (b-d) Details of basin area vs. cumulative sediment yield for each river with erosion rates for intermediate reaches along main stem rivers shown in (e-g).**



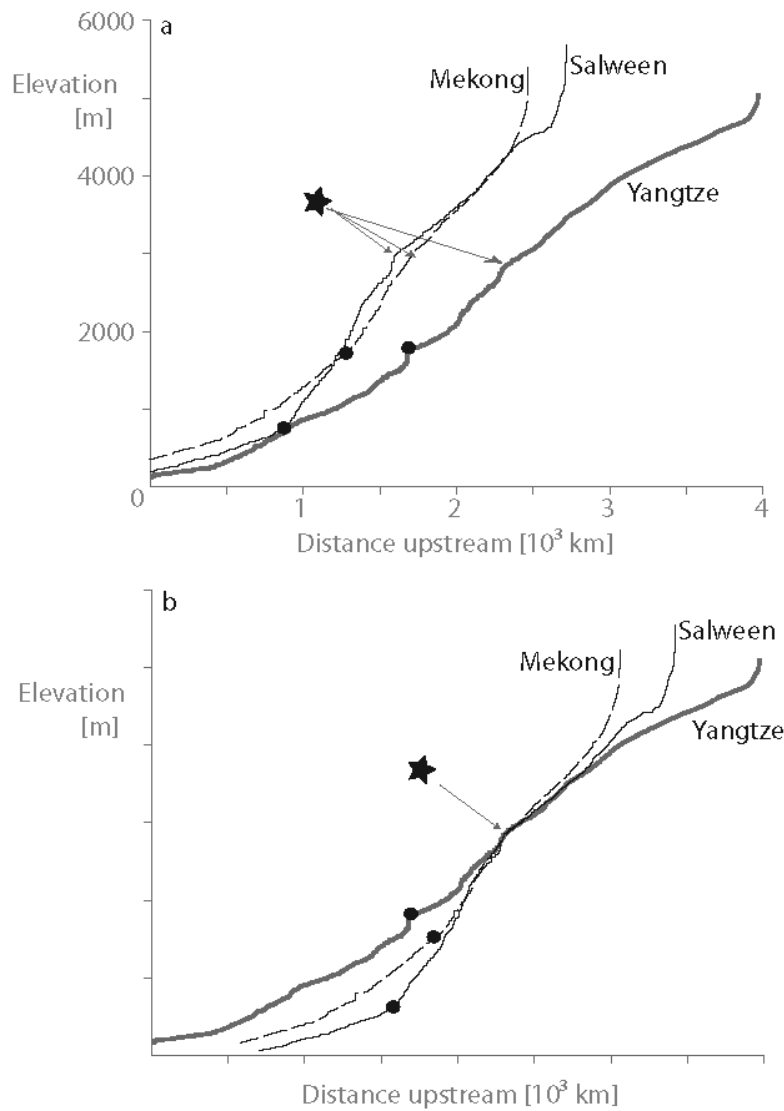


**Figure 2.7: Longitudinal profiles for main stem of each river. Star marks the break in longitudinal profile noted in figure 3 and small black circles mark the edge of the study area for each river. (a) Longitudinal profiles with actual elevations and distance downstream. (b) Longitudinal profiles lined up so that the break in the profile is at the same location on each river. The scale is the same but distance upstream and elevations are not accurate because the profiles have been moved. Note that below the break in the longitudinal profile, the Salween and Mekong Rivers have almost indistinguishable profiles and the Yangtze River has a less steep slope.**

## Tables for chapter 2

**Table 2.1: Details on location and sequence of samples used in analysis.**

Sample name	Details on collection location				Upstream area [km <sup>2</sup> ]
	Latitude	Longitude	River description	Samples upstream	
06-3R-52-SAL	29.78	96.71	Trib to Salween trib.	None	363
06-3R-50-SAL	30.04	97.15	Trib to Salween trib.	None	869
06-3R-49-SAL	30.11	97.19	Trib to Salween	06-3R-52-SAL, 06-3R-50-SAL	3108
06-3R-48-SAL	30.10	97.21	Salween	06-3R-49-SAL	283749
06-3R-46-SAL	30.10	97.30	Trib to Salween trib.	None	57
06-3R-30-SAL	30.60	97.07	Trib to Salween trib.	None	2136
06-3R-32-SAL	30.20	97.32	Trib to Salween trib.	06-3R-30-SAL	3280
06-3R-33-SAL	29.85	97.69	Trib to Salween trib.	None	251
06-3R-34-SAL	29.74	97.76	Trib to Salween trib.	06-3R-32-SAL, 06-3R-33-SAL	5787
06-3R-35-SAL	29.68	97.83	Trib to Salween trib.	None	131
05-3R-9-SAL	28.02	98.63	Salween	06-3R-34-SAL, 06-3R-35, SAL, 06-3R-46-SAL, 06-3R-48-SAL	303138
05-3R-10-SAL	27.58	98.79	Salween	05-3R-9-SAL	305003
05-3R-11a-SAL	27.23	98.89	Trib to Salween	None	2
05-3R-12-SAL	26.48	98.90	Salween	05-3R-10-SAL, 06-3R-11a-SAL	307894
05-3R-13b-SAL	25.85	98.86	Salween	06-3R-12-SAL	310028
06-3R-26-MEK	31.15	97.16	West branch of Mekong at Chamdo	None	16875
06-3R-27-MEK	31.15	97.18	East branch of Mekong at Chamdo	None	36710

Table 2.1 continued

06-3R-29-MEK	30.77	97.34	Trib to Mekong	None	6733
06-3R-38-MEK	29.62	98.35	Mekong	06-3R-26-MEK, 06-3R-27-MEK, 06-3R-29-MEK	73147
06-3R-39-MEK	29.66	98.37	Trib to Mekong	None	167
06-3R-43-MEK	29.55	98.21	Trib to Mekong	None	328
05-3R-4-MEK	28.56	98.81	Trib to Mekong	None	465
05-3R-6-MEK	28.10	98.92	Mekong	06-3R-38-MEK, 06-3R-39-MEK, 06-3R-43-MEK, 06-3R-4-MEK	77316
05-3R-7-MEK	27.57	99.04	Mekong	06-3R-6-MEK	80648
05-3R-14a-MEK	25.43	99.29	Mekong	06-3R-7-MEK	91031
06-3R-15-YANG	31.76	98.56	Trib to Yangtze	None	1376
06-3R-16-YANG	31.64	98.59	Trib to Yangtze	06-3R-15-YANG	1642
06-3R-17-YANG	31.63	98.59	Yangtze	06-3R-16-YANG	245160
06-3R-21-YANG	31.40	98.16	Trib to Yangtze trib.	None	1450
06-3R-20-YANG	31.59	98.37	Trib to Yangtze trib.	06-3R-21-YANG	1911
06-3R-19b-YANG	31.65	98.37	Trib to Yangtze trib.	None	1552
06-3R-19a-YANG	31.65	98.37	Trib to Yangtze trib.	06-3R-19a-YANG	1596
06-3R-18-YANG	31.62	98.60	Trib to Yangtze trib.	None	157
06-3R-22-YANG	31.30	98.00	Trib to Yangtze trib.	None	368
06-3R-24-YANG	31.40	97.88	Trib to Yangtze trib.	None	131

Table 2.1 continued

06-3R-41-YANG	29.76	99.00	Yangtze	06-3R-17-YANG, 06-3R-20-YANG, 06-3R-19a-YANG, 06-3R-18-YANG, 06-3R-22-YANG, 06-3R-24-YANG	277472
06-3R-42-YANG	29.76	99.01	Trib to Yangtze	None	617
05-3R-3-YANG	28.22	99.32	Yangtze	06-3R-41-YANG, 06-3R-42-YANG	300774
05-3R-1b-YANG	26.87	99.97	Yangtze	05-3R-3-YANG	310726

**Table 2.2: Concentrations of  $^{10}\text{Be}$  and derived erosion rates for entire upstream basins (a) and intermediate reaches between samples (b).**

Table 2.2a

Sample name	N	Error in N	Erosion Rate [mm/yr]	Error [mm/yr] 95% confidence
	[atoms/g]	atoms/g		
06-3R-52-SAL	277111	14909	0.22	0.03
06-3R-50-SAL	105850	5784	0.55	0.08
06-3R-49-SAL	231103	10285	0.24	0.03
06-3R-48-SAL	784949	20449	0.070	0.008
06-3R-46-SAL	367464	15764	0.12	0.016
06-3R-30-SAL	2078252	62058	0.026	0.003
06-3R-32-SAL	2120444	58616	0.025	0.003
06-3R-33-SAL	1553608	50391	0.034	0.004
06-3R-34-SAL	1092820	26768	0.048	0.005
06-3R-35-SAL	1237683	50806	0.041	0.006
05-3R-9-SAL	518500	12296	0.11	0.011
05-3R-10-SAL	427659	11859	0.13	0.015
05-3R-11a-SAL	161438	7129	0.08	0.010
05-3R-12-SAL	402267	15524	0.13	0.017
05-3R-13b-SAL	294362	12158	0.18	0.02
06-3R-26-MEK	317841	9684	0.18	0.02
06-3R-27-MEK	432965	12691	0.12	0.014
06-3R-29-MEK	678376	26294	0.08	0.010
06-3R-38-MEK	352113	10049	0.14	0.017
06-3R-39-MEK	344713	14531	0.11	0.015
06-3R-43-MEK	2768030	67592	0.017	0.002
05-3R-4-MEK	70117	5195	0.57	0.10
05-3R-6-MEK	308766	17071	0.16	0.02
05-3R-7-MEK	295439	12621	0.17	0.02
05-3R-14a-MEK	261412	14464	0.17	0.03
06-3R-15-YANG	360619	11421	0.13	0.016
06-3R-16-YANG	384297	13299	0.12	0.015
06-3R-17-YANG	4063015	59101	0.014	0.001
06-3R-21-YANG	949300	36916	0.048	0.006

Table 2.2a continued

06-3R-20-YANG	948113	30610	0.048	0.006
06-3R-19b-YANG	924199	20444	0.049	0.005
06-3R-19a-YANG	651735	29344	0.07	0.010
06-3R-18-YANG	360839	26401	0.12	0.021
06-3R-22-YANG	782810	33147	0.058	0.008
06-3R-24-YANG	881427	39199	0.060	0.008
06-3R-41-YANG	3262761	97513	0.017	0.002
06-3R-42-YANG	984334	38432	0.043	0.006
05-3R-3-YANG	2814015	45255	0.019	0.002
05-3R-1b-YANG	2661264	52493	0.020	0.002

Table 2.2b

Sample name	Area [sq. km]	Erosion Rate [mm/yr]	Error [mm/yr] 95% confidence
06-3R-49-SAL	1876	0.10	0.03
06-3R-48-SAL	280641	0.068	0.01
06-3R-32-SAL	1144	0.024	0.00
06-3R-34-SAL	2255	0.082	0.01
05-3R-9-SAL	13563	0.9	0.14
05-3R-10-SAL	1716	4	1.12
05-3R-12-SAL	3038	0.8	0.80
05-3R-13b-SAL	1985	8	2.13
06-3R-38-MEK	12830	0.22	0.03
05-3R-6-MEK	5067	0.4	0.40
05-3R-7-MEK	1474	0.5	0.66
05-3R-14a-MEK	10383	0.2	0.12
06-3R-16-YANG	266	0.07	0.04
06-3R-17-YANG	244894	0.0126	0.001
06-3R-20-YANG	461	0.047	0.01
06-3R-19a-YANG	45	0.8	0.19
06-3R-41-YANG	26774	0.042	0.01
05-3R-3-YANG	20546	0.04	0.01
05-3R-1b-YANG	11056	0.04	0.02

**Table 2.3: Details on data collection and preparation**

Sample name	Details on collection location				Upstream Area [km <sup>2</sup> ]	starting grain size fraction [microns]	Quartz yield
	Latitude	Longitude	River description	immediate upstream samples			
06-3R-52-SAL	29.78	96.71	Trib to Salween trib.	None	363	180-425	0.11
06-3R-53-SAL	29.78	96.71	Trib to Salween trib.	06-3R-52-SAL	661	180-425	0.54
06-3R-50-SAL	30.04	97.15	Trib to Salween trib.	None	869	180-425	0.17
06-3R-49-SAL	30.11	97.19	Trib to Salween	06-3R-53-SAL, 06-3R-50-SAL	3108	180-425	0.09
06-3R-48-SAL	30.10	97.21	Salween	06-3R-49-SAL	283749	180-425	0.10
06-3R-46-SAL	30.10	97.30	Trib to Salween trib.	None	57	180-425	0.05
06-3R-30-SAL	30.60	97.07	Trib to Salween trib.	None	2136	180-425	0.13
06-3R-32-SAL	30.20	97.32	Trib to Salween trib.	06-3R-30-SAL	3280	180-425	0.09
06-3R-33-SAL	29.85	97.69	Trib to Salween trib.	None	251	180-425	0.12
06-3R-34-SAL	29.74	97.76	Trib to Salween trib.	06-3R-32-SAL, 06-3R-33-SAL	5787	180-425	0.32
06-3R-35-SAL	29.68	97.83	Trib to Salween trib.	None	131	180-425	0.16
06-3R-36-SAL	29.67	97.85	Trib to Salween trib.	06-3R-34-SAL, 06-3R-35-SAL	6119	180-425	0.15
05-3R-9-SAL	28.02	98.63	Salween	06-3R-36-SAL, 06-3R-46-SAL, 06-3R-48-SAL	303287	180-425	0.22
05-3R-10-SAL	27.58	98.79	Salween	05-3R-9-SAL	305003	180-425	0.21
05-3R-11a-SAL	27.23	98.89	Trib to Salween	None	2	425-850	0.27

Table 2.3 continued

05-3R-11b-SAL	27.23	98.89	Salween	05-3R-10-SAL, 06-3R-11a-SAL	305964	180-425	0.07
05-3R-11b-SAL	27.23	98.89	Salween	05-3R-10-SAL, 06-3R-11a-SAL	305964	180-850	0.18
05-3R-12-SAL	26.48	98.90	Salween	06-3R-11b-SAL	308044	180-425	0.24
05-3R-13b-SAL	25.85	98.86	Salween	06-3R-12-SAL	310028	180-425	0.11
06-3R-26-MEK	31.15	97.16	West branch of Mekong at Chamdo	None	16875	180-425	0.41
06-3R-26-MEK	31.15	97.16	West branch of Mekong at Chamdo	None	16875	180-850	0.32
06-3R-27-MEK	31.15	97.18	East branch of Mekong at Chamdo	None	36710	180-425	0.32
06-3R-27-MEK	31.15	97.18	East branch of Mekong at Chamdo	None	36710	180-425	0.33
06-3R-28-MEK	30.85	97.34	Mekong	06-3R-26-MEK, 06-3R-27-MEK	54625	180-425	0.29
06-3R-29-MEK	30.77	97.34	Trib to Mekong	None	6733	180-425	0.24
06-3R-38-MEK	29.62	98.35	Mekong	06-3R-28-MEK, 06-3R-29-MEK	73147	180-425	0.24
06-3R-39-MEK	29.66	98.37	Trib to Mekong	None	167	180-425	0.35
06-3R-43-MEK	29.55	98.21	Trib to Mekong	None	346	425-850	0.31
05-3R-4-MEK	28.56	98.81	Trib to Mekong	None	465	180-425	0.30



Table 2.3 continued

05-3R-6-MEK	28.10	98.92	Mekong	06-3R-38-MEK, 06-3R-39-MEK, 06-3R-43-MEK, 06-3R-4-MEK	79193	180-425	0.23
05-3R-7-MEK	27.57	99.04	Mekong	06-3R-7-MEK	80667	180-425	0.13
05-3R-8-MEK	27.35	99.09	Mekong	06-3R-8-MEK	81317	180-425	0.23
05-3R-14a-MEK	25.43	99.29	Mekong	06-3R-14a-MEK	91049	180-425	0.13
06-3R-15-YANG	31.76	98.56	Trib to Yangtze	None	1376	180-425	0.06
06-3R-16-YANG	31.64	98.59	Trib to Yangtze	06-3R-15-YANG	1642	180-425	0.18
06-3R-17-YANG	31.63	98.59	Yangtze	06-3R-16-YANG	246535	180-425	0.34
06-3R-17-YANG	31.63	98.59	Yangtze	06-3R-16-YANG	246535	180-850	0.28
06-3R-21-YANG	31.40	98.16	Trib to Yangtze trib.	None	1450	180-425	0.17
06-3R-20-YANG	31.59	98.37	Trib to Yangtze trib.	06-3R-21-YANG	1911	180-425	0.11
06-3R-19b-YANG	31.65	98.37	Trib to Yangtze trib.	None	1552	180-425	0.10
06-3R-19a-YANG	31.65	98.37	Trib to Yangtze trib.	06-3R-19a-YANG	1596	180-425	0.24
06-3R-18-YANG	31.62	98.60	Trib to Yangtze trib.	None	157	180-425	0.10

Table 2.3 continued

06-3R-22-YANG	31.30	98.00	Trib to Yangtze trib.	None	368	180-425	0.27
06-3R-24-YANG	31.40	97.88	Trib to Yangtze trib.	None	131	180-425	0.16
06-3R-41-YANG	29.76	99.00	Yangtze	06-3R-17-YANG, 06-3R-20-YANG, 06-3R-19a-YANG, 06-3R-18-YANG, 06-3R-22-YANG, 06-3R-24-YANG	277472	180-425	0.31
06-3R-42-YANG	29.76	99.01	Trib to Yangtze	None	2756	180-425	0.36
05-3R-3-YANG	28.22	99.32	Yangtze	06-3R-41-YANG, 06-3R-42-YANG	300774	180-425	0.32
05-3R-1b-YANG	26.87	99.97	Yangtze	05-3R-3-YANG	311830	180-425	0.12

**Table 2.4: CRONUS calculator input.**

Sample name	Mean Latitude	Mean Longitude	Effective Mean Elevation [m]	Elevation/pressure flag	Sample thickness [cm]	Sample density [g/cm <sup>3</sup> ]	Conc. Be-10 (atoms/g)	Uncertainty in Be-10 conc.	Name of Be-10 stand.	Conc. Al-26	Uncertainty in Al-26	Name of Al-26 stand.
06-3R-52-SAL	29.70	96.80	5074	std	0.0001	2650.00	277111	14909	KNSTD	0	0	KNSTD
06-3R-53-SAL	29.74	96.70	5075	std	0.0001	2650.00	111701	7259	KNSTD	0	0	KNSTD
06-3R-50-SAL	29.83	97.10	4973	std	0.0001	2650.00	105850	5784	KNSTD	0	0	KNSTD
06-3R-49-SAL	29.88	96.89	4873	std	0.0001	2650.00	231103	10285	KNSTD	0	0	KNSTD
06-3R-48-SAL	31.44	94.16	4770	std	0.0001	2650.00	784949	20449	KNSTD	0	0	KNSTD
06-3R-46-SAL	30.12	97.31	4351	std	0.0001	2650.00	367464	15764	KNSTD	0	0	KNSTD
06-3R-30-SAL	30.73	96.82	4784	std	0.0001	2650.00	207825 2	62058	KNSTD	0	0	KNSTD
06-3R-32-SAL	30.62	96.94	4766	std	0.0001	2650.00	212044 4	58616	KNSTD	0	0	KNSTD
06-3R-33-SAL	29.91	97.77	4801	std	0.0001	2650.00	155360 8	50391	KNSTD	0	0	KNSTD
06-3R-34-SAL	30.38	97.21	4714	std	0.0001	2650.00	109282 0	26768	KNSTD	0	0	KNSTD

Table 2.4 continued

06-3R-35-SAL	29.77	97.87	4694	std	0.0001	2650.00	1237683	50806	KNSTD	0	0	KNSTD
06-3R-36-SAL	30.35	97.24	4708	std	0.0001	2650.00	1772162	37815	KNSTD	0	0	KNSTD
05-3R-9-SAL	31.31	94.39	4748	std	0.0001	2650.00	518500	12296	KNSTD	0	0	KNSTD
05-3R-10-SAL	31.29	94.42	4739	std	0.0001	2650.00	427659	11859	KNSTD	0	0	KNSTD
05-3R-11a-SAL	27.23	98.91	2018	std	0.0001	2650.00	161438	7129	KNSTD	0	0	KNSTD
05-3R-11b-SAL	31.28	94.43	4733	std	0.0001	2650.00	532386	18243	KNSTD	0	0	KNSTD
05-3R-11b-SAL	31.28	94.43	4733	std	0.0001	2650.00	591943	14123	KNSTD	0	0	KNSTD
05-3R-12-SAL	31.25	94.46	4720	std	0.0001	2650.00	402267	15524	KNSTD	0	0	KNSTD
05-3R-13b-SAL	31.22	94.49	4706	std	0.0001	2650.00	294362	12158	KNSTD	0	0	KNSTD
06-3R-26-MEK	32.11	95.65	4642	std	0.0001	2650.00	296760	10966	KNSTD	0	0	KNSTD
06-3R-26-MEK	32.11	95.65	4642	std	0.0001	2650.00	317841	9684	KNSTD	0	0	KNSTD

Table 2.4 continued

06-3R-27-MEK	32.56	96.13	4550	std	0.0001	2650.00	375523	13219	KNSTD	0	0	KNSTD
06-3R-27-MEK	32.56	96.13	4550	std	0.0001	2650.00	432965	12691	KNSTD	0	0	KNSTD
06-3R-28-MEK	32.40	96.00	4569	std	0.0001	2650.00	399126	18332	KNSTD	0	0	KNSTD
06-3R-29-MEK	31.35	96.37	4638	std	0.0001	2650.00	678376	26294	KNSTD	0	0	KNSTD
06-3R-38-MEK	31.98	96.35	4544	std	0.0001	2650.00	352113	10049	KNSTD	0	0	KNSTD
06-3R-39-MEK	29.72	98.42	4077	std	0.0001	2650.00	344713	14531	KNSTD	0	0	KNSTD
06-3R-43-MEK	29.69	98.24	4550	std	0.0001	2650.00	276803 0	67592	KNSTD	0	0	KNSTD
05-3R-4-MEK	28.66	98.90	4152	std	0.0001	2650.00	70117	5195	KNSTD	0	0	KNSTD
05-3R-6-MEK	31.75	96.52	4507	std	0.0001	2650.00	308766	17071	KNSTD	0	0	KNSTD
05-3R-7-MEK	31.68	96.56	4485	std	0.0001	2650.00	295439	12621	KNSTD	0	0	KNSTD
05-3R-8-MEK	31.65	96.58	4473	std	0.0001	2650.00	352419	10543	KNSTD	0	0	KNSTD
05-3R-14a-MEK	31.10	96.87	4288	std	0.0001	2650.00	261412	14464	KNSTD	0	0	KNSTD

Table 2.4 continued

06-3R-15-YANG	31.98	98.68	4384	std	0.0001	2650.00	360619	11421	KNSTD	0	0	KNSTD
06-3R-16-YANG	31.94	98.67	4352	std	0.0001	2650.00	384297	13299	KNSTD	0	0	KNSTD
06-3R-17-YANG	34.01	93.99	4744	std	0.0001	2650.00	421508 8	94795	KNSTD	0	0	KNSTD
06-3R-17-YANG	34.01	93.99	4744	std	0.0001	2650.00	406301 5	59101	KNSTD	0	0	KNSTD
06-3R-21-YANG	31.58	98.05	4327	std	0.0001	2650.00	949300	36916	KNSTD	0	0	KNSTD
06-3R-20-YANG	31.56	98.09	4317	std	0.0001	2650.00	948113	30610	KNSTD	0	0	KNSTD
06-3R-19b-YANG	31.64	98.43	4337	std	0.0001	2650.00	924199	20444	KNSTD	0	0	KNSTD
06-3R-19a-YANG	31.65	98.42	4333	std	0.0001	2650.00	651735	29344	KNSTD	0	0	KNSTD

Table 2.4 continued

06-3R-18-YANG	31.56	98.54	4142	std	0.0001	2650.00	360839	26401	KNSTD	0	0	KNSTD
06-3R-22-YANG	31.45	97.95	4327	std	0.0001	2650.00	782810	33147	KNSTD	0	0	KNSTD
06-3R-24-YANG	31.46	97.80	4681	std	0.0001	2650.00	881427	39199	KNSTD	0	0	KNSTD
06-3R-41-YANG	33.56	94.52	4695	std	0.0001	2650.00	326276 1	97513	KNSTD	0	0	KNSTD
06-3R-42-YANG	30.16	98.71	4253	std	0.0001	2650.00	984334	38432	KNSTD	0	0	KNSTD
05-3R-3-YANG	33.23	94.90	4651	std	0.0001	2650.00	281401 5	45255	KNSTD	0	0	KNSTD
05-3R-1b-YANG	33.04	95.06	4605	std	0.0001	2650.00	266126 4	52493	KNSTD	0	0	KNSTD

**Table 2.5: Information for calculating intermediate erosion rates**

Sample name	Total upstream basins				Intermediate reaches		
	Calculated production rate [atoms/g/yr]	Area [sq. km]	Erosion Rate [mm/yr]	Error [mm/yr]	Area [sq. km]	Erosion Rate [mm/yr]	Error [mm/yr] 95% confidence
06-3R-52-SAL	82	363	0.22	0.03	no upstream sample		
06-3R-53-SAL	82	661	0.55	0.09	incompatible data		
06-3R-50-SAL	78	869	0.55	0.08	no upstream sample		
06-3R-49-SAL	75	3108	0.24	0.03	1876	0.10	0.03
06-3R-48-SAL	74	283749	0.070	0.008	28064 1	0.068	0.01
06-3R-46-SAL	59	57	0.12	0.016	no upstream sample		
06-3R-30-SAL	74	2136	0.026	0.003	no upstream sample		
06-3R-32-SAL	73	3280	0.025	0.003	1144	0.024	0.00
06-3R-33-SAL	73	251	0.034	0.004	no upstream sample		
06-3R-34-SAL	71	5787	0.048	0.005	2255	0.082	0.01
06-3R-35-SAL	69	131	0.041	0.006	no upstream sample		
06-3R-36-SAL	70	6119	0.029	0.003	incompatible data		
05-3R-9-SAL	73	303287	0.11	0.011	13563	0.9	0.14
05-3R-10-SAL	73	305003	0.13	0.015	1716	4	1.12
05-3R-11a-SAL	15	2	0.08	0.010	no upstream sample		



Table 2.5 continued

05-3R-11b-SAL	73	305964	0.10	0.013	not used in mixing model		
05-3R-11b-SAL	73	305964	0.09	0.010	incompatible data		
05-3R-12-SAL	72	308044	0.13	0.017	3038	0.8	0.80
05-3R-13b-SAL	72	310028	0.18	0.02	1985	8	2.13
06-3R-26-MEK	71	16875	0.17	0.02	no upstream sample		
06-3R-26-MEK	71	16875	0.18	0.02	not used in mixing model		
06-3R-27-MEK	69	36710	0.14	0.017	no upstream sample		
06-3R-27-MEK	69	36710	0.12	0.014	not used in mixing model		
06-3R-28-MEK	69	54625	0.13	0.018	incompatible data		
06-3R-29-MEK	70	6733	0.08	0.010	no upstream sample		
06-3R-38-MEK	68	73147	0.14	0.017	12830	0.22	0.03
06-3R-39-MEK	51	167	0.11	0.015	no upstream sample		
06-3R-43-MEK	64	346	0.017	0.002	no upstream sample		
05-3R-4-MEK	52	465	0.57	0.10	no upstream sample		
05-3R-6-MEK	66	79193	0.16	0.02	5067	0.4	0.40
05-3R-7-MEK	66	80667	0.17	0.02	1474	0.5	0.66
05-3R-8-MEK	65	81317	0.14	0.016	incompatible data		
05-3R-14a-MEK	59	91049	0.17	0.03	10383	0.2	0.12

Table 2.5 continued

06-3R-15-YANG	63	1376	0.13	0.016	no upstream sample		
06-3R-16-YANG	62	1642	0.12	0.015	266	0.07	0.04
06-3R-17-YANG	79	246535	0.013	0.001	not used in mixing model		
06-3R-17-YANG	79	246535	0.014	0.001	24489 4	0.0126	0.001
06-3R-21-YANG	61	1450	0.048	0.006	no upstream sample		
06-3R-20-YANG	60	1911	0.048	0.006	461	0.047	0.01
06-3R-19b-YANG	61	1552	0.049	0.005	no upstream sample		
06-3R-19a-YANG	61	1596	0.07	0.010	45	0.8	0.19
06-3R-18-YANG	56	157	0.12	0.021	no upstream sample		
06-3R-22-YANG	61	368	0.058	0.008	no upstream sample		
06-3R-24-YANG	72	131	0.060	0.008	no upstream sample		
06-3R-41-YANG	76	277472	0.017	0.002	26774	0.042	0.01
06-3R-42-YANG	56	2756	0.043	0.006	no upstream sample		

Table 2.5 continued

05-3R- 3-YANG	74	300774	0.019	0.002	20546	0.04	0.01
05-3R- 1b- YANG	72	311830	0.020	0.002	11056	0.04	0.02

## Notes for chapter 2

- Aalto, R., Dunne, T., and Guyot, J. L. (2006). Geomorphic controls on Andean denudation rates. *Journal of Geology* 114, 85-99.
- Ahnert, F. (1970). Functional relationships between denudation, relief, and uplift in large mid-latitude drainage basins. *American Journal of Science* 268, 243-263.
- Anders, A., Roe, G. H., Hallet, B., Montgomery, D. R., Finnegan, N., and Putkonen, J. (2006). Spatial patterns of precipitation and topography in the Himalaya. In "Tectonics, Climate, and Landscape Evolution." (S. D. Willett, N. Hovius, M. T. Brandon, and D. Fisher, Eds.), pp. 39-53. Geological Society of America.
- Anders, A., Roe, G. H., Montgomery, D. R., and Hallet, B. (2008). Influence of precipitation phase on the form of mountain ranges. *Geology* 36, 479-482.
- Balco, G. (2006). Converting Al and Be isotope ratio measurements to nuclide concentrations in quartz. *Documentation - Be-10 / 26-Al exposure age calculator*  
Online: [http://hess.ess.washington.edu/math/docs/common/ams\\_data\\_reduction/](http://hess.ess.washington.edu/math/docs/common/ams_data_reduction/).
- Balco, G., Stone, J. O., Lifton, N. A., and Dunai, T. J. (2008). A complete and easily accessible means of calculating surface exposure ages or erosion rates from Be-10 and Al-26 measurements. *Quaternary Geochronology* 3, 174-195.
- Barnes, J. B., and Pelletier, J. D. (2006). Latitudinal variation of denudation in the evolution of the Bolivian Andes. *American Journal of Science* 306, 1-31.
- Bierman, P. R. (2004). Rock to sediment - Slope to sea with Be-10 - Rates of landscape change. *Annual Review of Earth and Planetary Sciences* 32, 215-255.
- Bierman, P. R., and Caffee, M. (2001). Slow rates of rock surface erosion and sediment production across the Namib Desert and escarpment, southern Africa. *American Journal of Science* 301, 326-358.

- Bierman, P. R., and Caffee, M. (2002). Cosmogenic exposure and erosion history of Australian bedrock landforms. *Geological Society of America Bulletin* 114, 787-803.
- Bierman, P. R., and Steig, E. J. (1996). Estimating rates of denudation using cosmogenic isotope abundances in sediment. *Earth Surface Processes and Landforms* 21, 125-139.
- Binnie, S. A., Phillips, W. M., Summerfield, M. A., and Fifield, L. K. (2007). Tectonic uplift, threshold hillslopes, and denudation rates in a developing mountain range. *Geology* 35, 743-746.
- Booth, A. L., Chamberlain, C. P., Kidd, W. S. F., and Zeitler, P. K. (2009). Constraints on the metamorphic evolution of the eastern Himalayan syntaxis from geochronologic and petrologic studies of Namche Barwa. *Geological Society of America Bulletin* 121, 385-407.
- Brookfield, M. E. (1998). The evolution of the great river systems of southern Asia during the Cenozoic India-Asia collision: rivers draining southwards. *Geomorphology* 22, 285-312.
- Brown, E. T., Stallard, R. F., Larsen, M. C., Raisbeck, G. M., and Yiou, F. (1995). Denudation rates determined from the accumulation of in situ-produced be-10 in the Luquillo Experimental Forest, Puerto-Rico. *Earth and Planetary Science Letters* 129, 193-202.
- Burbank, D. W., Blythe, A. E., Putkonen, J., Pratt-Sitaula, B., Gabet, E., Oskin, M., Barros, A., and Ojha, T. P. (2003). Decoupling of erosion and precipitation in the Himalayas. *Nature* 426, 652-655.
- Burg, J. P., Davy, P., Nievergelt, P., Oberli, F., Seward, D., Diao, Z. Z., and Meier, M. (1997). Exhumation during crustal folding in the Namche-Barwa syntaxis. *Terra Nova* 9, 53-56.

- Champagnac, J. D., Schlunegger, F., Norton, K., von Blanckenburg, F., Abbuhl, L. M., and Schwab, M. (2009). Erosion-driven uplift of the modern Central Alps. *Tectonophysics* 474, 236-249.
- Clark, M., and Royden, L. (2000). Topographic ooze: Building the eastern margin of Tibet by lower crustal flow. *Geology* 28, 703-706.
- Clark, M., Royden, L., Whipple, K., Burchfiel, B., Zhang, X., and Tang, W. (2006). Use of a regional, relict landscape to measure vertical deformation of the eastern Tibetan Plateau. *Journal of Geophysical Research-Earth Surface* 111, doi:10.1029/2005JF000294.
- Clark, M. K., Bush, J. W. M., and Royden, L. H. (2005a). Dynamic topography produced by lower crustal flow against rheological strength heterogeneities bordering the Tibetan Plateau. *Geophysical Journal International* 162, 575-590.
- Clark, M. K., House, M. A., Royden, L. H., Whipple, K. X., Burchfiel, B. C., Zhang, X., and Tang, W. (2005b). Late Cenozoic uplift of southeastern Tibet. *Geology* 33, 525-528.
- Clark, M. K., Schoenbohm, L. M., Royden, L. H., Whipple, K. X., Burchfiel, B. C., Zhang, X., Tang, W., Wang, E., and Chen, L. (2004). Surface uplift, tectonics, and erosion of eastern Tibet from large-scale drainage patterns. *Tectonics* 23, doi:10.1029/2005JF000294.
- Cyr, A. J., and Granger, D. E. (2008). Dynamic equilibrium among erosion, river incision, and coastal uplift in the northern and central Apennines, Italy. *Geology* 36, 103-106.
- Demoulin, A., Hallot, E., and Rixhon, G. (2009). Amount and controls of the Quaternary denudation in the Ardennes massif (western Europe). *Earth Surface Processes and Landforms* 34, 1487-1496.

- Ding, L., Zhong, D. L., Yin, A., Kapp, P., and Harrison, T. M. (2001). Cenozoic structural and metamorphic evolution of the eastern Himalayan syntaxis (Namche Barwa). *Earth and Planetary Science Letters* 192, 423-438.
- Dixon, J. L., Heimsath, A. M., and Amundson, R. (2009). The critical role of climate and saprolite weathering in landscape evolution. *Earth Surface Processes and Landforms* 34, 1507-1521.
- Enkelmann, E., Ratschbacher, L., Johnckheere, R., Nestler, R., Fleischer, M., Gloaguen, R., Hacker, B., Zhang, Y. Q., and Ma, Y. S. (2006). Cenozoic exhumation and deformation of northeastern Tibet and the Qinling; is Tibetan lower crustal flow diverging around the Sichuan Basin? *Geological Society of America Bulletin* 118, 651-671.
- Finlayson, D. P., Montgomery, D. R., and Hallet, B. (2002). Spatial coincidence of rapid inferred erosion with young metamorphic massifs in the Himalayas. *Geology* 30, 219-222.
- Finnegan, N. J., Hallet, B., Montgomery, D. R., Zeitler, P. K., Stone, J., Anders, A., and Liu, Y. (2008). Coupling of rock uplift and river incision in the Namche Barwa-Gyala Peri massif, Tibet. *Geological Society of America Bulletin* 120, 142-155.
- Finnegan, N. J., Roe, G., Montgomery, D. R., and Hallet, B. (2005). Controls on the channel width of rivers: Implications for modeling fluvial incision of bedrock. *Geology* 33, 229-232.
- Gabet, E. J., Pratt-Sitaula, B. A., and Burbank, D. W. (2004). Climatic controls on hillslope angle and relief in the Himalayas. *Geology* 32, 629-632.
- Granger, D. E., Kirchner, J. W., and Finkel, R. (1996). Spatially averaged long-term erosion rates measured from in situ-produced cosmogenic nuclides in alluvial sediment. *Journal of Geology* 104, 249-257.

- Hallet, B., and Molnar, P. (2001). Distorted drainage basins as markers of crustal strain east of the Himalaya. *Journal of Geophysical Research-Solid Earth* 106, 13697-13709.
- Harkins, N., Kirby, E., Heimsath, A., Robinson, R., and Reiser, U. (2007). Transient fluvial incision in the headwaters of the Yellow River, northeastern Tibet, China. *Journal of Geophysical Research-Earth Surface* 112, F03S04.
- Hodges, K. V., Wobus, C., Ruhl, K., Schildgen, T., and Whipple, K. (2004). Quaternary deformation, river steepening, and heavy precipitation at the front of the Higher Himalayan ranges. *Earth and Planetary Science Letters* 220, 379-389.
- Jayko, A. S. (2005). Late Quaternary denudation, Death and Panamint Valleys, eastern California. *Earth-Science Reviews* 73, 271-289.
- Kirby, E., Reiners, P. W., Krol, M. A., Whipple, K. X., Hodges, K. V., Farley, K. A., Tang, W. Q., and Chen, Z. L. (2002). Late Cenozoic evolution of the eastern margin of the Tibetan Plateau: Inferences from Ar-40/Ar-39 and (U-Th)/He thermochronology. *Tectonics* 21, 10.1029/2000TC001246.
- Kober, F., Ivy-Ochs, S., Schlunegger, F., Baur, H., Kubik, P. W., and Wieler, R. (2007). Denudation rates and a topography-driven rainfall threshold in northern Chile: Multiple cosmogenic nuclide data and sediment yield budgets. *Geomorphology* 83, 97-120.
- Kohl, C. P., and Nishiizumi, K. (1992). Chemical isolation of quartz for measurement of insitu-produced cosmogenic nuclides. *Geochimica Et Cosmochimica Acta* 56, 3583-3587.
- Kong, P., Na, C. G., Fink, D., Ding, L., and Huang, F. X. (2007). Erosion in northwest Tibet from in-situ-produced cosmogenic Be-10 and Al-26 in bedrock. *Earth Surface Processes and Landforms* 32, 116-125.



- Lal, D., Harris, N. B. W., Sharma, K. K., Gu, Z. Y., Ding, L., Liu, T. S., Dongal, W. Q., Caffee, M. W., and Jull, A. J. T. (2004). Erosion history of the Tibetan Plateau since the last interglacial: constraints from the first studies of cosmogenic Be-10 from Tibetan bedrock. *Earth and Planetary Science Letters* 217, 33-42.
- Liu, Y., and Zhong, D. (1997). Petrology of high-pressure granulites from the eastern Himalayan syntaxis. *Journal of Metamorphic Geology* 15, 451-466.
- Malloy, M. (2004). "Rapid erosion at the Tsangpo knickpoint and exhumation of southeastern Tibet." Unpublished M.S. thesis, Lehigh University.
- Matmon, A., Bierman, P. R., Larsen, J., Southworth, S., Pavich, M., and Caffee, M. (2003a). Temporally and spatially uniform rates of erosion in the southern Appalachian Great Smoky Mountains. *Geology* 31, 155-158.
- Matmon, A., Bierman, P. R., Larsen, J., Southworth, S., Pavich, M., Finkel, R., and Caffee, M. (2003b). Erosion of an ancient mountain range, the Great Smoky Mountains, North Carolina and Tennessee. *American Journal of Science* 303, 817-855.
- Molnar, P., Anderson, R. S., and Anderson, S. P. (2007). Tectonics, fracturing of rock, and erosion. *Journal of Geophysical Research-Earth Surface* 112, 10.1029/2005JF000433.
- Montgomery, D. R., Balco, G., and Willett, S. D. (2001). Climate, tectonics, and the morphology of the Andes. *Geology* 29, 579-582.
- Montgomery, D. R., and Brandon, M. T. (2002). Topographic controls on erosion rates in tectonically active mountain ranges. *Earth and Planetary Science Letters* 201, 481-489.
- Mora, A., Parra, M., Strecker, M. R., Sobel, E. R., Hooghiemstra, H., Torres, V., and Jaramillo, J. V. (2008). Climatic forcing of asymmetric orogenic evolution in the Eastern Cordillera of Colombia. *Geological Society of America Bulletin* 120, 930-949.

- Niemi, N. A., Oskin, M., Burbank, D. W., Heimsath, A. M., and Gabet, E. (2005). Effects of bedrock landslides on cosmogenically determined erosion rates. *Earth and Planetary Science Letters* 237, 489-498.
- Nishiizumi, K., Imamura, M., Caffee, M. W., Southon, J. R., Finkel, R. C., and McAninch, J. (2007). Absolute calibration of Be-10 AMS standards. *Nuclear Instruments & Methods in Physics Research Section B-Beam Interactions with Materials and Atoms* 258, 403-413.
- Ouimet, W. B. (2007). "Dissecting the eastern margin of the Tibetan plateau: a study of landslides, erosion and river incision in a transient landscape." Massachusetts Institute of Technology. PhD Dissertation.
- Ouimet, W. B., Whipple, K. X., and Granger, D. E. (2009). Beyond threshold hillslopes: Channel adjustment to base-level fall in tectonically active mountain ranges. *Geology* 37, 579-582.
- Quigley, M., Sandiford, M., Fifield, L. K., and Alimanovic, A. (2007). Landscape responses to intraplate tectonism: Quantitative constraints from Be-10 nuclide abundances. *Earth and Planetary Science Letters* 261, 120-133.
- Reiners, P. W., Ehlers, T. A., Mitchell, S. G., and Montgomery, D. R. (2003). Coupled spatial variations in precipitation and long-term erosion rates across the Washington Cascades. *Nature* 426, 645-647.
- Riebe, C. S., Kirchner, J. W., Granger, D. E., and Finkel, R. C. (2001). Minimal climatic control on erosion rates in the Sierra Nevada, California. *Geology* 29, 447-450.
- Roering, J. J., Kirchner, J. W., and Dietrich, W. E. (1999). Evidence for nonlinear, diffusive sediment transport on hillslopes and implications for landscape morphology. *Water Resources Research* 35, 853-870.

- Royden, L. H., Burchfiel, B. C., King, R. W., Wang, E., Chen, Z. L., Shen, F., and Liu, Y. P. (1997). Surface deformation and lower crustal flow in eastern Tibet. *Science* 276, 788-790.
- Safran, E. B., Bierman, P. R., Aalto, R., Dunne, T., Whipple, K. X., and Caffee, M. (2005). Erosion rates driven by channel network incision in the Bolivian Andes. *Earth Surface Processes and Landforms* 30, 1007-1024.
- Schoenbohm, L. M., Burchfiel, B. C., and Chen, L. Z. (2006a). Propagation of surface uplift, lower crustal flow, and Cenozoic tectonics of the southeast margin of the Tibetan Plateau. *Geology*. 34, 813-816.
- Schoenbohm, L. M., Burchfiel, B. C., Chen, L. Z., and Yin, J. Y. (2006b). Miocene to present activity along the Red River fault, China, in the context of continental extrusion, upper-crustal rotation, and lower-crustal flow. *Geological Society of America Bulletin*. 116, 895-909.
- Schoenbohm, L. M., Whipple, K. X., Burchfiel, B. C., and Chen, L. (2004). Geomorphic constraints on surface uplift, exhumation, and plateau growth in the Red River region, Yunnan Province, China. *Geological Society of America Bulletin* 116, 895-909.
- Seward, D., and Burg, J. P. (2008). Growth of the Namche Barwa syntaxis and associated evolution of the Tsangpo Gorge: Constraints from structural and thermochronological data. *Tectonophysics* 451, 282-289.
- Sklar, L. S., and Dietrich, W. E. (2001). Sediment and rock strength controls on river incision into bedrock. *Geology* 29, 1087-1090.
- Sol, S., Meltzer, A. S., Burgmann, R., Van der Hilst, R., King, R. W., Chen, Z., Koons, P. O., Lev, E., Liu, Y. P., Zeitler, P. K., Zhang, X., Zhang, J., and Zurek, B. (2007). Geodynamics of the southeastern Tibetan Plateau from seismic anisotropy and geodesy. *Geology* 35, 563-566.

- Stewart, R. J., Hallet, B., Zeitler, P. K., Mallor, M. A., Allen, C. M., and Trippett, D. (2008). Brahmaputra sediment flux dominated by highly localized rapid erosion from the easternmost Himalaya. *Geology* 36, 711-714.
- Stone, J. O. (2004). Extraction of Al and Be from quartz for isotopic analysis. *UW Cosmogenic Nuclide Lab Methods and Procedures Online*: <http://depts.washington.edu/cosmolab/chem.html>.
- Tapponnier, P., Xu, Z. Q., Roger, F., Meyer, B., Arnaud, N., Wittlinger, G., and Yang, J. S. (2001). Geology - Oblique stepwise rise and growth of the Tibet plateau. *Science* 294, 1671-1677.
- Taylor, M., and Yin, A. (2009). Active structures of the Himalayan-Tibetan orogen and their relationships to earthquake distribution, contemporary strain field, and Cenozoic volcanism. *Geosphere* 5, 199-214.
- Thiede, R. C., Bookhagen, B., Arrowsmith, J. R., Sobel, E. R., and Strecker, M. R. (2004). Climatic control on rapid exhumation along the Southern Himalayan Front. *Earth and Planetary Science Letters* 222, 791-806.
- Tomkins, K. M., Humphreys, G. S., Wilkinson, M. T., Fink, D., Hesse, P. P., Doerr, S. H., Shakesby, R. A., Wallbrink, P. J., and Blake, W. H. (2007). Contemporary versus long-term denudation along a passive plate margin: the role of extreme events. *Earth Surface Processes and Landforms* 32, 1013-1031.
- Tucker, G. E., and Slingerland, R. L. (1994). Erosional dynamics, flexural isostasy, and long-lived escarpments - a numerical modeling study. *Journal of Geophysical Research-Solid Earth* 99, 12229-12243.
- USGS. (2001). Global GIS database: digital atlas of South Asia. In "Global GIS Database, Digital Data Series DDS-62-C." (J. P. Hearn, T. Hare, P. Schruben, D. Sherrill, C. LaMar, and P. Tsushima, Ed.). USGS.

- USGS. (2008). HydroSHEDS. *World Wildlife Fund (WWF)* online:  
<http://hydrosheds.cr.usgs.gov/>, date accessed: 22 Jan 2009.
- Vanacker, V., von Blanckenburg, F., Hewawasam, T., and Kubik, P. W. (2007).  
Constraining landscape development of the Sri Lankan escarpment with  
cosmogenic nuclides in river sediment. *Earth and Planetary Science Letters* 253,  
402-414.
- Vance, D., Bickle, M., Ivy-Ochs, S., and Kubik, P. W. (2003). Erosion and exhumation in  
the Himalaya from cosmogenic isotope inventories of river sediments. *Earth and  
Planetary Science Letters* 206, 273-288.
- von Blanckenburg, F. (2005). The control mechanisms of erosion and weathering at basin  
scale from cosmogenic nuclides in river sediment. *Earth and Planetary Science  
Letters* 237, 462-479.
- von Blanckenburg, F., Hewawasam, T., and Kubik, P. W. (2004). Cosmogenic nuclide  
evidence for low weathering and denudation in the wet, tropical highlands of Sri  
Lanka. *Journal of Geophysical Research-Earth Surface* 109. F03008.
- Whipple, K. X., Kirby, E., and Brocklehurst, S. H. (1999). Geomorphic limits to climate-  
induced increases in topographic relief. *Nature* 401, 39-43.
- Whipple, K. X., and Tucker, G. E. (1999). Dynamics of the stream-power river incision  
model: Implications for height limits of mountain ranges, landscape response  
timescales, and research needs. *Journal of Geophysical Research-Solid Earth* 104,  
17661-17674.
- Whittaker, A. C., Cowie, P. A., Attal, M., Tucker, G. E., and Roberts, G. P. (2007).  
Bedrock channel adjustment to tectonic forcing: Implications for predicting river  
incision rates. *Geology* 35, 103-106.
- Willett, S. D. (1999). Orogeny and orography: The effects of erosion on the structure of  
mountain belts. *Journal of Geophysical Research-Solid Earth* 104, 28957-28981.

- Willett, S. D., Beaumont, C., and Fullsack, P. (1993). Mechanical model for the tectonics of doubly vergent compressional orogens. *Geology* 21, 371-374.
- Willett, S. D., Slingerland, R., and Hovius, N. (2001). Uplift, shortening, and steady-state topography in active mountain belts. *American Journal of Science* 301, 455-485.
- Wittmann, H., von Blanckenburg, F., Kruesmann, T., Norton, K. P., and Kubik, P. W. (2007). Relation between rock uplift and denudation from cosmogenic nuclides in river sediment in the Central Alps of Switzerland. *Journal of Geophysical Research-Earth Surface* 112. F04010.
- Zeitler, P. K., Meltzer, A. S., Koons, P. O., Craw, D., Hallet, B., Chamberlain, C. P., Kidd, W. S. F., Park, S. K., Seeber, L., Bishop, M., and Shroder, J. (2001). Erosion, Himalayan geodynamics, and the geomorphology of metamorphism. *GSA Today* January 2001, 11, 4-9.
- Zhang, P. Z., Shen, Z., Wang, M., Gan, W. J., Burgmann, R., and Molnar, P. (2004). Continuous deformation of the Tibetan Plateau from global positioning system data. *Geology* 32, 809-812.

### **Chapter 3: The myth of Communist land degradation: new evidence from local erosion and basin-wide sediment yield in SW China and SE Tibet**

#### **Introduction**

Let's wage war against the great earth!

Let the mountains and rivers surrender under our feet.

March on Nature,

Let's take over the power of rain and wind.

-- Zhang Zhimin

Poems such as the one above, by a noted revolutionary poet, illustrate poignantly communist-era attitudes towards nature, which the Chinese government promoted and that are widely blamed for increased flooding in recent decades along the lower Yangtze River (e.g., Yin and Li, 2001). This attitude towards nature is not new. Prior to the revolution, although small villages and isolated regions generally subscribed to Daoist and Buddhist ideals of living in harmony with nature and revering all living things, larger communities, scholars, and the ruling class held the Confucian ideals of controlling nature to suit humanity (Shapiro, 2001).

There are numerous reports of environmental destruction in imperial China. The degradation of the Loess Plateau and the Yellow River basin is one striking example. Thousand-fold population increase (70,000 to 70 million in 400 years) caused grassland and forested land on the Loess Plateau to decrease from 53% to

3% (Saito et al., 2001). Erosion “carved a maze and labyrinth of gullies up to 600 feet deep” (Lowdermilk, 1924), and increased flooding related to sedimentation resulted in levee building projects as early as 206 BC (Ma, 2004). Other early large-scale efforts to control nature include the irrigation projects at Dujiang Yan (Shapiro, 2001) and illegal clearing and levee building in the Dongting region of Hunan province during the Ming and Qing dynasties, which were blamed for causing massive Yangtze River floods in 1788 (Perdue, 1982).

Environmental destruction is also well documented in modern Chinese history. Three major policies, known as the “three great cuttings”, are blamed for mass deforestation since 1949: 1) the Great Leap Forward (1958-1960), when fueling widespread “backyard” steel furnaces induced extensive deforestation (Shapiro, 2001; Hyde et al., 2003); 2) the “Grain as a Key Link” policy (1966-1976) to clear land for expanding cropland (Hyde et al., 2003); and, 3) “opening and development” in the early 1980s when free markets opened and people could benefit financially from trees they cut and sold (Hyde et al., 2003).

Analysis of regional, quantitative data leads to complicated conclusions regarding the impact of such anthropogenic activity on erosion. For example, annual sediment yield in the Yellow River is second only to the Amazon (e.g., Saito et al., 2001), but recent conservation efforts appear to have been somewhat successful at reducing sediment yields (Hassan et al., 2008). Additionally, the Yellow River delta records a declining sediment load between 1951 and 1999



(Wang et al., 2006). Instead of conservation, this trend may reflect the increased water demand in the basin and the subsequent inability for the river to reach, let alone transport sediment to the delta; in 1997 the river did not reach the sea during 220 days, an increase from 20 dry days in 1961 (Wang et al., 2006).

The Yangtze River is more complicated. Up to 40% of the forests in Sichuan were cut in modern times (Winkler, 1996) and this has been blamed for increased sediment load and subsequent flooding (Chen, 2000; Yin and Li, 2001; Yi, 2003). In contrast, a number of studies conclude that human activity and modern policies have not, on average, increased sediment yield in the Yangtze River (Lu and Higgitt, 1998; Higgitt and Lu, 1999; 1999; Lu et al., 2003a; 2003b). Other studies find decreasing sediment yield to the river (Xu, 2000; Chen, 2001; 2005; Wang et al., 2007a; 2007b). Small-scale studies tell a different story. Several detailed studies find sediment loads increasing in mountainous tributaries and decreasing in urban tributaries (Zhang, 1999; Zhang and Wen, 2002; 2004). Another set of studies finds that in a rural, minority township in Sichuan, the local ethic for conservation did not stop the area from being heavily logged during all three “great cuttings” (Trac et al., 2007), transforming a single channel river set in a wooded floodplain into a widening channel actively eroding into hillslopes, and undercutting roads and houses (Urgenson et al., in review).

These seemingly contradictory results parallel the broader, international discussion of anthropogenic landscape change in the Himalaya, and, more

specifically, the Theory of Himalayan Environmental Degradation (THED). This theory postulates a general eight step process by which upstream anthropogenic changes, such as deforestation, cause enormous changes to the downstream environment (see review by Ives, 1987). A popular theory in the late 1980s, THED generally fell out of favor among those who study Himalayan environmental change as an overly simplistic representation of the environment (e.g., Ives, 1987). More recent research suggests that although THED does not hold on large scales, over small scales the environmental consequences of human activities can be great (e.g., Forsyth, 1996; Ali and Benjaminsen, 2004). Despite the scientific community moving away from such simplistic representations of environmental change, recent Chinese environmental policies are derived from THED. These policies largely ignore subtleties in the relationship between upstream land use and downstream effects, instead favoring blanket policies of controlling all anthropogenic land use as damaging to downstream areas (Blaikie and Muldavin, 2004).

This contrast in the results of large-scale and small-scale studies is corroborated by numerous studies showing that extensive deforestation greatly increases erosion by reducing soil cohesion but that humans have simultaneously increased storage of sediments, leading to a net effect of decreased sediment yield to oceans (Syvitski et al., 2005). Similarly, in China, Higgitt and Lu (1996) show that although soil erosion was increasing in the Upper Yangtze watersheds over the period from the late 1940s to late 1980s, sediment yield in rivers did not increase,

suggesting that sediment was stored and did not leave the basins. Thus, given the well-recognized tendency for deforestation to increase erosion, there are two possible hypotheses for the downstream effects of deforestation: 1) sediment yields increased regionally and, in turn, increased flooding by aggrading channel beds and decreasing channel space for water to flow in without over topping banks; or, 2) sediment yields increased locally but sediment storage in alluvial fans and floodplains upstream buffer downstream reaches from such changes.

In this context, we test the hypothesis that humans changed the nature of sediment supply to and transport in the large rivers making up the International Rivers of Yunnan and Tibet, China<sup>1</sup> (IRYT; Fig. 1). We use three measurements of anthropogenic effects on sediment yield: correlations between sediment yield and metrics of human development (i.e., population density, land cover, and fraction of land under cultivation), changes in the annual sediment yield, and changes in the nature of sediment rating curves. To account for natural spatial variability in sediment yield, we also analyze correlations between sediment yield and geomorphic parameters (i.e., mean local relief and rainfall). Following Wolman (1967), sediment yield is expected to increase with increasing population density until the point where the area becomes urban and sediment yield sharply decreases, whereas agricultural land use and the fraction of land under cultivation should correlate more directly with sediment yield. We also examine temporal variations

---

<sup>1</sup> Zangdian Guoji Heliu in Chinese.

in sediment yield reflecting the response of rivers to major changes in sediment supply. Finally, as a control for interannual variability in rainfall, we test for temporal variations in parameters of the sediment rating curves for each station. When watershed processes are disturbed, resulting in increased sediment delivery to stream channels, the sediment rating curve records changes in the way the river transports sediment by shifting upwards – either changing the slope or intercept of the regression (EPA, 2006). Well-documented examples of sediment rating curve shifts as a result of basin degradation include Missouri gully erosion (Piest et al., 1975), west Tennessee channelization (Simon and Hupp, 1986), and Arizona silvicultural impacts (Lopes et al., 2001).

The IRYT are the rivers which drain Yunnan and Tibet into foreign countries on their way to the ocean, mainly in the mountains that make up the eastern and southern margins of the Tibetan Plateau. The region includes the Tsangpo, Salween, Mekong, and Red Rivers<sup>2</sup> and lies between 20° and 34°N and 80° and 105°E at elevations ranging from 200 to over 6000 m. It is characterized by mean annual rainfall as high as 1500 mm/yr and as low as 180 mm/yr, and local relief ranging from 150 to over 3000 m measured over 10 km diameter areas.

---

<sup>2</sup> Yalong Zangbo Jiang, Nu Jiang, Lancang Jiang, and Hong He, respectively.

The IRYT is of particular interest because: 1) it contains part of the Three Rivers Region UNESCO World Heritage Site<sup>3</sup> and has been reported as possibly being moved to the World Heritage Sites at Risk List (IUCN, 2006) as a result of proposals for two cascades of dams along the Salween and Mekong Rivers (Feng and He, 2004; Magee, 2006); 2) the Yangtze River has been extensively studied during planning for and construction of the Three Gorges Dam; and 3) there is a long record (up to 27 years) of daily sediment yield measurements for 44 stations in the region.

## **Methods**

We used daily mean total suspended sediment and discharge data compiled for 44 stations in the IRYT operated by the Ministry of Hydrology of the People's Republic of China from 1953 to 1987 (Ministry of Hydrology, 1962-1989); data after 1987 are not publicly available. We photocopied all data for the Yangtze River – Jinsha and Yalong Regions, the Yellow River – Fen He Region, and all of the International Rivers of Yunnan and Tibet District from the original books. The organization of the books required us first to transliterate (into Pinyin) the names of all stations, rivers, and river basins so that we could match the stations between different years. As the numbers of the stations change from year to year, we matched stations based on their Chinese name and renumbered them such that each

---

<sup>3</sup> The Three Rivers Region is where the Salween, Mekong, and Yangtze Rivers flow parallel to one another in Eastern Tibet. This is not the Three Gorges; that is much further downstream on the Yangtze River.

station has a unique number. The location of the stations is tied to the year the location was reported because stations sometimes moved around or the location was misreported. After the stations were renumbered and the station information pages entered into the database, we input the daily data into the database.

Information about the relational database structure and how to access it are available at: <http://depts.washington.edu/shuiwen/>.

Xu and Cheng (2002) report that the data were collected using “standard procedures” described by the Ministry of Water Conservancy (1962) and the Ministry of Water Conservancy and Electric Power (1975). Unfortunately, these sources are not publicly available and we cannot evaluate the methods.

Nonetheless, a comparison of sediment concentration and discharge results indicates that the data were measured daily and not calculated using a rating curve, which assumes a linear relationship between sediment concentration and discharge. For one year of data at a representative station along the Mekong River, we show that a wide range of sediment concentrations are associated with any given discharge (Fig. 2a). Each of the stations exhibits interannual variability in the relationship between sediment concentration and discharge, and no station has sediment concentrations which correlate well with discharge.

The Ministry of Hydrology does not report errors for the data, and thus we estimate errors conservatively on the basis of previous sediment yield studies.

Singh and France-Lanord (2002) show that point sampling does not adequately

sample the distribution of suspended sediment in a river. We expect that the errors in erosion rates calculated from the sediment data measured by the Ministry of Hydrology can be as high as 50% due to errors in point sampling and the fact that these rates do not include bed load or dissolved load (Galy and France-Lanord, 2001).

Using data presented in Table 1 we calculated sediment yield (tonnes sediment·km<sup>-2</sup>·yr<sup>-1</sup>) for each of the stations, which individually have one to twenty-seven years of data available. For the eighteen stations with additional stations upstream of them in the same basin, we calculated the sediment yield for both the intermediate reaches between stations and the entire upstream area. Although reported station locations are accurate to the nearest minute, this resolution is insufficient to extract upstream basin areas from a digital elevation model, and thus we adjusted the station locations, placing each station on the nearest river of approximately the correct size. The adjustments were minor, with the revised locations placing the stations on rivers in approximately the same location and with nearly identical areas to those originally reported (Fig. 2b).

We compared mean annual sediment yields (both basin-wide and for reaches between successive stations) to three metrics of development in the region – population density, land cover, and fraction of land cultivated. We attempted to compare data for overlapping periods of time, but sediment yield data available to us only extend through 1987 while the population density data are from 1990

(Deichmann, 1996), the land cover data are based on satellite imagery from 1992 and 1993 and USGS classification schemes (USGS, 2008b), and the percent land under cultivation estimates are from 1997 county data from provincial yearbooks (CDC, 2009b; 2009a). In addition to these metrics of development, we compared mean annual sediment yields to two geomorphic metrics (mean annual rainfall and mean local relief) as indicators of geomorphic parameters that may influence sediment yields independently of anthropogenic factors. Mean local relief was used as a proxy for hillslope steepness, as it is relatively insensitive to quality or scale of topographic data. Rainfall was derived from Tropical Rainfall Measuring Mission (TRMM) satellite data and relief was derived from Satellite Radar Topography Mission (SRTM) data. TRMM data capture daily variability in rainfall but not total amount of rainfall, and therefore likely underestimate actual rainfall by 15-25% but portray accurate spatial distributions of rainfall (Anders et al., 2006).

For the temporal variations in sediment yield and sediment rating curves, we calculated the annual sediment yield and sediment rating curve parameters (i.e., slope and intercept) for every year through the period of record for stations with over 20 years of data (8 stations).

## **Results**

The sediment yields range from -8400 to 173,750 tonnes/km<sup>2</sup>/yr (mean and standard deviation are 3992 and 22304 tonnes/km<sup>2</sup>/yr, respectively) for the region and the measured basins range in size from 4 to 133,796 km<sup>2</sup> (Fig. 3a, Table 1).



The lowest sediment yields are along the Mekong River between 26° and 29°N where the river has negative net sediment yield (area upstream of station 4 and downstream of stations 55 and 57). Although other reaches with negative net sediment yield exist (upstream of stations 43, 104, and 302), they record much smaller amounts of sediment accumulation, fewer years of data, and/or significantly smaller basin areas. The area upstream of station 302 is mapped by Finnegan et al. (2008) as having extensive valley bottom sediment storage which they interpret to reflect high sediment supply and low transport capacity. This valley bottom sediment storage is likely the reason sediment yield in the region is negative. The highest sediment yield is for station 311, a 14-km<sup>2</sup> station in Tibet that operated for 5 years and had an annual sediment yield of 173,750 tonnes/km<sup>2</sup>/yr. This station has a sediment yield more than 6 standard deviations above the mean and so we omit it from future discussion as an outlier; no other station has a yield greater than one standard deviation from the mean. Aside from this station, the highest sediment yields are in the southern reaches of the study area. There is no correlation between basin area and sediment yield ( $r = -0.31$ ; Fig. 3a), but there is a clear trend indicating that as basin area increases, the inter-basin variation in unit sediment yield decreases (Figure 4a).

Mean local relief measured over a 10 km diameter circle and averaged over each basin analyzed ranges from 347 to 1505 m (Fig. 3b). The highest relief basins are in the narrow part of the Mekong River. The mean annual sediment yield is

poorly correlated with mean local relief ( $r = 0.24$ ; Fig. 4b), suggesting that hillslope steepness is not the major control on modern sediment yields in this region.

Mean annual rainfall values averaged over the basins analyzed range from 369 mm/yr to 1386 mm/yr (Fig. 3c). The highest rainfall values are in the southern basins of the region, which are those most affected by the Indian monsoon. A weak correlation exists between the mean annual rainfall for each basin and the mean annual sediment yield ( $r = 0.49$ ,  $p < 0.001$ ; Fig. 4c).

The population density in the region ranges from  $< 1$  to 516 people/km<sup>2</sup> averaged over the basins studied (Fig. 3d). Qualitatively, in general the highest population densities are in the southwestern portions of the region, the region with highest sediment yields. However, the annual sediment yield as a function of mean basin-averaged population density shows no trends ( $r = -0.20$ ; Fig. 4d).

Fraction of land under cultivation by county (as reported by the provincial governments) ranges from 0 to nearly 15% in the region (Fig. 3e). The highest proportion of land under cultivation is in the southern portions of the region and the lowest are in the Tibetan regions. Although several of the rapidly eroding areas are in counties more extensively cultivated, direct comparison of sediment yield and extent of agricultural land shows only a weak correlation ( $r = 0.41$ ,  $p < 0.001$ ; Fig. 4e).

The land cover for the study area consists primarily of grasses and forest (Fig. 3f). On average, only about 10% of each of the basins for which we calculated

sediment yield is cropland. The maximum percentage of cropland in a basin is as high as 86% (this value is for one intermediate reach) but sediment yield is low for basins with more than 40% agricultural land – the highest sediment yield among these basins is 1.41 kg/km<sup>2</sup>yr. There is no correlation between the proportion of a basin under agricultural use defined by satellite data and the sediment yield from the basin ( $r = 0.05$ ; Fig. 4f), potentially reflecting inaccuracies in the land use classification rather than a lack of relationship between sediment yield and agricultural land.

In the Jinsha and Yalong tributaries of the Yangtze River, Lu and Higgitt (1999) report sediment yields ranging from 65 to 1770 tonnes/km<sup>2</sup>/yr for thirteen watersheds. Using the sediment yields they report, sediment yields from these basins correlate poorly with both population density and percent cropland (from the land cover data) ( $r = 0.30$  and  $0.32$ , respectively); fraction agricultural land is not available for Sichuan counties.

None of the eight stations with over 20 years of record shows systematic, temporal variation in sediment yield or sediment rating curve parameters over time (Fig. 5). Most stations exhibit little variability in either sediment yield or rating curve parameters. Stations 4, 11, 103, and 106 exhibit temporal variability in sediment yield that is neither systematic nor related to the time periods of intense logging. Yang et al. (2007) conducted a similar sediment rating curve analysis on seven stations on the main stem of the Yangtze River and found that only two

stations show a systematic variation in the slope and intercept of sediment rating curves. In both of these cases, slope increases with time and intercept decreases. Although Yang et al. (2007) interpreted these data to indicate an increase in droughts and floods over time in the Yangtze River basin, we argue that this trend simply implies that less sediment is carried at low flows and more is carried at high flows, and does not suggest a systematic increase over time in sediment transported in the river.

## **Discussion**

Comparing regional sediment yields to indices of development and geomorphic parameters reveals a weak correlation between sediment yield and both rainfall and fraction of land under cultivation ( $r = 0.49$  and  $0.41$ , respectively;  $r = 0.54$  for the multiple regression with both variables). These two parameters are correlated ( $r = 0.79$ ), making it difficult to unravel the relative importance of each. These results suggest that the gradient in sediment yield across the IRYT is controlled by the rainfall gradient, and that the net influence of anthropogenic changes across this region is comparable to the variation in rainfall. Since there is a tendency for there to be more agricultural land in areas which have higher rainfall, it is not surprising that the rainfall and agricultural land generally follow parallel trends. Additionally, the strong qualitative coincidence of high sediment yields and high population densities, high rainfall, and higher fractions of agricultural land

suggest at least a weak anthropogenic control on sediment yield, the details of which are lost when comparing basin-wide averages.

Sediment yields and sediment rating parameters for stations with over 20 years of data show no systematic temporal changes, and the standard error of the annual means is below 5% for these stations. For these stations there is a systematic decrease in the inter-annual variation of all three parameters with increasing basin area (Fig. 4a). The most likely explanations for the lack of change in sediment yield and sediment rating curve parameters through time are (1) that deforestation and development activities are not profound enough to overcome natural variability in sediment yield in the IRYT, or (2) that any anthropogenic influence on patterns of sediment yield are a result of long term agricultural activity that pre-dates the establishment of the hydrology stations from which our data were collected.

Although it is possible that these sediment yields reflect agricultural practices, the erosion rates for most basins are lower than longer-term rates calculated from  $^{10}\text{Be}$  in modern river sand (Fig. 6) (Henck et al., 2007). This suggests that if there is an increase in sediment yield because of agricultural activity, it is either buffered in the system and not visible in short term records or is not large enough to exceed longer-term erosion rates. In contrast, two basins with extremely high modern sediment yields (basins upstream of stations 32 and 311) suggest erosion rates of 8 mm/yr and 65 mm/yr, respectively, which far exceed the longer-term rates (0.05 – 0.38 mm/yr). Basin 311 is a small watershed in Tibet and

sediment yield was only monitored in the watershed for 5 years. GoogleEarth images show extensive terracing and landslide scars in that basin. Erosion rates of 65 mm/yr are not sustainable over any significant period of time, therefore we hypothesize a major disturbance (such as a landslide, fire, logging, mining, etc.) occurred in the watershed immediately prior to when sediment yield measurements began. If this is the case, the sediment yield data reflect a transient response to disturbances, not a sustainable erosion rate. The watershed is roughly 20 km<sup>2</sup> (20 km<sup>2</sup> was reported in the Chinese data, but we calculated 14 km<sup>2</sup>) and at this size, it is conceivable that a disturbance could be widespread enough to cause this high an erosion rate. Basin 32 is a larger basin (17,000 km<sup>2</sup>) drained by a tributary to the Mekong River; on GoogleEarth this basin appears to be heavily agricultural and largely logged. The average erosion rate here, over 5 years, is over 8 mm/yr. Again, although the basin is much larger, the short period of record makes it more likely that the station records a major change in the land use for the basin or the legacy of a large natural event, such as a storm or series of landslides or a human disturbance. Given the potential inaccuracies in how we scale county-data to basin-wide data, it is possible that a much higher percentage of land in this watershed is under cultivation than we estimate. This is the only example we have of a large basin with modern sediment yields significantly higher than expected background rates.

The decrease in variation of mean sediment yield and the inter-annual changes in sediment yield and sediment rating curve parameters with increasing

basin area suggest a buffering effect of large basins which may mask any anthropogenic changes. This buffering is most likely to happen through small-scale storage of sediment as it leaves the altered sub-basin and enters the larger river system. Large alluvial fans at the mouths of tributary valleys are common in the narrow reaches of the Salween and Mekong Rivers, providing evidence for active sediment storage along these rivers. In addition, the presence of two large intermediate reaches with apparently negative sediment yields provides further evidence of sediment storage (the areas upstream of stations 4 and 302, on the Mekong and Tsangpo Rivers, respectively). To show the magnitude of sediment storage in these two reaches, we plot the total sediment yield as a function of basin area for the stations along the main stems of the Mekong and Tsangpo Rivers (Fig. 7). In both of the reaches with negative sediment yields, there are numerous sand bars, small flood plains, and alluvial fans in which some sediment could be stored.

In light of a large body of literature showing that agriculture, development, and logging locally increase erosion rates (e.g., see review by Syvitski, 2003), we suggest that to the extent that these anthropogenic activities locally increase erosion, the sediment is stored locally and does not make it to the rivers in the larger basins. In addition, the weak correlation between sediment yield and both rainfall and fraction of land under cultivation suggests that the variability we see in sediment yield is weakly controlled by these two factors (which are strongly correlated). Any additional variation from anthropogenic activities is almost

certainly smaller than the magnitude of these controls, especially in larger rivers. In any case, however, the data show no sign of the dramatic increase in sediment yield argued to have resulted from Communist programs. However, due to the apparent buffering effect that large river basins have on sediment yield, we suggest that future research on anthropogenic effects on sediment yield in this region focus on basins under 5000 km<sup>2</sup>. Another possibility is that the response to anthropogenic or natural disturbances is short-lived and that over short periods of time we could see a high erosion rate, as we see with the basins upstream of stations 32 and 311.

Extending these results brings into focus the differences between the IRYT, the Yangtze River basin, and the Yellow River basin. Of the large body of literature on anthropogenic impacts to Yangtze River sediment yield, only three studies find sediment yield to be increasing with time. These either infer sediment yield from flood frequency data (Yin and Li, 2001), infer changes in sediment yield based on land use data (Chen, 2000), or present figures and tables which do not support the conclusion that sediment yield increased with time (Yi, 2003). None of these studies uses the methods presented here or those used in other studies in this region. Other studies find that sediment yield decreased or remained steady through time, primarily using data from stations downstream on the Yangtze River rather than smaller tributaries (Lu and Higgitt, 1998; Higgitt and Lu, 1999; Lu and Higgitt, 1999; Chen, 2001; Lu et al., 2003a; 2003b; Xu, 2005; Wang et al., 2007a; 2007b). Higgitt and Lu (1996) suggest that erosion rates in the Yangtze River do not



currently reflect increased hillslope erosion due to human activities, a hypothesis supported by Cs-137 measurements (Lu and Higgitt, 2000).

The Yellow River has an extremely long history of human disturbance and, in modern times, an acute water supply deficit. The history of disturbance means that conservation efforts were started in the early 1900s and, thus far, appear to be successful in curbing sediment loss (Hassan et al., 2008), although the lack of water in the river as many as 220 days a year (Wang et al., 2006) now means that it is impossible to know what the basin-wide sediment yields would be if there were flow to transport it. Obviously there is a large amount of sediment storage in the basin because there is no water with which to transport the sediment out of the basin. The decrease in sediment yield in the Yellow River basin due to sediment storage is parallel to our results for the IRYT that sediment yield is not necessarily commensurate with increasing local erosion or development.

## **Conclusions**

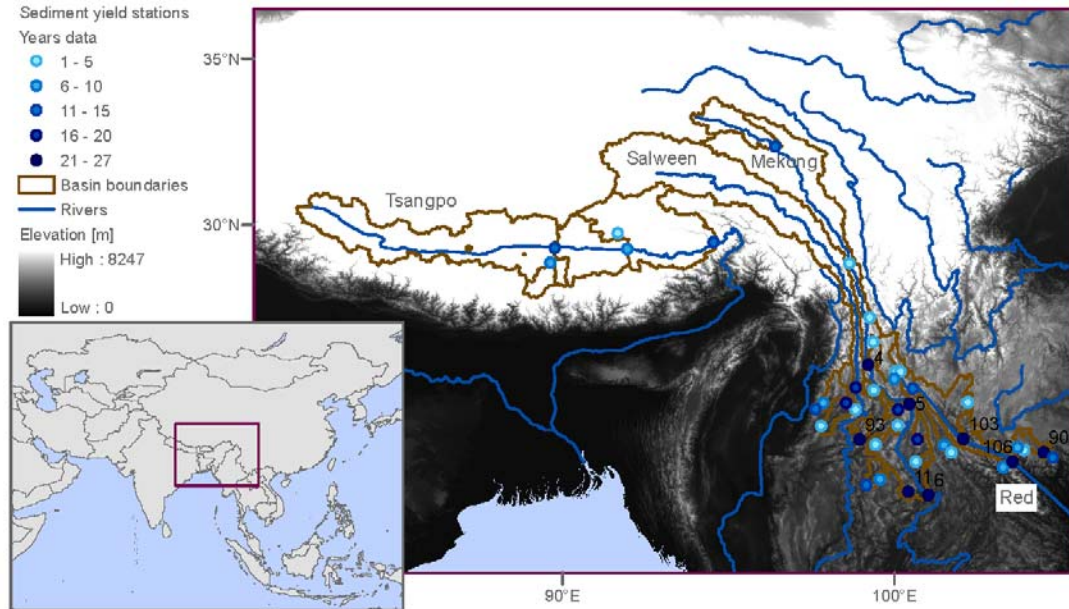
Our data extend the complicated story of China's relationship with the environment and the effects of modern policies on erosion rates throughout the country. Despite reported environmental devastation to the countryside and accelerated erosion, we present a substantial data set on sediment yield that reveals only weak correlation between modern sediment yield and fraction of land under cultivation and a qualitative correlation with population density. In addition, we find no correlation of sediment yield with other geomorphic and human activity

metrics and instead find remarkable temporal stability over several decades. These results do not, however, show that development activities and logging do not mobilize large amounts of sediment. Rather, we consider it more likely that they indicate that such sediment is being stored in higher order, ungauged channels, floodplains, or alluvial fans and is not being transported out of the study basins by the rivers. This is particularly likely to be true for larger basins as they show less variability in annual sediment yield. If our interpretation is correct, the data indicate that larger basins are effectively buffered against rapid and extreme variations in sediment yield, suggesting that smaller basins are more likely to show the expected changes due to anthropogenic activity. Hence, particular caution is needed in relating regional sediment fluxes in and degradation of rivers to agriculture, logging, and construction. Although these activities may have large local effects, in southwestern China they have comparable effects to regional patterns in rainfall in controlling basin-wide sediment yield. Smaller-scale studies over a wide region are required to improve understanding of the processes related to producing, transporting, and storing sediment in this region. Such small-scale studies may provide a means to quantify the apparent qualitative correlation between sediment yield and both agricultural land and population density which are apparent upon visual inspection of the data but basin-scale averaging and regressions do not reflect.

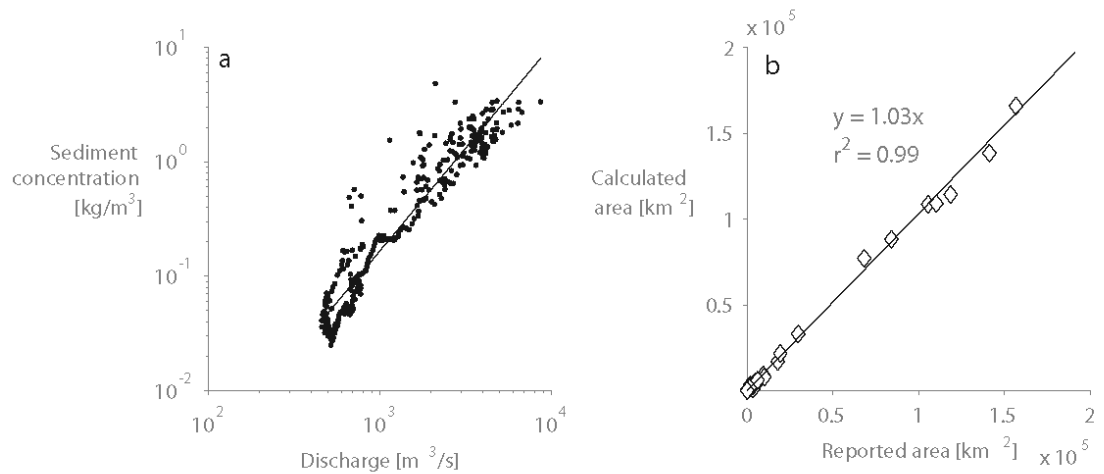
**Acknowledgements**

This chapter was submitted for publication with David R. Montgomery, Katharine W. Huntington, and Liang Chuan as coauthors. We thank Harvey Greenberg for GIS help, numerous students for data entry, and Alison Anders, Tom Hinckley, Steve Harrell, and Tom Carpenter for helpful comments on early versions of the paper. This work was supported by the UW Quaternary Research Center, UW Earth and Space Sciences department, the Geological Society of America Fahnestock Award, the Geological Society of America Mackin Award, and the UW Graduate School Top Scholar Award. Henck was supported by NSF-IGERT grant 0333408 and an NSF Graduate Research Fellowship.

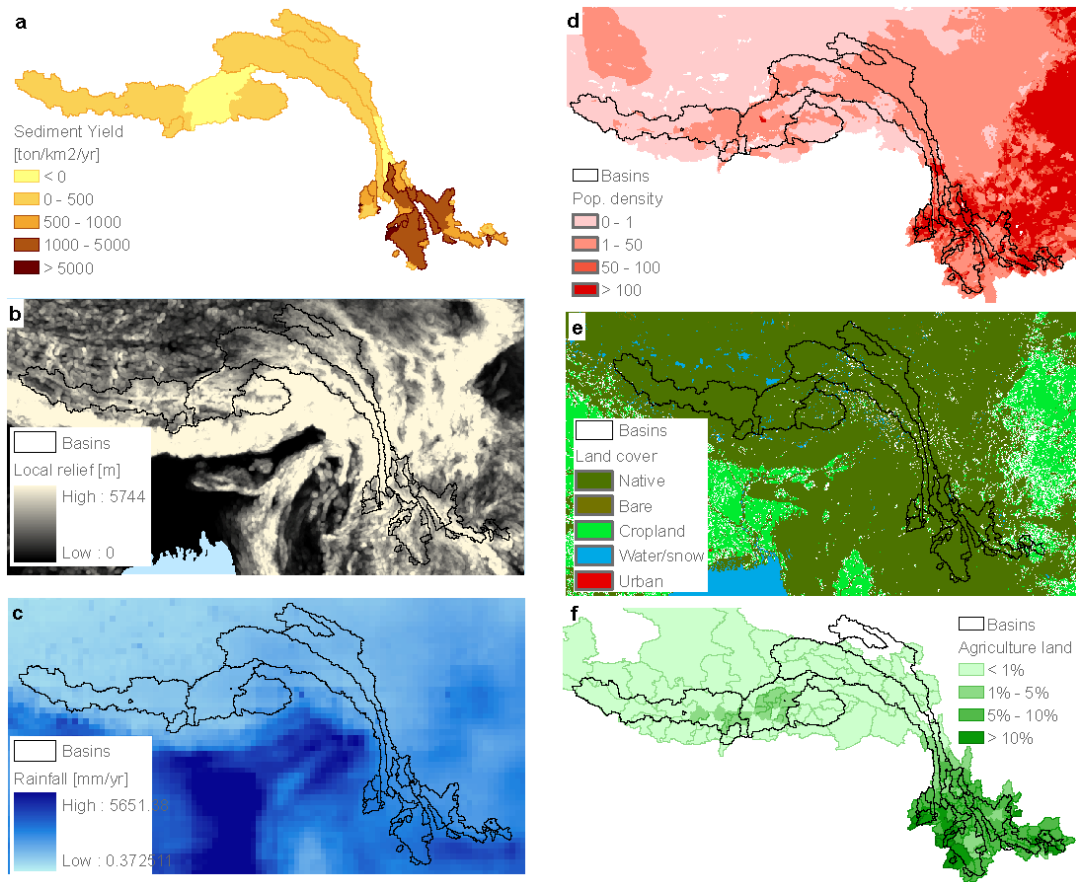
### Figures for chapter 3



**Figure 3.1: Location of the study region in the inset figure and details about that location in the larger figure. Stations for which we analyze sediment yield are shown with blue circles – the darker colors indicated longer periods of record for the stations. Basin boundaries for the area uniquely sampled by each station are shown with brown. Underlying the image are major rivers in the region and elevations in grey scale.**

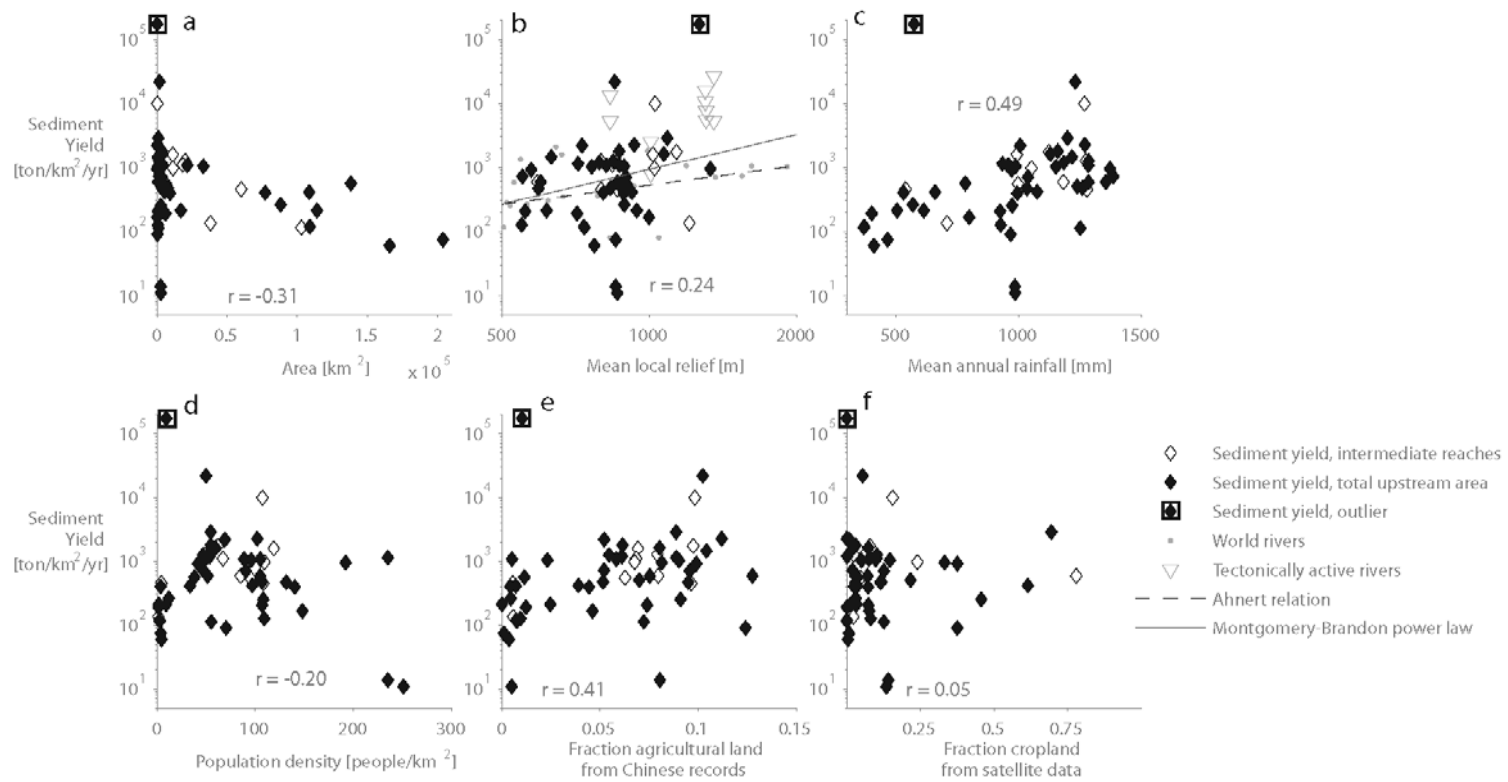


**Figure 3.2: Details on location and quality of sediment yield data. (a) Total suspended sediment as a function of discharge for station 6 in 1969. The scattering of data strongly supports the hypothesis that total suspended sediment was measured daily rather than calculated from a rating curve. This figure also shows how we calculate the slope and y-intercept for figure 5 and the time series analysis. For each year of data we calculate the best fit line in log-log space for concentration of suspended sediment as a function of discharge. The slope and intercept for that best-fit line are used in subsequent analysis. (b) Area above a station calculated from where we located stations against the upstream area reported in the original data books. The correlation has a slope just above 1 and an  $r^2$  value  $> 0.99$ , suggesting that we placed the stations in the correct locations.**



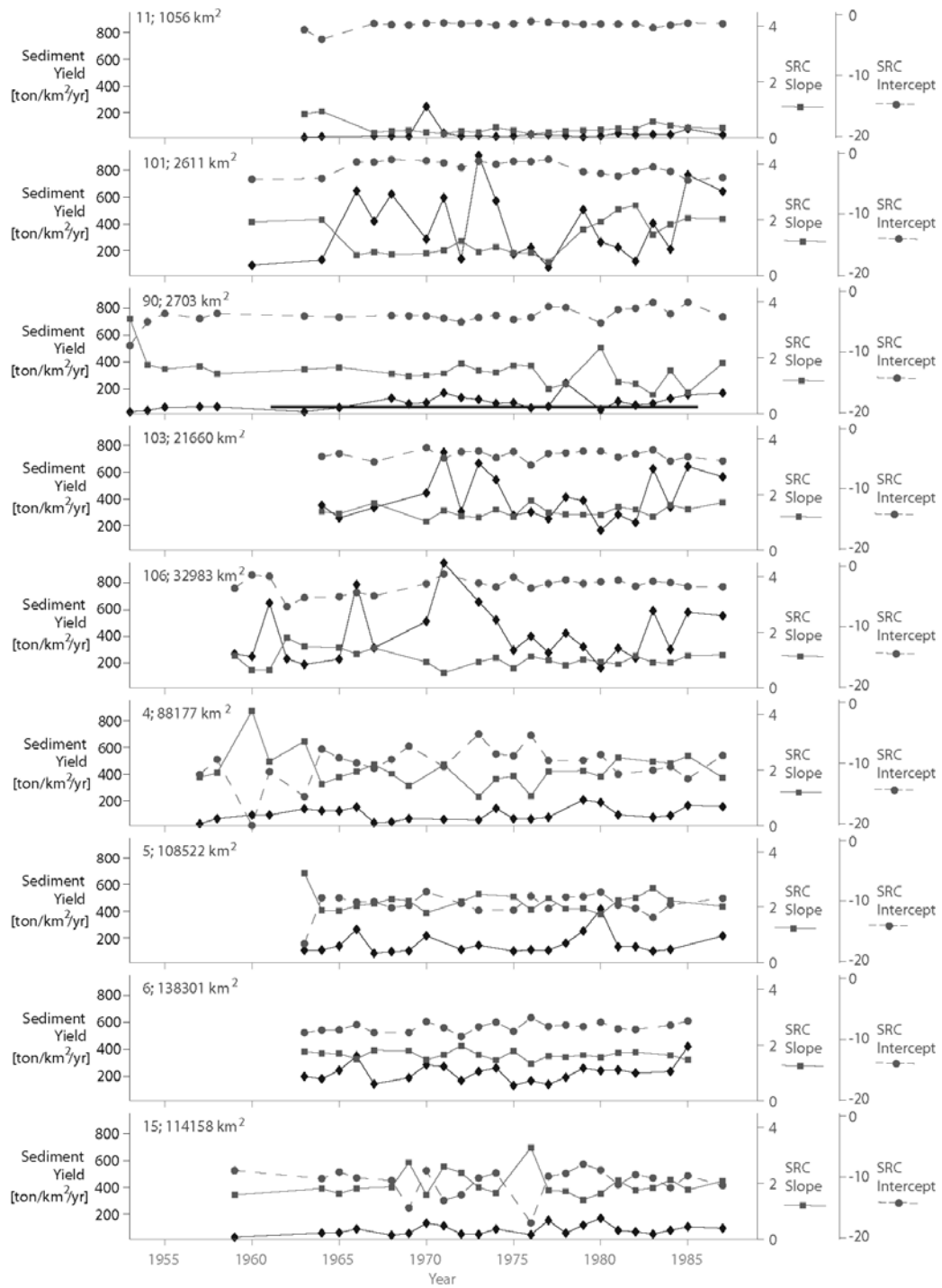
**Figure 3.3: Geomorphic and anthropogenic data about the region. Panel (a) shows the mean annual sediment yield for unique areas sampled by stations. Panels (b) and (c) show geomorphic parameters which are proposed to correlate with sediment yield data – local relief (b) and mean annual rainfall (c). Panels (d), (e), and (f) show the anthropogenic parameters predicted to be related to sediment yield – population density (d), land cover from satellite data (e), and fraction land under cultivation by county from Chinese records (f).**

**Figure 3.4: Scatter plots showing the relation between various geomorphic and anthropogenic metrics and sediment yield. Black diamonds indicate sediment yield for entire upstream area and open diamonds indicate sediment yield for an intermediate reach between two stations. A box is around an outlier point which was left out of correlation analyses. (a) The sediment yield as a function of area. Note the decreasing variation in mean annual sediment yield with increasing basin area, suggesting that basins effectively buffer against sediment loading. (b) The sediment yield as a function of mean local relief. Global data from Montgomery and Brandon (2002) are shown in grey in the background as well as the Ahnert Relation and the power law proposed by Montgomery and Brandon (2002). Our sediment yield values approximately plot on top of world data for the same relief, but with higher scatter. (c) The sediment yield as a function of rainfall reveals a weak correlation between the two. (d) Sediment yield as a function of population density has no correlation. (e) Sediment yield is weakly correlated to fraction agricultural land (based on Chinese county-wide data). Note that on a county-by-county basis, rainfall is strongly correlated with agricultural land, suggesting that people farm more in places with more rain and making it impossible to unravel the two signals. (f) Sediment yield is not correlated to land use as classified with USGS classifications from satellite data.**





**Figure 3.5: Sediment yield and sediment rating curve parameters as a function of time (black line is sediment yield, grey dashed line with circles is the y-intercept, and grey solid line with squares is the slope). Each plot has the station number (for reference to table 1) and upstream area of the station noted. These sediment yield values are for the entire upstream area, not for any intermediate reaches. Details for how we obtained these values are shown in figure 2. An interesting trend in the sediment rating curve figures is that the intercept and slope are inversely correlated to one another. None of the parameters show major trends during the period of record for any station.**



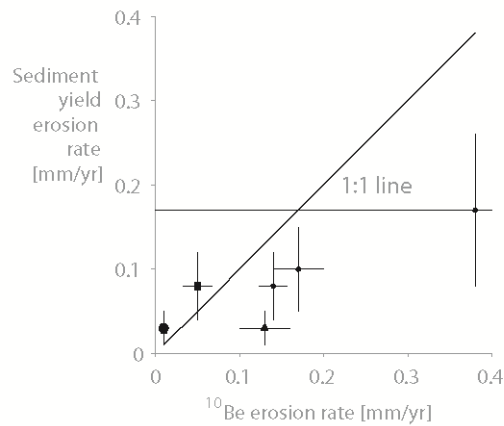


**Figure 3.6: Erosion rate calculated from sediment yield as a function of erosion rate measured over millennial timescales from  $^{10}\text{Be}$  data. Salween data are shown with a square, Mekong data with circles, Yangtze data with a hexagon, and Tsangpo data with a triangle. The modern erosion rates are generally lower than would be expected from the longer term data, with the notable exception of the point on the Yangtze River where sediment yield erosion rates are higher than  $^{10}\text{Be}$  erosion rates and on the Salween River where sediment yield erosion rates are slightly higher than  $^{10}\text{Be}$  erosion rates, but within the error of the sediment yield data. We use reported errors for  $^{10}\text{Be}$  data and estimate 50% errors on sediment yield data. Unfortunately, the areas of data do not overlap for a large area. Salween, Mekong, and Yangtze River  $^{10}\text{Be}$  data are from Henck et al. (2007), Tsangpo River  $^{10}\text{Be}$  data are from Finnegan et al. (2008), and Yangtze River sediment yield erosion rates are calculated from Higgitt and Lu (1996).**

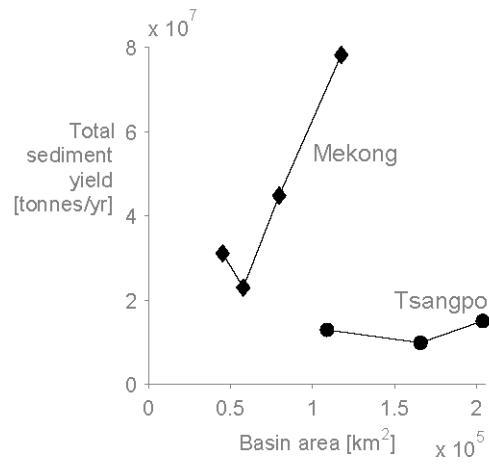


**Figure 3.7: Cumulative sediment yield as a function of upstream area. The slope of the line is the erosion rate between two points. It is apparent from this figure that the upper Tsangpo River has a much lower overall erosion rate than the Mekong River.**

### Tables for chapter 3

**Table 3.1: Summary details on all the stations, including the (a) watershed, river name, station name, and stations upstream, (b) reported station location, our best location for the station, and upstream area, (c) sediment yield, mean annual rainfall, mean local relief, mean population density, fraction cropland, and fraction agricultural land, and (d) all of these parameters for the intermediate reaches between two stations.**

Table 3.1a

Station number	Watershed	River name	Station name	Stations immediately upstream
87	Bu Gu Jiang	Bu Gu Jiang	Zhong Ai Qiao	None
84	Da Ying Jiang	Da Ying Jiang	La He Lian	None
85	Da Ying Jiang	Da Ying Jiang	Xia La Xian	84
96	Dong He	Dong He	Bing Ma	None
55	Lan Cang Jiang (Mekong)	Za Qu He	Xiang Da	None
57	Lan Cang Jiang (Mekong)	Lan Cang Jiang	Liu Tong Jiang	55
35	Lan Cang Jiang (Mekong)	Yong Chun He	Tang Shang	None
4	Lan Cang Jiang (Mekong)	Lan Cang Jiang	Jiu Zhou	35, 57
75	Lan Cang Jiang (Mekong)	Xi Er He	Tian Sheng Qiao	None
43	Lan Cang Jiang (Mekong)	Xi Er He	Si Shi Li Qiao	75
86	Lan Cang Jiang (Mekong)	Hei Hui Jiang	Tian Kou	43
5	Lan Cang Jiang (Mekong)	Lan Cang Jiang	Ga Jiu	86, 4
11	Lan Cang Jiang (Mekong)	Liu Sha He	Meng Hai	None
32	Lan Cang Jiang (Mekong)	Nan Bi He	Meng Sheng	None

Table 3.1a continued

49	Lan Cang Jiang (Mekong)	Jing Gu Da He	Jing Gu	None
70	Lan Cang Jiang (Mekong)	Pu Er He	San Ke Zhuang	None
89	Lan Cang Jiang (Mekong)	Jin Ping He	Xiao He Gou	None
97	Lan Cang Jiang (Mekong)	Ku Ke He	Ke Jie	None
110	Lan Cang Jiang (Mekong)	Bi Jiang	Yun Long	None
6	Lan Cang Jiang (Mekong)	Lan Cang Jiang	Yun Jing Hong	5, 11, 32, 49, 70, 89, 97, 110
100	Long Chuan Jiang	Long Chuan Jiang	Teng Chong Qiao	None
99	Long Chuan Jiang	Long Chuan Jiang	Ga Zhong	100
105	Lv Shui He	Lv Shui He	Lv Shui He	None
108	Lv Shui He	Lv Shui He	Zuo Bei Wu	None
261	Nan Ding He	Nan Ding He	Da Wen	None
93	Nan Ding He	Nan Ding He	Gu Lao He	261
94	Nan Lei He	Nan Lei He	Meng Lian	None
98	Nan Wan He	Nan Wan He	Ma Li Ba	None
109	Nan Xi He	Nan Xi He	Nan Xi Jie	None
15	Nu Jiang (Salween)	Nu Jiang	Dao Jie Ba	None
90	Pan Long He	Pan Long He	Long Tan Zhai	None
91	Pan Long He	Pan Long He	Tian Bao	90
88	Si Nan Jiang	Si Nan Jiang	Da Qiao	None
95	Su Pa He	Su Pa He	Chao Yang	None
102	Yuan Jiang	Pa He	Shui Gou	None
104	Yuan Jiang	Pa He	Mu Gou	102
101	Yuan Jiang	Zha Jiang	Da Dong Yong	None
103	Yuan Jiang	Yuan Jiang	Yuan Jiang	101, 104
106	Yuan Jiang	Yuan Jiang	Man Hao	103
306	Ya Long Zang Bu Jiang (Yarlung Tsangpo)	Nian Chu He	Jiang Ze	None

Table 3.1a continued

301	Ya Long Zang Bu Jiang (Yarlung Tsangpo)	Ya Long Zang Bu Jiang	Nu Ge Sha	306
311	Ya Long Zang Bu Jiang (Yarlung Tsangpo)	La Sa He	Kang Jia	None
302	Ya Long Zang Bu Jiang (Yarlung Tsangpo)	Ya Long Zang Bu Jiang	Yang Cun	301, 311
305	Ya Long Zang Bu Jiang (Yarlung Tsangpo)	Ya Long Zang Bu Jiang	Nu Xia	302

Table 3.1b

Station number	Reported location			Years of data	Where I put the station		
	Latitude	Longitude	Entire upstream area [sq. km]		Latitude	Longitude	Area [sq. km]
87	23.35	101.50	3564	17	23.35	101.50	3610
84	24.70	97.97	4225	6	24.75	98.05	4022
85	24.68	98.27	5476	17	24.69	97.92	4243
96	25.00	99.40	N/A	2	25.00	99.40	3641
55	32.30	96.20	17909	20	32.35	96.43	16959
57	28.82	98.82	68280	4	28.83	98.65	77090
35	27.17	99.63	247	18	27.15	99.32	199
4	25.83	99.38	84220	26	25.81	99.20	88177
75	25.62	100.20	2513	2	25.62	100.22	2519
43	25.60	100.10	2591	6	25.56	100.10	2693
86	25.35	100.02	9394	12	25.35	100.01	9209
5	24.60	100.47	105660	23	24.60	100.47	108522
11	21.95	100.42	1032	23	21.95	100.43	1056
32	23.38	99.42	1766	5	23.38	99.42	1746
49	23.50	100.70	2773	20	23.55	100.71	1891
70	22.88	100.70	1372	2	22.89	100.70	1381
89	22.65	103.30	109	10	22.85	103.14	231
97	24.87	99.77	1755	17	24.52	100.49	3235
110	25.90	99.37	211	1	25.85	99.51	182
6	21.88	101.07	141380	22	21.85	101.03	138301
100	24.63	98.83	3487	18	24.64	98.63	3684
99	24.00	98.43	10084	6	24.07	97.98	7905
105	23.00	103.27	181	6	23.29	103.73	285
108	23.03	103.45	63	7	23.26	103.63	318
261	23.95	100.10	657	1	23.68	99.24	690
93	23.68	99.23	3628	20	23.95	100.10	3924
94	22.33	99.58	775	16	22.33	99.58	746
98	24.42	97.97	294	2	24.42	97.98	280
109	22.65	104.05	3476	18	22.82	103.90	907
15	25.10	99.15	118760	23	25.11	98.85	114158



Table 3.1b continued

90	23.45	104.28	3410	27	23.40	104.22	2704
91	22.95	104.77	5123	14	22.98	104.79	5299
88	22.97	101.90	2083	9	23.10	101.85	1610
95	24.43	98.80	459	1	24.43	98.78	441
102	24.67	102.27	691	10	24.69	102.24	537
104	24.65	102.22	691	6	24.68	102.23	610
101	25.10	100.57	2373	23	25.07	100.56	2611
103	23.63	102.15	19320	21	23.63	101.99	21660
106	22.85	103.55	29889	25	22.85	103.57	32983
306	28.90	89.60	6200	10	28.85	89.65	5980
301	29.38	89.78	110415	11	29.30	89.79	108957
311	29.88	91.78	20.367	5	29.89	91.82	14
302	29.30	91.97	156808	10	29.26	91.97	165838
305	29.45	94.57	191222	12	29.46	94.56	203904

Table 3.1c

Station number	Mean annual sediment yield [ton/km <sup>2</sup> /yr]	Mean local relief [m]	Mean annual rainfall [mm/yr]	Mean population density (people/km <sup>2</sup> )	Fraction cropland (from satellite data)	Fraction agricultural land (from Chinese data)
87	1790	869	1160	55	0.03	0.06
84	589	862	1285	105	0.07	0.08
85	1074	870	1284	105	0.08	0.01
96	472	594	1034	132	0.11	0.10
55	211	617	505	2	0.01	0.00
57	404	806	532	4	0.02	0.00
35	167	1000	799	148	0.08	0.05
4	261	890	570	12	0.03	0.00
75	14	854	986	235	0.14	0.08
43	11	861	986	251	0.13	0.01
86	395	887	995	140	0.07	0.04
5	413	922	660	34	0.04	0.01
11	113	486	1252	55	0.13	0.07
32	21919	850	1231	50	0.05	0.10
49	1196	790	1184	54	0.00	0.06
70	720	551	1386	47	0.02	0.05
89	950	1334	1372	192	0.33	0.08
97	709	896	1039	91	0.13	0.10
110	2198	729	1007	69	0.01	0.05
6	566	895	783	38	0.04	0.01
100	507	874	1239	106	0.22	0.07
99	476	833	1260	107	0.12	0.05
105	913	574	973	42	0.38	0.10
108	90	368	968	70	0.38	0.12
261	1027	763	1153	48	0.05	0.09
93	1624	1071	1130	59	0.07	0.08
94	593	600	1356	51	0.03	0.13
98	2266	932	1270	102	0.00	0.11
109	2879	1090	1200	55	0.69	0.09
15	212	944	614	9	0.03	0.02
90	252	347	974	108	0.46	0.09

Table 3.1c continued

91	419	466	1076	97	0.61	0.04
88	1252	844	1286	47	0.10	0.05
95	1455	631	1218	55	0.01	0.10
102	205	558	925	107	0.07	0.07
104	127	549	927	109	0.08	0.01
101	1139	716	935	235	0.08	0.09
103	1076	818	955	89	0.10	0.06
106	1038	889	989	96	0.15	0.02
306	191	712	402	1	0.00	0.01
301	119	736	371	3	0.00	0.01
311	173750	1266	574	9	0.00	0.01
302	60	773	411	4	0.00	0.00
305	74	854	466	4	0.01	0.00

Table 3.1d

Station	Area [km <sup>2</sup> ]	Mean annual sediment yield [ton/km <sup>2</sup> /yr]	Mean local relief [m]	Mean annual rainfall [mm/yr]	Mean population density [people/km <sup>2</sup> ]	Fraction cropland (from satellite data)	Fraction agricultural land (from Chinese data)
104	72	-452	480	944	126	0.14	0.08
85	221	9900	1028	1268	108	0.16	0.10
57	60131	458	861	539	4	0.03	0.01
4	10888	-747	1505	844	69	0.07	0.04
75	2519	14	854	986	235	0.14	0.08
43	174	-30	960	994	480	0.04	0.08
86	6516	554	898	998	95	0.05	0.06
5	11136	1598	1018	993	119	0.04	0.07
6	20058	1273	796	1275	48	0.02	0.08
99	4220	450	798	1279	108	0.03	0.10
93	3234	1752	1137	1125	62	0.08	0.10
91	2595	593	591	1183	85	0.78	0.08
103	18439	1098	841	959	67	0.10	0.07
106	11323	966	1025	1053	109	0.24	0.07
301	102977	115	737	369	3	0.00	0.01
302	56867	-66	843	487	8	0.01	0.01
305	38066	135	1209	708	1	0.02	0.01

### Notes for chapter 3

- Ali, J., and Benjaminsen, T. A. (2004). Fuelwood, timber and deforestation in the Himalayas - The case of Basho Valley, Baltistan Region, Pakistan. *Mountain Research and Development* 24, 312-318.
- Anders, A., Roe, G. H., Hallet, B., Montgomery, D. R., Finnegan, N., and Putkonen, J. (2006). Spatial patterns of precipitation and topography in the Himalaya. In "Tectonics, Climate, and Landscape Evolution." (S. D. Willett, N. Hovius, M. T. Brandon, and D. Fisher, Eds.), pp. 39-53. Geological Society of America.
- Blaikie, P. M., and Muldavin, J. S. S. (2004). Upstream, downstream, China, India: The politics of environment in the Himalayan region. *Annals of the Association of American Geographers* 94, 520-548.
- CDC, C. D. C. (2009a). Tibet Provincial Yearbook (1997). In "Provincial Yearbook." All China Data Center, url: <http://chinadataonline.org>.
- CDC, C. D. C. (2009b). Yunnan Provincial Yearbook (1997). In "Provincial Yearbooks." All China Data Center, url: <http://chinadataonline.org>.
- Chen, G. J. (2000). Major causes of soil erosion in the Upper Yangtze River valley and the control countermeasures (in Chinese). *Rural Eco2Environment* 16, 5-8.
- Chen, Z., Li, J, Shen, H, Wang, Z. (2001). Yangtze River of China: historical analysis of discharge variability and sediment flux. *Geomorphology* 41, 77-91.
- Deichmann, U. (1996). The ASIA Population Database (G. Geneva, Ed.). United Nations Environment Programme, url: <http://www.grida.no/prog/global/cgiar/htmls/asiademo.htm>.
- EPA. (2006). Integration of Stream Stability, Reference Condition & Sediment Rating Curves. In "Watershed Assessment of River Stability & Sediment Supply."

Environmental Protection Agency, url:  
<http://www.epa.gov/warsss/sedsource/rivrelat.htm>.

- Feng, J. K., and He, Y. H. (2004). Nu Jiang, Lancang Jiang, and Jinsha Jiang: Researches on the Exploitation of Hydropower Resources and the Protection of the Environment. Social Sciences Academic Press (China).
- Finnegan, N. J., Hallet, B., Montgomery, D. R., Zeitler, P. K., Stone, J., Anders, A., and Liu, Y. (2008). Coupling of rock uplift and river incision in the Namche Barwa-Gyala Peri massif, Tibet. *Geological Society of America Bulletin* 120, 142-155.
- Forsyth, T. (1996). Science, myth, and knowledge: testing Himalayan environmental degradation in Thailand. *Geoforum* 27, 375-392.
- Galy, A., and France-Lanord, C. (2001). Higher erosion rates in the Himalaya: Geochemical constraints on riverine fluxes. *Geology* 29, 23-26.
- Hassan, M. A., Church, M., Xu, J. X., and Yan, Y. X. (2008). Spatial and temporal variation of sediment yield in the landscape: Example of Huanghe (Yellow River). *Geophysical Research Letters* 35, L06401.
- Henck, A., Stone, J. O., Montgomery, D. R., and Hallet, B. (2007). Patterns of erosion in the Three Rivers Area, Eastern Tibet. *Geological Society of America Abstracts with Programs* 39, 183.
- Higgitt, D. L., and Lu, X. (1996). Patterns of sediment yield in the Upper Yangtze basin, China. *Erosion and Sediment Yield: Global and Regional Perspectives* IAHS Pub. No. 236, 205-214.
- Higgitt, D. L., and Lu, X. X. (1999). Challenges in relating land use to sediment yield in the Upper Yangtze. *Hydrobiologia* 410, 269-277.

- Hyde, W. F., Belcher, B., and Xu, J. T. (2003). *China's Forest: Global Lessons from Market Reforms. Resources for the Future*, Washington, DC.
- IUCN, W. C. U. (2006). A report of a joint reactive monitoring mission to the Three Parallel Rivers of Yunnan Protected Areas, China. *In "Report to the UNESCO committee."*
- Ives, J. D. (1987). The Theory of Himalayan Environmental Degradation - Its validity and application challenged by recent research. *Mountain Research and Development* 7, 189-199.
- Lopes, V. L., Follitt, P. F., and Baker, J., M.B. (2001). Impacts of vegetative practices on suspended sediment from watersheds in Arizona. *Journal of Water Resource Planning and Management* 127, ASCE.
- Lowdermilk, W. C. (1924). Erosion and floods in the Yellow River watershed. *Journal of Forestry* 22, 11-18.
- Lu, X. X., Ashmore, P., and Wang, J. (2003a). Sediment yield mapping in a large river basin: the Upper Yangtze, China. *Environmental Modelling & Software* 18, 339-353.
- Lu, X. X., Ashmore, P., and Wang, J. F. (2003b). Seasonal water discharge and sediment load changes in the Upper Yangtze, China. *Mountain Research and Development* 23, 56-64.
- Lu, X. X., and Higgitt, D. L. (1998). Recent changes of sediment yield in the Upper Yangtze, China. *Environmental Management* 22, 697-709.
- Lu, X. X., and Higgitt, D. L. (1999). Sediment yield variability in the Upper Yangtze, China. *Earth Surface Processes and Landforms* 24, 1077-1093.

- Lu, X. X., and Higgitt, D. L. (2000). Estimating erosion rates on sloping agricultural land in the Yangtze Three Gorges, China, from caesium-137 measurements. *Catena* 39, 33-51.
- Ma, J. (2004). "China's Water Crisis (translated from Zhongguo Shui Weiji)." East Bridge, Norwalk.
- Magee, D. (2006). Powershed Politics: Hydropower and Interprovincial Relations under Great Western Development. *The China Quarterly* 185.
- Ministry of Hydrology, P. (1962-1989). "Zangdian Guoji Heliu Shuiwen Ziliao (District 9 Region 2 1947-1987) (in Chinese)." Yunnansheng Shuiwen Zongzhan Geming Weiyuanhui Kanyin.
- Ministry of Water Conservancy and Electric Power, P. (1962). "National Standards for Hydrological Survey (in Chinese)." China Industry Press, Beijing.
- Ministry of Water Conservancy and Electric Power, P. (1975). "Handbook for Hydrological Survey (in Chinese)." Water Conservancy and Electric Power Press, Beijing.
- Perdue, P. C. (1982). Water Control in the Dongting Lake Region during the Ming and Qing Periods. *Journal of Asian Studies* 41, 747-765.
- Piest, R. F., Bradford, J., and Spomer, R. G. (1975). Mechanisms of erosion and sediment movement from gullies. In "Present and Prospective Technology for Predicting Sediment Yields and Sources." pp. ARS-S-40. USDA, USDA Sed. Lab, Oxford, Mississippi.
- Saito, Y., Yang, Z. S., and Hori, K. (2001). The Huange (Yellow River) and Changjiang (Yangtze River) deltas: a review on their characteristics, evolution and sediment discharge during the Holocene. *Geomorphology* 41, 219-231.



- Shapiro, J. (2001). *Mao's War Against Nature: Politics and the Environment in Revolutionary China*. Cambridge University Press, Cambridge.
- Simon, A., and Hupp, C. R. (1986). Channel evolution in modified Tennessee stream. *In* "4th Federal Interagency Sedimentation Conference." pp. 5.71-5.82. US Government Printing Offices, Washington, DC, Las Vegas, Nevada.
- Singh, S. K., and France-Lanord, C. (2002). Tracing the distribution of erosion in the Brahmaputra watershed from isotopic compositions of stream sediments. *Earth and Planetary Science Letters* 202, 645-662.
- Syvitski, J. P. M. (2003). Supply and flux of sediment along hydrological pathways: research for the 21st century. *Global and Planetary Change* 39, 1-11.
- Syvitski, J. P. M., Vorosmarty, C. J., Kettner, A. J., and Green, P. (2005). Impact of humans on the flux of terrestrial sediment to the global coastal ocean. *Science* 308, 376-380.
- Trac, C. J., Harrell, S., Hinckley, T. M., and Henck, A. (2007). Reforestation programs in Southwest China: reported success, observed failure, and the reasons why. *Journal of Mountain Science* 4, 275 - 292.
- Urgenson, L. S., Harrell, S., Hinckley, T. M., Hagmann, R. K., Grub, B. L., Henck, A., Chi, P. M., and Shepler, S. J. (in review). Social-ecological dynamics of a forested watershed in SW China. *Society and Ecology*.
- USGS. (2008). Eurasia land cover characteristics data base version 2.0. *In* "Global Land Cover Characterization." (USGS, Ed.).
- Wang, S. J., Hassan, M. A., and Xie, X. P. (2006). Relationship between suspended sediment load, channel geometry and land area increment in the Yellow River Delta. *Catena* 65, 302-314.

- Wang, Z. Y., Huang, W. D., and Li, Y. T. (2007a). Sediment budget of the Yangtze River. *Journal of Sediment Research*, 1-10.
- Wang, Z. Y., Li, Y. T., and He, Y. P. (2007b). Sediment budget of the Yangtze River. *Water Resources Research* 43, 14.
- Winkler, D. (1996). Forests, forest economy and deforestation in the Tibetan Prefectures of west Sichuan. *Commonwealth Forest Review* 75, 296-301.
- Wolman, M. (1967). A cycle of sedimentation and erosion in urban river channels. *Geografiska Annaler* 49, 385-395.
- Xu, J. X. (2000). Runoff and sediment variations in the upper reaches of Changjiang River and its tributaries due to deforestation (in Chinese). *Shuili Xuebao*, 72-80.
- Xu, J. X. (2005). Variation in grain size of suspended load in upper Changjiang River and its tributaries by human activities (in Chinese). *Journal of Sediment Research*, 8-16.
- Xu, J. X., and Cheng, D. S. (2002). Relation between erosion and sedimentation zones in the Yellow River, China. *Geomorphology* 48, 365-382.
- Yang, G. F., Chen, Z. Y., Yu, F. L., Wang, Z. H., Zhao, Y. W., and Wang, Z. Q. (2007). Sediment rating parameters and their implications: Yangtze River, China. *Geomorphology* 85, 166-175.
- Yi, Z. W. (2003). Upper Yangtze River sediments (in Chinese). *Sichuan Shuili*, 29-32.
- Yin, H. F., and Li, C. G. (2001). Human impact on floods and flood disasters on the Yangtze River. *Geomorphology* 41, 105-109.
- Zhang, X. B. (1999). Status and causes of sediment change in the Upper Yangtze River and sediment reduction measures - comparison of Jialing River with Jinsha River (in Chinese). *Soil Water Conservation in China*, 22-24.

Zhang, X. B., and Wen, A. B. (2002). Variations of sediment in upper stream of Yangtze River and its tributary (in Chinese). *Shuili Xuebao*, 56-59.

Zhang, X. B., and Wen, A. B. (2004). Current changes of sediment yields in the upper Yangtze River and its two biggest tributaries, China. *Global and Planetary Change* 41, 221-227.

## **Chapter 4: Monsoon control of effective discharge, Yunnan and Tibet**

### **Introduction**

As recent interest in the interplay between climate, tectonics, and erosion has focused on the Himalayas and Tibet as a natural laboratory for understanding such processes (e.g., Brozovic et al., 1997; Galy and France-Lanord, 2001; Finlayson et al., 2002; Burbank et al., 2003; Thiede et al., 2008), some researchers have concluded that mean annual rainfall is strongly correlated with, and possibly driving, average erosion rates (Gabet et al., 2008), whereas others conclude that erosion and precipitation are decoupled (Burbank et al., 2003). Although these analyses have more typically employed mean annual rainfall, it is often assumed that up to 90% of sediment transport happens during only the highest 10% of discharges (Meade, 1982), suggesting that mean annual rainfall will not necessarily set erosion rates. Therefore, some researchers suggest that monsoon (Craddock et al., 2007) or storm event (Snyder et al., 2003) rainfall may be the controlling factor on erosion rates, rather than annual rainfall. In monsoon regions, the longstanding question of whether frequent events, such as monsoons, or infrequent events, such as large storms, transport more sediment remains little explored.

The concept of effective discharge ( $Q_{\text{eff}}$ ) is a useful tool for evaluating the relative roles of large and small storms and the monsoon climate of south and southeast Tibet in transporting sediment. Following Wolman and Miller (1960), we

define  $Q_{\text{eff}}$  as the discharge which transports the most suspended sediment, integrated over the record available. The concept initially was used by Wolman and Miller (1960) to show that large, infrequent events do less work over time than moderate events which occur more frequently. They calculated  $Q_{\text{eff}}$  using a flow-frequency curve and a sediment rating curve, the product of which had a peak they defined as  $Q_{\text{eff}}$ .

Since this initial analysis, two schools of thought have emerged around the concept of  $Q_{\text{eff}}$  (Crowder and Knapp, 2005). The first is that  $Q_{\text{eff}}$  is the dominant discharge in setting channel properties (i.e., channel forming flow), is approximately equal to the flow which recurs every 1.5 years and fills the banks of the channel (e.g., Wolman and Miller, 1960; Leopold et al., 1964; Dury, 1973; Andrews, 1980; Leopold, 1994; Rosgen, 1994; Andrews and Nankervis, 1995; Rosgen and Silvey, 1996). The second is that rivers respond differently to a variety of discharges and the concept of a dominant discharge is virtually meaningless. This is in part because some researchers have found widely varying recurrence intervals associated with  $Q_{\text{eff}}$  which are thought to be the result of varying morphology, hydrologic regimes, size of sediment transported, and watershed areas (e.g., Benson and Thomas, 1966; Pickup and Warner, 1976; Williams, 1978; Ashmore and Day, 1988; Nash, 1994; Hey, 1998; Castro and Jackson, 2001; Phillips, 2002). Subsequently, some have proposed that rivers have two important

discharges; one for suspended sediment that transports the most sediment and one for bedload that forms the channel (Phillips, 2002).

Rivers dominated by monsoon climates have received little attention in this ongoing debate surrounding  $Q_{\text{eff}}$ . Kale (2002) reports that Indian rivers are dominated by the monsoon climate of the region and that in this environment large floods control channel form. A detailed analysis of discharges and stream power for Narmada River (Kale, 2008) and Tapi River (Kale and Hire, 2004; 2007), both on the Indian Peninsula, reveals that monsoon flows are geomorphically effective for transporting pebbles during most of the monsoon, but that channel altering flows recur much less frequently (possibly with recurrence intervals longer than 100 years). However, these analyses are primarily based on potential stream power estimated from discharge and channel cross-sections rather than sediment concentration and yield in the rivers.

Instead of estimating potential for sediment transport from stream power or estimating sediment yield from a rating curve, we calculate effective discharges using complete years of daily mean discharge and daily mean total suspended sediment data for 44 hydrology stations in Yunnan and Tibet (Fig. 1). We use these data to investigate climatic controls on sediment yield in monsoon rivers. Based on the results discussed above, we expect that  $Q_{\text{eff}}$  will recur for up to 3-6 months a year if the monsoon controls suspended sediment transport and less than once a year if channel forming flows are also  $Q_{\text{eff}}$  for suspended sediment transport.

Additionally, we expect that if  $Q_{\text{eff}}$  is monsoon controlled, then those discharges would be exceeded only during the monsoon.

## Methods

Reported values of  $Q_{\text{eff}}$  are highly dependent on the way the calculation is performed (Crowder and Knapp, 2005). In particular, the discharge must be binned to create a histogram and the value calculated for  $Q_{\text{eff}}$  depends on the size and number of bins used (Biedenharn and Copeland, 2000). Typically, discharge measurements are taken much more frequently than sediment yield measurements, meaning that sediment yield must be estimated. The method used to estimate sediment yield has been the subject of much debate and can potentially greatly affect the calculated  $Q_{\text{eff}}$  (Wolman and Miller, 1960; Benson and Thomas, 1966; Pickup and Warner, 1976; Crowder and Knapp, 2005). To avoid many of these problems, we use sediment concentrations and discharges measured daily over periods of complete years.

We use data from rivers in southwest China and Tibet collected by the Chinese Ministry of Hydrology and compiled in a series of books (Ministry of Hydrology, 1962-1989) which we digitized for this analysis. The stations have upstream areas ranging in size from 14 to 203,904 km<sup>2</sup> and 1 to 27 years of data (data repository item, Fig. 1). Although no methods are given for how the data were collected, based on analysis of sediment rating curves which show poor correlation between discharge and suspended sediment at all stations, we conclude that

suspended sediment is not likely to have been measured using a rating curve. No error estimates are reported for these data in the original sources.

We calculated  $Q_{\text{eff}}$  for all stations in the region with at least one full year (365 days in the same calendar year) of total suspended sediment and discharge data and only use data from years for which there is a full year of both sediment and discharge data. Because we are in the unique position of having sediment yield data available for entire years of the data record, we calculated the sediment yield for each day, then binned the daily sediment yield by discharge, creating a histogram of daily sediment yield. Following Crowder and Knapp (2005), we initially used 25 bins for discharge and added bins until the peak of the histogram is not in the first bin. The peak of the histogram of daily sediment yield is the  $Q_{\text{eff}}$  for that station.

To calculate the recurrence interval (RI) of  $Q_{\text{eff}}$ , we used the daily flow frequency curves created with all the discharge data used to calculate  $Q_{\text{eff}}$  rather than a flood frequency curve. We did this because many studies have found  $Q_{\text{eff}}$  is smaller than the lowest annual flood on record (e.g., Benson and Thomas, 1966; Nolan et al., 1987; Ashmore and Day, 1988; Crowder and Knapp, 2005). This is a systematic way to treat recurrence frequencies which are lower than annual and we report recurrence frequencies measured in days rather than years.

To further investigate the spatial and temporal scaling of  $Q_{\text{eff}}$ , we calculated the range of possible values of  $Q_{\text{eff}}$  and RI as if only a subset of data years were



available. Starting with one year of data, we calculated all the possible  $Q_{\text{eff}}$  and RI values for each individual year of data. We then performed this calculation for all pairs of data, all triplets, and so on up to using all the data for a given station. For sets of years for which there would be more than 10,000 possible combinations of years of data, we used a Monte Carlo simulation to choose 10,000 random combinations of the correct number of years. We repeated this calculation for all stations with more than one complete year of data.

## Results and discussion

RI for  $Q_{\text{eff}}$  for these data varies between 2 and 243 days (Table 1). A probability density function of RI shows a peak at 11 days for both calculations which included all years of data for each station and calculations which included only a subset of years of data selected using a Monte Carlo simulation (Fig. 2). As would be expected, there is a log-linear relationship between  $Q_{\text{eff}}$  and the ratio of effective discharge to mean daily flow (Fig. 3a;  $r = 0.80$ ). We find no relationship between recurrence interval of  $Q_{\text{eff}}$  and either basin area or the number of years of data available (Fig. 3b-c).

Typical annual hydrographs for all stations show that the monsoon base flow is approximately equal to  $Q_{\text{eff}}$  (Fig. 4), suggesting that an RI of 11 days does not mean that  $Q_{\text{eff}}$  is exceeded during 33 individual storms, but instead that it is exceeded for the entire month which is the peak of the monsoon. These results demonstrate that in the monsoon region of Yunnan and Tibet, rivers move the most

sediment during the peak of the monsoon. In this case,  $Q_{\text{eff}}$  is not a function of individual stochastic events; it is simply a measure of the strength of the monsoon. Since these flows recur many times a year and are lower than the annual flood, they are not likely to be channel-forming flows (Kale, 2002; Kale and Hire, 2004; 2007; Kale, 2008), showing that in monsoon climates  $Q_{\text{eff}}$  and channel forming flows are distinct discharges.

### **Conclusions**

Our analysis demonstrates that monsoon base flow is  $Q_{\text{eff}}$  in Yunnan and Tibet and suggests that monsoon discharge is more important than individual storms in sediment transport for rivers in monsoon regions. In general, suspended sediment is transported in these systems during the monsoon and the base flow during the peak of the monsoon exceeds the  $Q_{\text{eff}}$  each year. The fact that  $Q_{\text{eff}}$  for most stations is higher than the mean annual flow and the peak distribution of RI is only 11 days shows that  $Q_{\text{eff}}$  in this part of the world is different from the channel forming flows.

If our observations in Tibet and Yunnan are characteristic of other monsoon systems, the adage that up to 90% of the sediment transport happens 10% of the time (Meade, 1982) does not hold for monsoonal rivers. Instead, in rivers dominated by a monsoon climate, the base flow during the monsoon is the discharge which transports the most sediment. This discharge recurs for several months a year and is distinct from the channel forming discharge.

In light of these results, models of landscape evolution or erosion processes in the Himalaya and other monsoonal regions should model sediment transport as happening during monsoon discharges rather than during stochastic large flood events. Similarly, studies of correlations between rainfall and erosion rate should focus on monsoon rainfall rather than mean annual rainfall.

**Acknowledgments**

This chapter was submitted for publication with David R. Montgomery, Katharine W. Huntington, and Liang Chuan as coauthors. Henck was supported by an NSF Graduate Research Fellowship while doing this research. Thanks to Vivian Leung for encouraging the analysis and to Alison Anders for suggesting it.

### Figures for chapter 4

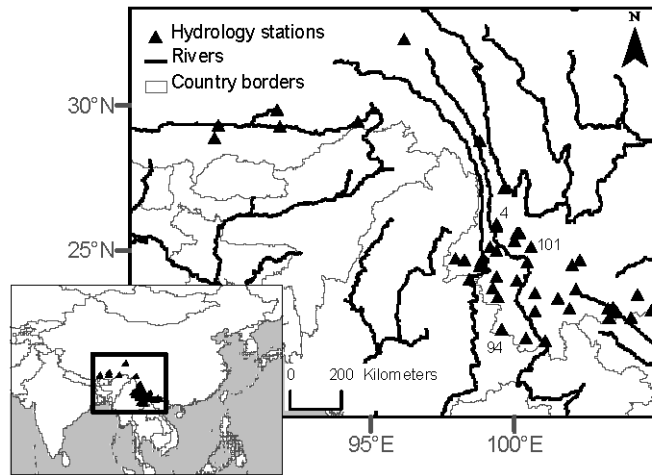


**Figure 4.1:** Map showing location of stations analyzed. Stations 4, 94, 101 are labeled since data about them are shown in more detail in figure 4.

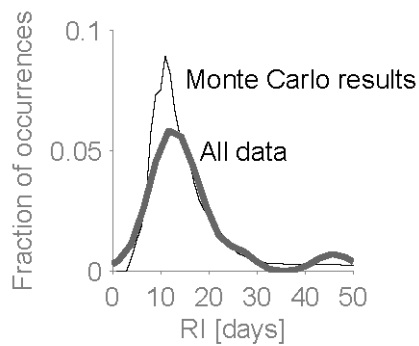


**Figure 4.2:** Histograms of distribution of RI for calculations using all data for each station (wider grey line) and using all permutations for 1 to all years of data for each station (thin black line). Both have peaks below at 11 days with large tails to higher RI, showing a strong controlling influence of monsoons on  $Q_{\text{eff}}$  in this region. We have truncated the figure at  $RI = 50$  days because of the long tails.

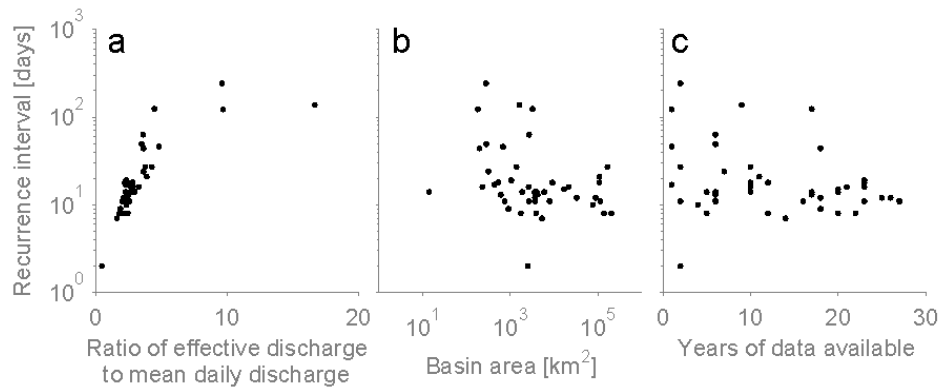


**Figure 4.3: RI as a function of ratio of effective discharge to mean daily discharge, basin area, and years of data available. (a) The relationship between the ratio of effective discharge to mean daily discharge and the recurrence interval. This is a log-linear relationship with  $r^2 = 0.84$ . (b) The variation in calculated recurrence intervals does not decrease with basin area. (c) The variation in calculated recurrence intervals does not change with increasing number of years of data.**

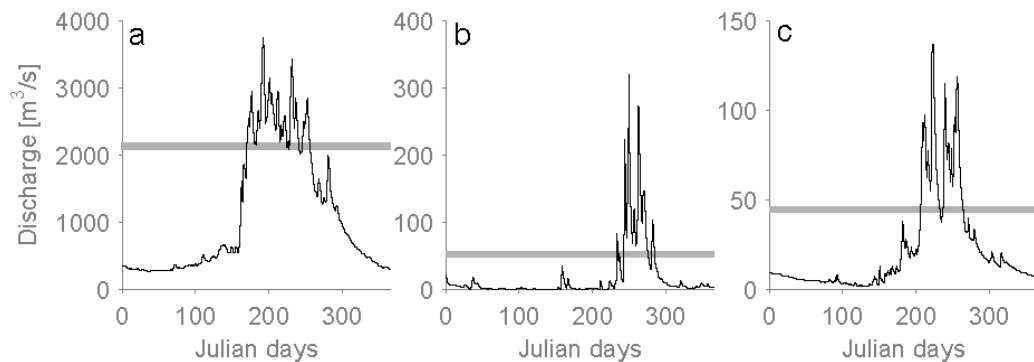


**Figure 4.4: Hydrographs (thin black line) and  $Q_{eff}$  (wider grey line) for (a) station 4 in 1963, (b) station 101 in 1987, and (c) station 94 in 1974. These show that  $Q_{eff}$  is exceeded for most of the monsoon. These years and stations are typical among the stations analyzed.**

## Tables for chapter 4

**Table 4.1: Details on stations and effective discharge calculations**

Station number	Longitude	Latitude	Upstream area [km <sup>2</sup> ]	Years of data available	Q <sub>eff</sub> [m <sup>3</sup> /s]	RI [days]	Mean daily flow [m <sup>3</sup> /s]
87	101.50	23.35	3610	17	210	14	80
84	97.97	24.70	4022	6	449	14	193
85	98.27	24.68	4243	17	423	13	175
96	99.40	25.00	3641	2	46	11	18
55	96.20	32.30	16959	20	383	15	136
57	98.82	28.82	77090	4	1817	10	771
35	99.63	27.17	199	18	11	44	3
4	99.38	25.83	88177	26	2138	12	939
75	100.20	25.62	2519	2	14	2	28
43	100.10	25.60	2693	6	98	63	27
86	100.02	25.35	9209	12	358	18	126
5	100.47	24.60	108522	23	3059	18	1236
11	100.42	21.95	1056	23	42	19	18
32	99.42	23.38	1746	5	111	8	45
49	100.70	23.50	1891	20	144	14	54
70	100.70	22.88	1381	2	99	27	23
89	103.30	22.65	231	10	20	16	7
97	99.37	24.08	3235	17	99	124	22
110	99.37	25.90	182	1	185	122	19
6	101.07	21.88	138301	22	3296	8	1797
100	98.83	24.63	3684	18	371	12	155
99	98.43	24.00	7905	6	589	11	226
105	103.27	23.00	285	6	74	49	21
108	103.45	23.03	318	7	11	24	3
93	99.23	23.68	690	1	68	46	14
261	100.10	23.95	3924	20	176	8	89
94	99.57	22.27	746	16	45	11	18
98	98.25	24.43	280	2	135	243	14
109	104.05	22.65	907	18	165	9	86
15	99.15	25.10	114158	23	3801	11	1665

Table 4.1 continued

90	104.28	23.45	2704	27	53	11	26
91	104.77	22.95	5299	14	154	7	93
88	101.90	22.97	1610	9	735	137	44
95	98.80	24.43	441	1	53	17	23
102	102.27	24.67	537	10	9	18	4
104	102.02	24.48	610	6	5	13	2
101	100.57	25.10	2611	23	53	16	16
103	102.15	23.63	21660	21	455	16	168
106	103.55	22.85	32983	25	609	12	285
311	91.78	29.88	5980	10	65	14	22
306	89.60	28.90	108957	11	1806	21	461
301	89.72	29.33	14	5	771	14	256
302	91.88	29.28	165838	10	3281	27	863
305	94.57	29.47	203904	12	3927	8	1801



## Notes for chapter 4

- Andrews, E. D. (1980). Effective and Bankfull Discharges of Streams in the Yampa River Basin, Colorado and Wyoming. *Journal of Hydrology* 46, 311-330.
- Andrews, E. D., and Nankervis, J. M. (1995). Effective discharge and the design of channel maintenance flows for gravel-bed rivers. In "Natural and Anthropogenic Influences in Fluvial Geomorphology." (J. E. Costa, A. J. Miller, K. W. Potter, and P. R. Wilcock, Eds.), pp. 151-164. American Geophysical Union.
- Ashmore, P., and Day, T. J. (1988). Effective discharge for suspended sediment transport in streams of the Saskatchewan River Basin. *Water Resources Research* 24, 864-870.
- Benson, M. A., and Thomas, D. M. (1966). A definition of dominant discharge. *Bulletin of the International Association of Hydrologists* 11, 76-80.
- Biedenharn, D. S., and Copeland, R. R. (2000). Effective discharge calculation. *ERDC/CHL CHETN-VIII-4* US Army Corps of Engineers.
- Brozovic, N., Burbank, D. W., and Meigs, A. J. (1997). Climatic limits on landscape development in the northwestern Himalaya. *Science* 276, 571-574.
- Burbank, D. W., Blythe, A. E., Putkonen, J., Pratt-Sitaula, B., Gabet, E., Oskin, M., Barros, A., and Ojha, T. P. (2003). Decoupling of erosion and precipitation in the Himalayas. *Nature* 426, 652-655.
- Castro, J. M., and Jackson, P. L. (2001). Bankfull discharge recurrence intervals and regional hydraulic geometry relationships: Patterns in the Pacific Northwest, USA. *Journal of the American Water Resources Association* 37, 1249-1262.
- Craddock, W. H., Burbank, D. W., Bookhagen, B., and Gabet, E. J. (2007). Bedrock channel geometry along an orographic rainfall gradient in the upper Marsyandi River valley in central Nepal. *Journal of Geophysical Research-Earth Surface* 112, F03008, doi:10.1029/2006JF000717.

- Crowder, D. W., and Knapp, H. V. (2005). Effective discharge recurrence intervals of Illinois streams. *Geomorphology* 64, 167-184.
- Dury, G. H. (1973). Magnitude-frequency analysis and channel morphology. In "Fluvial Geomorphology." (M. Morisawa, Ed.), pp. 281-293. SUNY, Binghamton.
- Finlayson, D. P., Montgomery, D. R., and Hallet, B. (2002). Spatial coincidence of rapid inferred erosion with young metamorphic massifs in the Himalayas. *Geology* 30, 219-222.
- Gabet, E. J., Burbank, D. W., Pratt-Sitaula, B., Putkonen, J., and Bookhagen, B. (2008). Modern erosion rates in the High Himalayas of Nepal. *Earth and Planetary Science Letters* 267, 482-494.
- Galy, A., and France-Lanord, C. (2001). Higher erosion rates in the Himalaya: Geochemical constraints on riverine fluxes. *Geology* 29, 23-26.
- Hey, R. D. (1998). Frequency and duration of bankfull flow and application for natural channel design. In "Wetlands Engineering and River Restoration Conference." (D. F. Hays, Ed.), Denver, CO, USA.
- Kale, V. S. (2002). Fluvial geomorphology of Indian rivers: an overview. *Progress in Physical Geography* 26, 400-433.
- Kale, V. S. (2008). A half-a-century record of annual energy expenditure and geomorphic effectiveness of the monsoon-fed Narmada River, central India. *Catena* 75, 154-163.
- Kale, V. S., and Hire, P. S. (2004). Effectiveness of monsoon floods on the Tapi River, India: role of channel geometry and hydrologic regime. *Geomorphology* 57, 275-291.

- Kale, V. S., and Hire, P. S. (2007). Temporal variations in the specific stream power and total energy expenditure of a monsoonal river: The Tapi River, India. *Geomorphology* 92, 134-146.
- Leopold, L. B. (1994). "A View of the River." Harvard University Press, Cambridge, MA, USA.
- Leopold, L. B., Wolman, M. G., and Miller, J. P. (1964). "Fluvial Processes in Geomorphology." W.H. Freeman, San Francisco.
- Meade, R. H. (1982). Sources, sinks, and storage of river sediment in the atlantic drainage of the United States. *The Journal of Geology* 90, 235-252.
- Ministry of Hydrology, P. (1962-1989). "Zangdian Guoji Heliu Shuiwen Ziliao (District 9 Region 2 1947-1987) (in Chinese)." Yunnansheng Shuiwen Zongzhan Geming Weiyuanhui Kanyin.
- Nash, D. B. (1994). Effective Sediment-Transporting Discharge from Magnitude-Frequency Analysis. *Journal of Geology* 102, 79-95.
- Nolan, K. M., Lisle, T. E., and Kelsey, H. M. (1987). Bankfull discharge and sediment transport in northwestern California. In "Erosion and Sedimentation in the Pacific Rim." pp. 439-449. IAHS Publication.
- Phillips, J. D. (2002). Geomorphic impacts of flash flooding in a forested headwater basin. *Journal of Hydrology* 269, 236-250.
- Pickup, G., and Warner, R. F. (1976). Effects of Hydrologic Regime on Magnitude and Frequency of Dominant Discharge. *Journal of Hydrology* 29, 51-75.
- Rosgen, D. L. (1994). A Classification of Natural Rivers. *Catena* 22, 169-199.
- Rosgen, D. L., and Silvey, H. L. I. (1996). "Applied River Morphology." Wildland Hydrology, Pagosa Springs, CO.

- Snyder, N. P., Whipple, K. X., Tucker, G. E., and Merritts, D. J. (2003). Importance of a stochastic distribution of floods and erosion thresholds in the bedrock river incision problem. *Journal of Geophysical Research-Solid Earth* 108, 2117.
- Thiede, R. C., Ehlers, T. A., Bookhagen, B., and Strecker, M. R. (2008). Erosional variability along the northwest Himalaya.
- Williams, G. P. (1978). Bank-Full Discharge of Rivers. *Water Resources Research* 14, 1141-1154.
- Wolman, M. G., and Miller, J. P. (1960). Magnitude and Frequency of Forces in Geomorphic Processes. *Journal of Geology* 68, 54-74.

## Bibliography

Aalto, R., Dunne, T., and Guyot, J. L. (2006). Geomorphic controls on Andean denudation rates. *Journal of Geology* 114, 85-99.

Ahnert, F. (1970). Functional relationships between denudation, relief, and uplift in large mid-latitude drainage basins. *American Journal of Science* 268, 243-263.

Ali, J., and Benjaminsen, T. A. (2004). Fuelwood, timber and deforestation in the Himalayas - The case of Basho Valley, Baltistan Region, Pakistan. *Mountain Research and Development* 24, 312-318.

Anders, A., Roe, G. H., Hallet, B., Montgomery, D. R., Finnegan, N., and Putkonen, J. (2006). Spatial patterns of precipitation and topography in the Himalaya. In "Tectonics, Climate, and Landscape Evolution." (S. D. Willett, N. Hovius, M. T. Brandon, and D. Fisher, Eds.), pp. 39-53. Geological Society of America.

Anders, A., Roe, G. H., Montgomery, D. R., and Hallet, B. (2008). Influence of precipitation phase on the form of mountain ranges. *Geology* 36, 479-482.

Andrews, E. D. (1980). Effective and Bankfull Discharges of Streams in the Yampa River Basin, Colorado and Wyoming. *Journal of Hydrology* 46, 311-330.

Andrews, E. D., and Nankervis, J. M. (1995). Effective discharge and the design of channel maintenance flows for gravel-bed rivers. In "Natural and Anthropogenic Influences in Fluvial Geomorphology." (J. E. Costa, A. J. Miller, K. W. Potter, and P. R. Wilcock, Eds.), pp. 151-164. American Geophysical Union.

Ashmore, P., and Day, T. J. (1988). Effective discharge for suspended sediment transport in streams of the Saskatchewan River Basin. *Water Resources Research* 24, 864-870.

- Balco, G. (2006). Converting Al and Be isotope ratio measurements to nuclide concentrations in quartz. *Documentation - Be-10 / 26-Al exposure age calculator*  
Online: [http://hess.ess.washington.edu/math/docs/common/ams\\_data\\_reduction/](http://hess.ess.washington.edu/math/docs/common/ams_data_reduction/).
- Balco, G., Stone, J. O., Lifton, N. A., and Dunai, T. J. (2008). A complete and easily accessible means of calculating surface exposure ages or erosion rates from Be-10 and Al-26 measurements. *Quaternary Geochronology* 3, 174-195.
- Barnes, J. B., and Pelletier, J. D. (2006). Latitudinal variation of denudation in the evolution of the Bolivian Andes. *American Journal of Science* 306, 1-31.
- Benson, M. A., and Thomas, D. M. (1966). A definition of dominant discharge. *Bulletin of the International Association of Hydrologists* 11, 76-80.
- Biedenharn, D. S., and Copeland, R. R. (2000). Effective discharge calculation. *ERDC/CHL CHETN-VIII-4* US Army Corps of Engineers.
- Bierman, P. R., and Steig, E. J. (1996). Estimating rates of denudation using cosmogenic isotope abundances in sediment. *Earth Surface Processes and Landforms* 21, 125-139.
- Bierman, P. R., and Caffee, M. (2001). Slow rates of rock surface erosion and sediment production across the Namib Desert and escarpment, southern Africa. *American Journal of Science* 301, 326-358.
- Bierman, P. R., and Caffee, M. (2002). Cosmogenic exposure and erosion history of Australian bedrock landforms. *Geological Society of America Bulletin* 114, 787-803.
- Bierman, P. R. (2004). Rock to sediment - Slope to sea with Be-10 - Rates of landscape change. *Annual Review of Earth and Planetary Sciences* 32, 215-255.

- Binnie, S. A., Phillips, W. M., Summerfield, M. A., and Fifield, L. K. (2007). Tectonic uplift, threshold hillslopes, and denudation rates in a developing mountain range. *Geology* 35, 743-746.
- Blaikie, P. M., and Muldavin, J. S. S. (2004). Upstream, downstream, China, India: The politics of environment in the Himalayan region. *Annals of the Association of American Geographers* 94, 520-548.
- Booth, A. L., Chamberlain, C. P., Kidd, W. S. F., and Zeitler, P. K. (2009). Constraints on the metamorphic evolution of the eastern Himalayan syntaxis from geochronologic and petrologic studies of Namche Barwa. *Geological Society of America Bulletin* 121, 385-407.
- Brookfield, M. E. (1998). The evolution of the great river systems of southern Asia during the Cenozoic India-Asia collision: rivers draining southwards. *Geomorphology* 22, 285-312.
- Brown, E. T., Stallard, R. F., Larsen, M. C., Raisbeck, G. M., and Yiou, F. (1995). Denudation rates determined from the accumulation of in situ-produced be-10 in the Luquillo Experimental Forest, Puerto-Rico. *Earth and Planetary Science Letters* 129, 193-202.
- Brozovic, N., Burbank, D. W., and Meigs, A. J. (1997). Climatic limits on landscape development in the northwestern Himalaya. *Science* 276, 571-574.
- Burbank, D. W., Leland, J., Fielding, E., Anderson, R. S., Brozovic, N., Reid, M. R., and Duncan, C. (1996). Bedrock incision, rock uplift and threshold hillslopes in the northwestern Himalayas. *Nature* 379, 505-510.
- Burbank, D. W., Blythe, A. E., Putkonen, J., Pratt-Sitaula, B., Gabet, E., Oskin, M., Barros, A., and Ojha, T. P. (2003). Decoupling of erosion and precipitation in the Himalayas. *Nature* 426, 652-655.

- Burg, J. P., Davy, P., Nievergelt, P., Oberli, F., Seward, D., Diao, Z. Z., and Meier, M. (1997). Exhumation during crustal folding in the Namche-Barwa syntaxis. *Terra Nova* 9, 53-56.
- Burtman, V. S., and Molnar, P. (1993). Geological and geophysical evidence for deep subduction of continental crust beneath the Pamir. *Geological Society of America Special Paper* 281, 1-76.
- Castro, J. M., and Jackson, P. L. (2001). Bankfull discharge recurrence intervals and regional hydraulic geometry relationships: Patterns in the Pacific Northwest, USA. *Journal of the American Water Resources Association* 37, 1249-1262.
- CDC, C. D. C. (2009a). Yunnan Provincial Yearbook (1997). In "Provincial Yearbooks." All China Data Center, url: <http://chinadataonline.org>.
- CDC, C. D. C. (2009b). Tibet Provincial Yearbook (1997). In "Provincial Yearbook." All China Data Center, url: <http://chinadataonline.org>.
- Champagnac, J. D., Schlunegger, F., Norton, K., von Blanckenburg, F., Abbuhl, L. M., and Schwab, M. (2009). Erosion-driven uplift of the modern Central Alps. *Tectonophysics* 474, 236-249.
- Chen, G. J. (2000). Major causes of soil erosion in the Upper Yangtze River valley and the control countermeasures (in Chinese). *Rural Eco2Environment* 16, 5-8.
- Chen, Z., Li, J, Shen, H, Wang, Z. (2001). Yangtze River of China: historical analysis of discharge variability and sediment flux. *Geomorphology* 41, 77-91.
- Clark, M., and Royden, L. (2000). Topographic ooze: Building the eastern margin of Tibet by lower crustal flow. *Geology* 28, 703-706.



- Clark, M., Royden, L., Whipple, K., Burchfiel, B., Zhang, X., and Tang, W. (2006). Use of a regional, relict landscape to measure vertical deformation of the eastern Tibetan Plateau. *Journal of Geophysical Research-Earth Surface* 111, doi:10.1029/2005JF000294.
- Clark, M. K., Schoenbohm, L. M., Royden, L. H., Whipple, K. X., Burchfiel, B. C., Zhang, X., Tang, W., Wang, E., and Chen, L. (2004). Surface uplift, tectonics, and erosion of eastern Tibet from large-scale drainage patterns. *Tectonics* 23. doi: 10.1029/2002TC001402.
- Clark, M. K., Bush, J. W. M., and Royden, L. H. (2005a). Dynamic topography produced by lower crustal flow against rheological strength heterogeneities bordering the Tibetan Plateau. *Geophysical Journal International* 162, 575-590.
- Clark, M. K., House, M. A., Royden, L. H., Whipple, K. X., Burchfiel, B. C., Zhang, X., and Tang, W. (2005b). Late Cenozoic uplift of southeastern Tibet. *Geology* 33, 525-528.
- Craddock, W. H., Burbank, D. W., Bookhagen, B., and Gabet, E. J. (2007). Bedrock channel geometry along an orographic rainfall gradient in the upper Marsyandi River valley in central Nepal. *Journal of Geophysical Research-Earth Surface* 112, -.
- Crowder, D. W., and Knapp, H. V. (2005). Effective discharge recurrence intervals of Illinois streams. *Geomorphology* 64, 167-184.
- Cyr, A. J., and Granger, D. E. (2008). Dynamic equilibrium among erosion, river incision, and coastal uplift in the northern and central Apennines, Italy. *Geology* 36, 103-106.

- Dadson, S. J., Hovius, N., Chen, H. G., Dade, W. B., Hsieh, M. L., Willett, S. D., Hu, J. C., Horng, M. J., Chen, M. C., Stark, C. P., Lague, D., and Lin, J. C. (2003). Links between erosion, runoff variability and seismicity in the Taiwan orogen. *Nature* 426, 648-651.
- DeCelles, P. G., Robinson, D. M., and Zandt, G. (2002). Implications of shortening in the Himalayan fold-thrust belt for uplift of the Tibetan Plateau. *Tectonics* 21, 10.1029/2001TC001322.
- Deichmann, U. (1996). The ASIA Population Database (G. Geneva, Ed.). United Nations Environment Programme, url:  
<http://www.grida.no/prog/global/cgiar/htmls/asiademo.htm>.
- Demoulin, A., Hallot, E., and Rixhon, G. (2009). Amount and controls of the Quaternary denudation in the Ardennes massif (western Europe). *Earth Surface Processes and Landforms* 34, 1487-1496.
- Ding, L., Zhong, D. L., Yin, A., Kapp, P., and Harrison, T. M. (2001). Cenozoic structural and metamorphic evolution of the eastern Himalayan syntaxis (Namche Barwa). *Earth and Planetary Science Letters* 192, 423-438.
- Dixon, J. L., Heimsath, A. M., and Amundson, R. (2009). The critical role of climate and saprolite weathering in landscape evolution. *Earth Surface Processes and Landforms* 34, 1507-1521.
- Dury, G. H. (1973). Magnitude-frequency analysis and channel morphology. In "Fluvial Geomorphology." (M. Morisawa, Ed.), pp. 281-293. SUNY, Binghamton.
- Enkelmann, E., Ratschbacher, L., Johnckheere, R., Nestler, R., Fleischer, M., Gloaguen, R., Hacker, B., Zhang, Y. Q., and Ma, Y. S. (2006). Cenozoic exhumation and deformation of northeastern Tibet and the Qinling; is Tibetan lower crustal flow diverging around the Sichuan Basin? *Geological Society of America Bulletin* 118, 651-671.

- EPA. (2006). Integration of Stream Stability, Reference Condition & Sediment Rating Curves. In "Watershed Assessment of River Stability & Sediment Supply." Environmental Protection Agency, url: <http://www.epa.gov/warsss/sedsource/rivrelat.htm>.
- Feng, J. K., and He, Y. H. (2004). Nu Jiang, Lancang Jiang, and Jinsha Jiang: Researches on the Exploitation of Hydropower Resources and the Protection of the Environment. Social Sciences Academic Press (China).
- Fielding, E., Isacks, B., Barazangi, M., and Duncan, C. (1994). How flat is Tibet. *Geology* 22, 163-167.
- Finlayson, D. P., Montgomery, D. R., and Hallet, B. (2002). Spatial coincidence of rapid inferred erosion with young metamorphic massifs in the Himalayas. *Geology* 30, 219-222.
- Finnegan, N. J., Roe, G., Montgomery, D. R., and Hallet, B. (2005). Controls on the channel width of rivers: Implications for modeling fluvial incision of bedrock. *Geology* 33, 229-232.
- Finnegan, N. J., Hallet, B., Montgomery, D. R., Zeitler, P. K., Stone, J., Anders, A., and Liu, Y. (2008). Coupling of rock uplift and river incision in the Namche Barwa-Gyala Peri massif, Tibet. *Geological Society of America Bulletin* 120, 142-155.
- Forsyth, T. (1996). Science, myth, and knowledge: testing Himalayan environmental degradation in Thailand. *Geoforum* 27, 375-392.
- Gabet, E. J., Pratt-Sitaula, B. A., and Burbank, D. W. (2004). Climatic controls on hillslope angle and relief in the Himalayas. *Geology* 32, 629-632.
- Gabet, E. J., Burbank, D. W., Pratt-Sitaula, B., Putkonen, J., and Bookhagen, B. (2008). Modern erosion rates in the High Himalayas of Nepal. *Earth and Planetary Science Letters* 267, 482-494.

- Galy, A., and France-Lanord, C. (2001). Higher erosion rates in the Himalaya: Geochemical constraints on riverine fluxes. *Geology* 29, 23-26.
- Granger, D. E., Kirchner, J. W., and Finkel, R. (1996). Spatially averaged long-term erosion rates measured from in situ-produced cosmogenic nuclides in alluvial sediment. *Journal of Geology* 104, 249-257.
- Hallet, B., and Molnar, P. (2001). Distorted drainage basins as markers of crustal strain east of the Himalaya. *Journal of Geophysical Research-Solid Earth* 106, 13697-13709.
- Harkins, N., Kirby, E., Heimsath, A., Robinson, R., and Reiser, U. (2007). Transient fluvial incision in the headwaters of the Yellow River, northeastern Tibet, China. *Journal of Geophysical Research-Earth Surface* 112, F03S04.
- Hassan, M. A., Church, M., Xu, J. X., and Yan, Y. X. (2008). Spatial and temporal variation of sediment yield in the landscape: Example of Huanghe (Yellow River). *Geophysical Research Letters* 35, L06401.
- Henck, A., Stone, J. O., Montgomery, D. R., and Hallet, B. (2007). Patterns of erosion in the Three Rivers Area, Eastern Tibet. *Geological Society of America Abstracts with Programs* 39, 183.
- Hey, R. D. (1998). Frequency and duration of bankfull flow and application for natural channel design. In "Wetlands Engineering and River Restoration Conference." (D. F. Hays, Ed.), Denver, CO, USA.
- Higgitt, D. L., and Lu, X. (1996). Patterns of sediment yield in the Upper Yangtze basin, China. *Erosion and Sediment Yield: Global and Regional Perspectives* IAHS Pub. No. 236, 205-214.
- Higgitt, D. L., and Lu, X. X. (1999). Challenges in relating land use to sediment yield in the Upper Yangtze. *Hydrobiologia* 410, 269-277.

- Hodges, K. V. (2000). Tectonics of the Himalaya and southern Tibet from two perspectives. *Geological Society of America Bulletin* 112, 324-350.
- Hodges, K. V., Wobus, C., Ruhl, K., Schildgen, T., and Whipple, K. (2004). Quaternary deformation, river steepening, and heavy precipitation at the front of the Higher Himalayan ranges. *Earth and Planetary Science Letters* 220, 379-389.
- Hooke, R. L. (1999). Spatial distribution of human geomorphic activity in the United States: Comparison with rivers. *Earth Surface Processes and Landforms* 24, 687-692.
- Hooke, R. L. (2000). On the history of humans as geomorphic agents. *Geology* 28, 843-846.
- Hyde, W. F., Belcher, B., and Xu, J. T. (2003). China's Forest: Global Lessons from Market Reforms. Resources for the Future, Washington, DC.
- IUCN, W. C. U. (2006). A report of a joint reactive monitoring mission to the Three Parallel Rivers of Yunnan Protected Areas, China. In "Report to the UNESCO committee."
- Ives, J. D. (1987). The Theory of Himalayan Environmental Degradation - Its validity and application challenged by recent research. *Mountain Research and Development* 7, 189-199.
- Jayko, A. S. (2005). Late Quaternary denudation, Death and Panamint Valleys, eastern California. *Earth-Science Reviews* 73, 271-289.
- Kale, V. S. (2002). Fluvial geomorphology of Indian rivers: an overview. *Progress in Physical Geography* 26, 400-433.

- Kale, V. S., and Hire, P. S. (2004). Effectiveness of monsoon floods on the Tapi River, India: role of channel geometry and hydrologic regime. *Geomorphology* 57, 275-291.
- Kale, V. S., and Hire, P. S. (2007). Temporal variations in the specific stream power and total energy expenditure of a monsoonal river: The Tapi River, India. *Geomorphology* 92, 134-146.
- Kale, V. S. (2008). A half-a-century record of annual energy expenditure and geomorphic effectiveness of the monsoon-fed Narmada River, central India. *Catena* 75, 154-163.
- Kirby, E., Reiners, P. W., Krol, M. A., Whipple, K. X., Hodges, K. V., Farley, K. A., Tang, W. Q., and Chen, Z. L. (2002). Late Cenozoic evolution of the eastern margin of the Tibetan Plateau: Inferences from Ar-40/Ar-39 and (U-Th)/He thermochronology. *Tectonics* 21, 10.1029/2000TC001246.
- Kober, F., Ivy-Ochs, S., Schlunegger, F., Baur, H., Kubik, P. W., and Wieler, R. (2007). Denudation rates and a topography-driven rainfall threshold in northern Chile: Multiple cosmogenic nuclide data and sediment yield budgets. *Geomorphology* 83, 97-120.
- Kohl, C. P., and Nishiizumi, K. (1992). Chemical isolation of quartz for measurement of insitu-produced cosmogenic nuclides. *Geochimica Et Cosmochimica Acta* 56, 3583-3587.
- Kong, P., Na, C. G., Fink, D., Ding, L., and Huang, F. X. (2007). Erosion in northwest Tibet from in-situ-produced cosmogenic Be-10 and Al-26 in bedrock. *Earth Surface Processes and Landforms* 32, 116-125.
- Koons, P. O., Hallet, B., Henck, A., Liu, Y., and Zeitler, P. K. (2005). Topographic expression of crustal velocity curls: an example from Eastern Himalaya to Burma. *Eos Transactions AGU; Fall Meeting Supplement* 87.

- Lal, D., Harris, N. B. W., Sharma, K. K., Gu, Z. Y., Ding, L., Liu, T. S., Dongal, W. Q., Caffee, M. W., and Jull, A. J. T. (2004). Erosion history of the Tibetan Plateau since the last interglacial: constraints from the first studies of cosmogenic Be-10 from Tibetan bedrock. *Earth and Planetary Science Letters* 217, 33-42.
- Leopold, L. B., Wolman, M. G., and Miller, J. P. (1964). "Fluvial Processes in Geomorphology." W.H. Freeman, San Francisco.
- Leopold, L. B. (1994). "A View of the River." Harvard University Press, Cambridge, MA, USA.
- Liu, Y., and Zhong, D. (1997). Petrology of high-pressure granulites from the eastern Himalayan syntaxis. *Journal of Metamorphic Geology* 15, 451-466.
- Lopes, V. L., Folliott, P. F., and Baker, J., M.B. (2001). Impacts of vegetative practices on suspended sediment from watersheds in Arizona. *Journal of Water Resource Planning and Management* 127, ASCE.
- Lowdermilk, W. C. (1924). Erosion and floods in the Yellow River watershed. *Journal of Forestry* 22, 11-18.
- Lu, X. X., and Higgitt, D. L. (1998). Recent changes of sediment yield in the Upper Yangtze, China. *Environmental Management* 22, 697-709.
- Lu, X. X., and Higgitt, D. L. (1999). Sediment yield variability in the Upper Yangtze, China. *Earth Surface Processes and Landforms* 24, 1077-1093.
- Lu, X. X., and Higgitt, D. L. (2000). Estimating erosion rates on sloping agricultural land in the Yangtze Three Gorges, China, from caesium-137 measurements. *Catena* 39, 33-51.

- Lu, X. X., Ashmore, P., and Wang, J. (2003a). Sediment yield mapping in a large river basin: the Upper Yangtze, China. *Environmental Modelling & Software* 18, 339-353.
- Lu, X. X., Ashmore, P., and Wang, J. F. (2003b). Seasonal water discharge and sediment load changes in the Upper Yangtze, China. *Mountain Research and Development* 23, 56-64.
- Ma, J. (2004). "China's Water Crisis (translated from Zhongguo Shui Weiji)." East Bridge, Norwalk.
- Magee, D. (2006). Powershed Politics: Hydropower and Interprovincial Relations under Great Western Development. *The China Quarterly* 185.
- Malloy, M. (2004). "Rapid erosion at the Tsangpo knickpoint and exhumation of southeastern Tibet." Unpublished M.S. thesis, Lehigh University.
- Matmon, A., Bierman, P. R., Larsen, J., Southworth, S., Pavich, M., and Caffee, M. (2003a). Temporally and spatially uniform rates of erosion in the southern Appalachian Great Smoky Mountains. *Geology* 31, 155-158.
- Matmon, A., Bierman, P. R., Larsen, J., Southworth, S., Pavich, M., Finkel, R., and Caffee, M. (2003b). Erosion of an ancient mountain range, the Great Smoky Mountains, North Carolina and Tennessee. *American Journal of Science* 303, 817-855.
- Meade, R. H. (1982). Sources, sinks, and storage of river sediment in the atlantic drainage of the United States. *The Journal of Geology* 90, 235-252.
- Ministry of Hydrology, P. (1962-1989). "Zangdian Guoji Heliu Shuiwen Ziliao (District 9 Region 2 1947-1987) (in Chinese)." Yunnansheng Shuiwen Zongzhan Geming Weiyuanhui Kanyin.



- Ministry of Water Conservancy and Electric Power, P. (1962). "National Standards for Hydrological Survey (in Chinese)." China Industry Press, Beijing.
- Ministry of Water Conservancy and Electric Power, P. (1975). "Handbook for Hydrological Survey (in Chinese)." Water Conservancy and Electric Power Press, Beijing.
- Molnar, P., Anderson, R. S., and Anderson, S. P. (2007). Tectonics, fracturing of rock, and erosion. *Journal of Geophysical Research-Earth Surface* 112, 10.1029/2005JF000433.
- Montgomery, D. R., Balco, G., and Willett, S. D. (2001). Climate, tectonics, and the morphology of the Andes. *Geology* 29, 579-582.
- Montgomery, D. R., and Brandon, M. T. (2002). Topographic controls on erosion rates in tectonically active mountain ranges. *Earth and Planetary Science Letters* 201, 481-489.
- Mora, A., Parra, M., Strecker, M. R., Sobel, E. R., Hooghiemstra, H., Torres, V., and Jaramillo, J. V. (2008). Climatic forcing of asymmetric orogenic evolution in the Eastern Cordillera of Colombia. *Geological Society of America Bulletin* 120, 930-949.
- Nash, D. B. (1994). Effective Sediment-Transporting Discharge from Magnitude-Frequency Analysis. *Journal of Geology* 102, 79-95.
- Niemi, N. A., Oskin, M., Burbank, D. W., Heimsath, A. M., and Gabet, E. (2005). Effects of bedrock landslides on cosmogenically determined erosion rates. *Earth and Planetary Science Letters* 237, 489-498.

- Nishiizumi, K., Imamura, M., Caffee, M. W., Southon, J. R., Finkel, R. C., and McAninch, J. (2007). Absolute calibration of Be-10 AMS standards. *Nuclear Instruments & Methods in Physics Research Section B-Beam Interactions with Materials and Atoms* 258, 403-413.
- Nolan, K. M., Lisle, T. E., and Kelsey, H. M. (1987). Bankfull discharge and sediment transport in northwestern California. In "Erosion and Sedimentation in the Pacific Rim." pp. 439-449. IAHS Publication.
- Ouimet, W. B. (2007). "Dissecting the eastern margin of the Tibetan plateau: a study of landslides, erosion and river incision in a transient landscape." Massachusetts Institute of Technology. PhD Dissertation.
- Ouimet, W. B., Whipple, K. X., and Granger, D. E. (2009). Beyond threshold hillslopes: Channel adjustment to base-level fall in tectonically active mountain ranges. *Geology* 37, 579-582.
- Perdue, P. C. (1982). Water Control in the Dongting Lake Region during the Ming and Qing Periods. *Journal of Asian Studies* 41, 747-765.
- Phillips, J. D. (2002). Geomorphic impacts of flash flooding in a forested headwater basin. *Journal of Hydrology* 269, 236-250.
- Pickup, G., and Warner, R. F. (1976). Effects of Hydrologic Regime on Magnitude and Frequency of Dominant Discharge. *Journal of Hydrology* 29, 51-75.
- Piest, R. F., Bradford, J., and Spomer, R. G. (1975). Mechanisms of erosion and sediment movement from gullies. In "Present and Prospective Technology for Predicting Sediment Yields and Sources." pp. ARS-S-40. USDA, USDA Sed. Lab, Oxford, Mississippi.

- Quigley, M., Sandiford, M., Fifield, L. K., and Alimanovic, A. (2007). Landscape responses to intraplate tectonism: Quantitative constraints from Be-10 nuclide abundances. *Earth and Planetary Science Letters* 261, 120-133.
- Reiners, P. W., Ehlers, T. A., Mitchell, S. G., and Montgomery, D. R. (2003). Coupled spatial variations in precipitation and long-term erosion rates across the Washington Cascades. *Nature* 426, 645-647.
- Riebe, C. S., Kirchner, J. W., Granger, D. E., and Finkel, R. C. (2001). Minimal climatic control on erosion rates in the Sierra Nevada, California. *Geology* 29, 447-450.
- Roering, J. J., Kirchner, J. W., and Dietrich, W. E. (1999). Evidence for nonlinear, diffusive sediment transport on hillslopes and implications for landscape morphology. *Water Resources Research* 35, 853-870.
- Rosgen, D. L. (1994). A Classification of Natural Rivers. *Catena* 22, 169-199.
- Rosgen, D. L., and Silvey, H. L. I. (1996). "Applied River Morphology." Wildland Hydrology, Pagosa Springs, CO.
- Royden, L. H., Burchfiel, B. C., King, R. W., Wang, E., Chen, Z. L., Shen, F., and Liu, Y. P. (1997). Surface deformation and lower crustal flow in eastern Tibet. *Science* 276, 788-790.
- Safran, E. B., Bierman, P. R., Aalto, R., Dunne, T., Whipple, K. X., and Caffee, M. (2005). Erosion rates driven by channel network incision in the Bolivian Andes. *Earth Surface Processes and Landforms* 30, 1007-1024.
- Saito, Y., Yang, Z. S., and Hori, K. (2001). The Huange (Yellow River) and Changjiang (Yangtze River) deltas: a review on their characteristics, evolution and sediment discharge during the Holocene. *Geomorphology* 41, 219-231.

- Schoenbohm, L. M., Whipple, K. X., Burchfiel, B. C., and Chen, L. (2004). Geomorphic constraints on surface uplift, exhumation, and plateau growth in the Red River region, Yunnan Province, China. *Geological Society of America Bulletin* 116, 895-909.
- Schoenbohm, L. M., Burchfiel, B. C., and Chen, L. Z. (2006a). Propagation of surface uplift, lower crustal flow, and Cenozoic tectonics of the southeast margin of the Tibetan Plateau. *Geology*. 34, 813-816.
- Schoenbohm, L. M., Burchfiel, B. C., Chen, L. Z., and Yin, J. Y. (2006b). Miocene to present activity along the Red River fault, China, in the context of continental extrusion, upper-crustal rotation, and lower-crustal flow. *Geological Society of America Bulletin*. 118, 672-688.
- Searle, M. P., and Tirrul, R. (1991). Structural and Thermal Evolution of the Karakoram Crust. *Journal of the Geological Society* 148, 65-82.
- Seward, D., and Burg, J. P. (2008). Growth of the Namche Barwa syntaxis and associated evolution of the Tsangpo Gorge: Constraints from structural and thermochronological data. *Tectonophysics* 451, 282-289.
- Shapiro, J. (2001). Mao's War Against Nature: Politics and the Environment in Revolutionary China. Cambridge University Press, Cambridge.
- Simon, A., and Hupp, C. R. (1986). Channel evolution in modified Tennessee stream. *In* "4th Federal Interagency Sedimentation Conference." pp. 5.71-5.82. US Government Printing Offices, Washington, DC, Las Vegas, Nevada.
- Singh, S. K., and France-Lanord, C. (2002). Tracing the distribution of erosion in the Brahmaputra watershed from isotopic compositions of stream sediments. *Earth and Planetary Science Letters* 202, 645-662.

- Sklar, L. S., and Dietrich, W. E. (2001). Sediment and rock strength controls on river incision into bedrock. *Geology* 29, 1087-1090.
- Snyder, N. P., Whipple, K. X., Tucker, G. E., and Merritts, D. J. (2003). Importance of a stochastic distribution of floods and erosion thresholds in the bedrock river incision problem (vol 108, pg 2117, 2003). *Journal of Geophysical Research-Solid Earth* 108, -.
- Sol, S., Meltzer, A. S., Burgmann, R., Van der Hilst, R., King, R. W., Chen, Z., Koons, P. O., Lev, E., Liu, Y. P., Zeitler, P. K., Zhang, X., Zhang, J., and Zurek, B. (2007). Geodynamics of the southeastern Tibetan Plateau from seismic anisotropy and geodesy. *Geology* 35, 563-566.
- Stewart, R. J., Hallet, B., Zeitler, P. K., Mallor, M. A., Allen, C. M., and Trippett, D. (2008). Brahmaputra sediment flux dominated by highly localized rapid erosion from the easternmost Himalaya. *Geology* 36, 711-714.
- Stone, J. O. (2004). Extraction of Al and Be from quartz for isotopic analysis. *UW Cosmogenic Nuclide Lab Methods and Procedures Online*: <http://depts.washington.edu/cosmolab/chem.html>.
- Syvitski, J. P. M. (2003). Supply and flux of sediment along hydrological pathways: research for the 21st century. *Global and Planetary Change* 39, 1-11.
- Syvitski, J. P. M., Vorosmarty, C. J., Kettner, A. J., and Green, P. (2005). Impact of humans on the flux of terrestrial sediment to the global coastal ocean. *Science* 308, 376-380.
- Tapponnier, P., Xu, Z. Q., Roger, F., Meyer, B., Arnaud, N., Wittlinger, G., and Yang, J. S. (2001). Geology - Oblique stepwise rise and growth of the Tibet plateau. *Science* 294, 1671-1677.

- Taylor, M., and Yin, A. (2009). Active structures of the Himalayan-Tibetan orogen and their relationships to earthquake distribution, contemporary strain field, and Cenozoic volcanism. *Geosphere* 5, 199-214.
- Thiede, R. C., Bookhagen, B., Arrowsmith, J. R., Sobel, E. R., and Strecker, M. R. (2004). Climatic control on rapid exhumation along the Southern Himalayan Front. *Earth and Planetary Science Letters* 222, 791-806.
- Tomkins, K. M., Humphreys, G. S., Wilkinson, M. T., Fink, D., Hesse, P. P., Doerr, S. H., Shakesby, R. A., Wallbrink, P. J., and Blake, W. H. (2007). Contemporary versus long-term denudation along a passive plate margin: the role of extreme events. *Earth Surface Processes and Landforms* 32, 1013-1031.
- Trac, C. J., Harrell, S., Hinckley, T. M., and Henck, A. (2007). Reforestation programs in Southwest China: reported success, observed failure, and the reasons why. *Journal of Mountain Science* 4, 275 - 292.
- Tucker, G. E., and Slingerland, R. L. (1994). Erosional dynamics, flexural isostasy, and long-lived escarpments - a numerical modeling study. *Journal of Geophysical Research-Solid Earth* 99, 12229-12243.
- Urgenson, L. S., Harrell, S., Hinckley, T. M., Hagmann, R. K., Grub, B. L., Henck, A., Chi, P. M., and Shepler, S. J. (in review). Social-ecological dynamics of a forested watershed in SW China. *Society and Ecology*.
- USGS. (2001). Global GIS database: digital atlas of South Asia. In "Global GIS Database, Digital Data Series DDS-62-C." (J. P. Hearn, T. Hare, P. Schruben, D. Sherrill, C. LaMar, and P. Tsushima, Ed.). USGS.
- USGS. (2008a). HydroSHEDS. *World Wildlife Fund (WWF)* online: <http://hydrosheds.cr.usgs.gov/>, date accessed: 22 Jan 2009.

- USGS. (2008b). Eurasia land cover characteristics data base version 2.0. In "Global Land Cover Characterization." (USGS, Ed.).
- Vanacker, V., von Blanckenburg, F., Hewawasam, T., and Kubik, P. W. (2007). Constraining landscape development of the Sri Lankan escarpment with cosmogenic nuclides in river sediment. *Earth and Planetary Science Letters* 253, 402-414.
- Vance, D., Bickle, M., Ivy-Ochs, S., and Kubik, P. W. (2003). Erosion and exhumation in the Himalaya from cosmogenic isotope inventories of river sediments. *Earth and Planetary Science Letters* 206, 273-288.
- von Blanckenburg, F., Hewawasam, T., and Kubik, P. W. (2004). Cosmogenic nuclide evidence for low weathering and denudation in the wet, tropical highlands of Sri Lanka. *Journal of Geophysical Research-Earth Surface* 109.
- von Blanckenburg, F. (2005). The control mechanisms of erosion and weathering at basin scale from cosmogenic nuclides in river sediment. *Earth and Planetary Science Letters* 237, 462-479.
- Wang, E., and Burchfiel, B. (2000). Late Cenozoic to Holocene deformation in southwestern Sichuan and adjacent Yunnan, China, and its role in formation of the southeastern part of the Tibetan Plateau. *Geological Society of America Bulletin* 112, 413-423.
- Wang, S. J., Hassan, M. A., and Xie, X. P. (2006). Relationship between suspended sediment load, channel geometry and land area increment in the Yellow River Delta. *Catena* 65, 302-314.
- Wang, Z. Y., Huang, W. D., and Li, Y. T. (2007a). Sediment budget of the Yangtze River. *Journal of Sediment Research*, 1-10.

- Wang, Z. Y., Li, Y. T., and He, Y. P. (2007b). Sediment budget of the Yangtze River. *Water Resources Research* 43, 14.
- Whipple, K. X., Kirby, E., and Brocklehurst, S. H. (1999). Geomorphic limits to climate-induced increases in topographic relief. *Nature* 401, 39-43.
- Whipple, K. X., and Tucker, G. E. (1999). Dynamics of the stream-power river incision model: Implications for height limits of mountain ranges, landscape response timescales, and research needs. *Journal of Geophysical Research-Solid Earth* 104, 17661-17674.
- Whittaker, A. C., Cowie, P. A., Attal, M., Tucker, G. E., and Roberts, G. P. (2007). Bedrock channel adjustment to tectonic forcing: Implications for predicting river incision rates. *Geology* 35, 103-106.
- Willett, S. D., Beaumont, C., and Fullsack, P. (1993). Mechanical model for the tectonics of doubly vergent compressional orogens. *Geology* 21, 371-374.
- Willett, S. D. (1999). Orogeny and orography: The effects of erosion on the structure of mountain belts. *Journal of Geophysical Research-Solid Earth* 104, 28957-28981.
- Willett, S. D., Slingerland, R., and Hovius, N. (2001). Uplift, shortening, and steady-state topography in active mountain belts. *American Journal of Science* 301, 455-485.
- Williams, G. P. (1978). Bank-Full Discharge of Rivers. *Water Resources Research* 14, 1141-1154.
- Winkler, D. (1996). Forests, forest economy and deforestation in the Tibetan Prefectures of west Sichuan. *Commonwealth Forest Review* 75, 296-301.



- Wittmann, H., von Blanckenburg, F., Kruesmann, T., Norton, K. P., and Kubik, P. W. (2007). Relation between rock uplift and denudation from cosmogenic nuclides in river sediment in the Central Alps of Switzerland. *Journal of Geophysical Research-Earth Surface* 112.
- Wobus, C. W., Hodges, K. V., and Whipple, K. X. (2003). Has focused denudation sustained active thrusting at the Himalayan topographic front? *Geology* 31, 861-864.
- Wolman, M. (1967). A cycle of sedimentation and erosion in urban river channels. *Geografiska Annaler* 49, 385-395.
- Wolman, M. G., and Miller, J. P. (1960). Magnitude and Frequency of Forces in Geomorphic Processes. *Journal of Geology* 68, 54-74.
- Xu, J. X. (2000). Runoff and sediment variations in the upper reaches of Changjiang River and its tributaries due to deforestation (in Chinese). *Shuili Xuebao*, 72-80.
- Xu, J. X., and Cheng, D. S. (2002). Relation between erosion and sedimentation zones in the Yellow River, China. *Geomorphology* 48, 365-382.
- Xu, J. X. (2005). Variation in grain size of suspended load in upper Changjiang River and its tributaries by human activities (in Chinese). *Journal of Sediment Research*, 8-16.
- Yang, G. F., Chen, Z. Y., Yu, F. L., Wang, Z. H., Zhao, Y. W., and Wang, Z. Q. (2007). Sediment rating parameters and their implications: Yangtze River, China. *Geomorphology* 85, 166-175.
- Yi, Z. W. (2003). Upper Yangtze River sediments (in Chinese). *Sichuan Shuili*, 29-32.
- Yin, H. F., and Li, C. G. (2001). Human impact on floods and flood disasters on the Yangtze River. *Geomorphology* 41, 105-109.

- Zeitler, P. K., Meltzer, A. S., Koons, P. O., Craw, D., Hallet, B., Chamberlain, C. P., Kidd, W. S. F., Park, S. K., Seeber, L., Bishop, M., and Shroder, J. (2001). Erosion, Himalayan geodynamics, and the geomorphology of metamorphism. *GSA Today* January 2001, 11, 4-9.
- Zhang, P. Z., Shen, Z., Wang, M., Gan, W. J., Burgmann, R., and Molnar, P. (2004). Continuous deformation of the Tibetan Plateau from global positioning system data. *Geology* 32, 809-812.
- Zhang, X. B. (1999). Status and causes of sediment change in the Upper Yangtze River and sediment reduction measures - comparison of Jialing River with Jinsha River (in Chinese). *Soil Water Conservation in China*, 22-24.
- Zhang, X. B., and Wen, A. B. (2002). Variations of sediment in upper stream of Yangtze River and its tributary (in Chinese). *Shuili Xuebao*, 56-59.
- Zhang, X. B., and Wen, A. B. (2004). Current changes of sediment yields in the upper Yangtze River and its two biggest tributaries, China. *Global and Planetary Change* 41, 221-227.

## VITA

Amanda Henck was raised in Hong Kong and there discovered her lifelong love for China. She completed a Bachelor of Science in Engineering in Environmental Engineering from Princeton University in 2002 where she also studied Mandarin. Prior to arriving at UW in September 2003, she tried her hand at teaching English in Harbin, China. While at UW she was a student in Geological Sciences and a fellow in the Multinational Collaborations on Challenges to the Environment IGERT program. Through that program she spent a year studying at Sichuan University and working as a site director for the undergraduate exchange program there. Amanda graduated from the University of Washington with a PhD in Geological Sciences in March 2010. She will be continuing her academic career with a Fulbright Student Fellowship to Jiuzhaigou National Park, Sichuan, China from March – December 2010 followed by an assistant professorship at Oberlin College starting in January 2011. She intends to continue to research in China.